

UNCLASSIFIED

AD NUMBER
AD911150
NEW LIMITATION CHANGE
TO Approved for public release, distribution unlimited
FROM Distribution authorized to U.S. Gov't. agencies only; Test and Evaluation; MAR 1972. Other requests shall be referred to Air Force Avionics Laboratory, Attn: TEL/405B, Wright-Patterson AFB, OH 45433.
AUTHORITY
AFWAL ltr, 9 May 1980

THIS PAGE IS UNCLASSIFIED



AFAL-TR-73-180

EVALUATION of CONCEPTS for a LASER ACQUISITION and TRACKING SYSTEM

ROBERT C. CULVER
Ball Brothers Research Corporation

June 1973

D D C
RECEIVED
JUN 25 1973
REGISTRATION
C

AD 911 1000

DISTRIBUTION IS LIMITED TO U.S. GOVERNMENT
AGENCIES ONLY BY REASON OF INCLUSION OF TEST
AND EVALUATION DATA; APPLIED MARCH 1972.
OTHER REQUESTS FOR THIS DOCUMENT MUST BE
REFERRED TO AFAL/TEL/405B, WRIGHT-PATTERSON
AFB, OHIO, 45433

Air Force Avionics Laboratory
Air Force Systems Command
Wright Patterson Air Force Base, Ohio

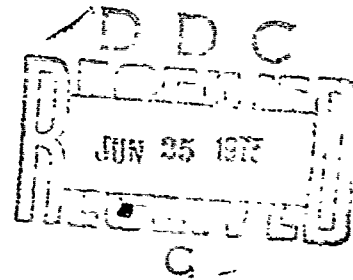
NOTICE

When Government drawings, specifications, or other data are used for any purpose other than in connection with a definitely related Government procurement operation, the United States Government thereby incurs no responsibility nor any obligation whatsoever; and the fact that the government may have formulated, furnished, or in any way supplied the said drawings, specifications, or other data, is not to be regarded by implication or otherwise as in any manner licensing the holder or any other person or corporation, or conveying any rights or permission to manufacture, use, or sell any patented invention that may in any way be related thereto.

Copies of this report should not be returned unless return is required by security considerations, contractual obligations, or notice on a specific document.

EVALUATION OF CONCEPTS
FOR A LASER ACQUISITION AND TRACKING SUBSYSTEM

Robert C. Culver



Distribution is limited to U.S. Government agencies only, by reason of inclusion of test and evaluation data; applied March, 1972. Other requests for this document must be referred to AFAL/TEL/405B, Wright Patterson AFB, Ohio, 45433.

FOREWORD

This report was prepared by Ball Brothers Research Corporation under Contract No. F33615-72-C-2053, Advanced Development Program 405B. This report covers the period June 1972 to April 1973 and is the final report on this contract. The work described herein was carried out by Ball Brothers Research Corporation, P.O. Box 1062, Boulder, Colorado 80302.

The Project Engineer was Robert C. Culver.

The report was submitted in May, 1973 and has been reviewed and approved for publication.

Paul Freedman

Paul M. Freedman, Maj. USAF
Program Manager
405B Advanced Development Program

ABSTRACT

The program objective was to evaluate the starting and running friction characteristics of bearings rotating at 0.001 - 1.0 degree/second and to determine the pointing accuracy that can be achieved on a bearing supported gimbal system. The bearing tests measured the friction of bearings with pitch diameters of 0.25, 1.4 and 2.6 inches, using liquid and dry film lubricants, at high and low temperatures, and with various axial preloads. The running friction results were generally lower than predicted, varying from less than detectable to 0.9 ounce inches. The starting friction tests showed that the bearings have a spring-like characteristic when small torque levels are applied, that the starting friction levels were much lower than expected (0.03 ounce inch), and that a starting friction peak larger than the low speed running friction level does not exist. The pointing accuracy tests were performed on a single axis gimbal which was controlled by a conventional servo system. Tests were run on the repeatability of the system in attaining null, the ability to point while the gimbal housing was rotating at 1°/second, and the effects of disturbances on the system. The tests showed that pointing accuracies in the range of 10-35 microradian can be achieved on bearing supported systems and that the bearings are not the limiting cause of errors.

TABLE OF CONTENTS

<u>Section</u>	<u>Description</u>	<u>Page</u>
I	INTRODUCTION	1
II	BEARING TECHNOLOGY REVIEW	3
III	BEARING TEST EQUIPMENT DESCRIPTION	8
IV	BEARING TESTS	16
V	POINTING TEST EQUIPMENT DESCRIPTION	69
VI	POINTING TESTS	76
VII	ALTERNATE APPROACHES TO BEARING SUPPORTED SYSTEMS	82
 <u>Appendices</u>		
A	REFERENCE BIBLIOGRAPHY OF BEARING TECHNOLOGY	88
B	SCHEMATICS OF TEST ELECTRONICS	95
 <u>Figures</u>		
1	Bearing Test Fixture	9
2	LVDT Schematic	11
3	Bearing Test Electronics	12
4	Servo Block Diagram	14
5	Bearing Spring Effect	22
6	Breakaway Torque	23
7	Spring Effect Data	24
8a & b	Speed-Torque Models	25
9	Torque Vs. Preload for Bearing 33267	27
10	Torque Vs. Preload for Bearing 36563	27
11	Torque Vs. Preload for SR156	28
12	$Y=X^{2/3}$	28
13	Speed-Torque of Bearing 36563	29

TABLE OF CONTENTS

<u>Figures</u>	<u>Description</u>	<u>Page</u>
14	Speed-Torque of Bearing SR156	30
15	Speed-Torque of Bearing 33267	30
16	$Y=X^{2/3}$ Piece-wise Linear	21
17	Bearing 9A Speed-Torque	33
18	Bearing 9B Speed-Torque	33
19	Bearing 13A Speed-Torque	34
20	Bearing 13B Speed-Torque	34
21	Bearing 12A Speed-Torque	35
22	Bearing 12B Speed-Torque	35
23	Bearing 14A Speed-Torque	36
24	Bearing 14B Speed-Torque	36
25	Bearing 13A Temp. Test at Zero Preload	37
26	Bearing 13A Temp. Test at 10 Lb. Preload	37
27	Bearing 13A Temp. Test at 30 Lb. Preload	38
28	Bearing 9A Temperature Test	38
29	Bearing 9B Temperature Test	39
30	Bearing 13B Temperature Test at 10 Lb. Preload	39
31	Bearing 12A Temp. Test at Zero Preload	40
32	Bearing 12A Temp. Test at 10 Lb. Preload	40
33	Bearing 12A Temp. Test at 30 Lb. Preload	41
34	Bearing 12B Temp. Test at 10 Lb. Preload	41
35	Bearing 14A Temp. Test at 10 Lb. Preload	42
36	Bearing 14B Temp. Test at 10 Lb. Preload	42
37	Breakaway Torque Vs. Preload	44

TABLE OF CONTENTS

<u>Figures</u>	<u>Description</u>	<u>Page</u>
38	Brg. 33267 Starting Data 0 and 10 Lb. Preload	44
39	Brg. 33267 Starting Data 20 and 30 Lb. Preload	45
40	Brg. 33267 Starting Data 43 and 53 Lb. Preload	46
41	Bearing 36563 Speed-Torque	48
42	Bearing 36563 Temp. Test at 0 Lbs. Preload	48
43	Bearing 56563 Temp. Test at 10 Lb. Preload	49
44	Bearing 36563 Temp. Test, 30 Lb. Preload	49
45	Bearing 36563 Speed-Torque	50
46	Bearing 36563 Temp. Test at 0 Lb. Preload	50
47	Bearing 36563 Temp. Test at 10 Lb. Preload	51
48	Bearing 36563 Temp. Test at 30 Lbs. Preload	51
49	Brg. 36563 Starting Data 10 & 20 Lb. Preload	53
50	Brg. 36563 Starting Data 40 & 50 Lb. Preload	54
51	Bearing SR156-A Speed Vs. Torque	55
52	Bearing SR156-B Speed Vs. Torque	55
53	Bearing SR156-C Speed Vs. Torque	56
54	Bearing SR156-D Speed Vs. Torque	
55	Bearing SR156-A Temp. Tests at 5 lb. Preload	57
56	Bearing SR156-B Temperature Tests	57
57	Bearing SR156-C Temperature Tests	58
58	Bearing SR156-D Temperature Tests	58
59	Bearing SR156-E Speed Vs. Torque	59
60	Bearing SR156-F Speed Vs. Torque	59

TABLE OF CONTENTS

<u>Figures</u>	<u>Description</u>	<u>Page</u>
61	Bearing SR156-G Speed Vs. Torque	60
62	Bearing SR156-H Speed Vs. Torque	60
63	Bearing SR156-F Temp. Tests, Zero Preload	61
64	Bearing SR156-F Temp. Test, 2 Lb. Preload	61
65	Bearing SR156-F Temp. Test, 4 Lb. Preload	62
66	Bearing SR156-E Temp. Test, 2 Lb. Preload	62
67	Bearing SR156-G Temp. Test, 2 Lb. Preload	63
68	Bearing SR156-H Temp. Test, 2 Lb. Preload	63
69	SR156 Breakaway - 0 & 1 Lb. Preload	65
70	SR156 Breakaway - 5 Lbs. Preload	66
71	Pointing Test Fixture	70
72	Test Gimbal and Motion Input Mechanism	71
73	Pointing Gimbal Control System	73
74	Pointing Gimbal Control Servo Root Locus	73
75	Closed Loop Frequency Response of the Pointing Servo	74
76	Root Locus for Friction Effects	75
77	Angular Pointing Frequency Histogram	77
78	Moving Gimbal Position Traces	79
79	Closed Loop Response to Disturbance Torques	81
80	A Simplified Magnetic Bearing	83
81	Flexure Pivot Types	85
 <u>Tables</u>		
I	Bearing Test Conditions	20

SECTION I INTRODUCTION

Satellite laser communications require that the laser beams be pointed and tracked to accuracies in the range of 0.5-1.0 micro-rad. Systems have been conceived which call for bearing supported elements that must point with accuracies in the range of 10-35 microrad, and move at rates between 0.001 and 1.0 degree/second. No known data was available on the starting and running friction characteristics of bearings at these speeds. In addition, data was needed on the pointing accuracy which can be achieved with bearing supported gimbal systems. The 405B Space Bearing Test Program was undertaken to provide data in both of these areas. The effort was divided into two phases; the first to provide bearing data, and the second to provide pointing accuracy data.

Phase I centered on the testing of three sizes of bearings, using both liquid and dry lubricants. The test bearings have pitch diameters of approximately 0.25, 1.4, and 2.6 inches. All were lubricated with BBRC Vac Kote; half with the liquid type, and half with the dry. The bearings and lubricant are described in Section IV. Two test methods were used, one for starting and one for running friction measurements. Both were performed with the same test fixture which is described in Section III. A considerable amount of fixture development was necessary because with the speeds and bearing sizes tested, the torque levels were far below those encountered in other similar tests. The development effort is also described in Section III.

A literature review of previous bearing effort, including tests, analyses, reference works, and test techniques was performed. While no tests were found at the speeds required on this test program, a number of relevant documents were found and are reviewed in Section II below.

The running friction tests were performed by rotating the outer bearing race at a steady speed and measuring the torque necessary to maintain the inner race still (zero position). The inner race is attached to a frictionless position transducer and to a brushless torque motor. The transducer generates a position signal which is fed to servo electronics, which in turn drive the torque motor to maintain the inner race at its zero position. The torque motor current required to maintain this position is a direct measure of the bearing torque. The outer race is driven from a dc torque motor through an adjustable transmission and a worm gear/wheel combination, at speeds between 0.001 and 1.0 degree/second. The friction torque of the bearings was recorded on a strip chart for preloads varying from less than one pound to 50 pounds, and at high, low, and room temperatures.

The starting friction was measured without the use of the servo electronics. While the outer race was maintained stationary, small steps of torque were applied to the inner race via the brushless torque motor. The position of the inner race was monitored to detect movements in response to the applied torque. Increasing torque steps were applied and position changes observed for each bearing. The tests were repeated for a number of preloads applicable to the bearing size. The tests, results, and conclusions drawn are discussed in Section IV.

In Phase II a single axis gimbal assembly was fabricated and tested to determine the accuracy to which bearing supported systems can be pointed and the effects of friction on this accuracy. The gimbal assembly was installed in a test fixture which rotated the gimbal outer housing at the speeds defined for laser pointing while the inner shaft was accurately pointed by a closed loop servo. A description of the gimbal and its associated test fixture is given in Section V.

The pointing tests were run at room temperature in a laboratory environment. Pointing accuracy was defined as the ability of the system to keep the position transducer nulled in the presence of bearing, slipping, motor, and disturbance torques. The test description, results, and conclusions drawn are found in Section VI.

An additional task associated with Phase II was to review gimbal support mechanisms other than bearings. A review of magnetic bearings and of flexure pivots is given in Section VII.

SECTION II
BEARING TECHNOLOGY REVIEW

A literature review of bearing test programs which could be relevant to the bearing requirements of the 405B program was made. A review of each of those which contains applicable information is given. Appendix A is a bibliography of articles reviewed at BBRC and which are not considered applicable to the laser pointing task but do supply data on the technology of bearings and lubricants.

2.1 BARDEN TEST SUMMARY REPORT

February 1968. This report is the most relevant of those reviewed because the sizes and speeds of the bearings tested are close to those of this program. The tests were run by the Barden Corporation for General Electric. Bearing running torque was measured for three bearings with pitch diameters of 0.437", 1.81" and 3.05". The smallest bearing was preloaded at 10 pounds, the 1.8" bearings at 5, 10, 20, 100 and 200 pounds, and the larger bearings at 600 pounds. The two smaller bearings are within the size of our test program. The smallest bearings were run at 1°/second and the 1.8" bearings at 1 and 2°/second. Two lubricants, Kendall KG-80 and SR-0839 were used. The 1°/second rate is the fastest that the 405B task is concerned with; i.e., the lower rate data needed for 405B are not available. In addition, the starting friction data which is of paramount importance to our test program was not attempted.

The small bearing, preloaded to 10 pounds had running torque of approximately 0.07 oz.in. The 1.81 inch bearing exhibited torques of approximately 0.17, 0.24, and 0.42 oz.in. when preloaded at 5, 10, and 20 pounds respectively. The same size bearings had running torques of approximately 4.2 and 8.4 oz.in. when preloaded to 100 and 200 pounds. This preload, as well as the large bearings loaded to 600 pounds, are not considered relevant to 405B. A method of predicting low speed torque, which had been developed in a reference document, was compared favorably to the experimental data. Comparisons between the reported data and that taken on our program are made in Section IV below. A check was made with Barden on further tests but no more have been done following those reported.

2.2 GENERAL ELECTRIC MOL TESTING

1968-1969. As a part of the MOL program, the General Electric Space Systems group performed bearing tests that, although not directly applicable, are relevant to the laser pointing task. ABEC class VII bearings of 2.4, 5 and 9 inch bore diameters were tested. Only the 2.4 inch bore bearing (3.7 inches O.D.) is

considered relevant, and this not directly because of its large size. Tests were run to obtain information on running torque, starting friction and bearing smoothness, with the emphasis on smoothness. The running torque data showed large variations which were attributed to imbalance in the test equipment.

The smoothness data were evaluated by spectrum analysis on an IBM 7094 computer, which gave power spectral density curves. The test setup used was similar in concept to that which we used for 405B, in that one race of the bearing was rotated at a known speed (0.5-3°/second) and the motor currents used as a measure of torque. The torque levels determined by this test were higher than those we measured, although for undetermined reasons. Some of the measured torques may have resulted from test fixture hardware such as an iron core motor, which has too much residual torque for our tests. The test fixture used a gyro as a rate sensor to control the drive motor. This made it difficult to measure breakaway torque accurately and sensitively, since no position sensor was used and open loop tests were not run. The best data obtainable was that the stiction seemed to be of the same magnitude as the running friction without a starting friction peak. A check with G. . indicated that no further tests of this type have been conducted.

2.3 MECHANICAL SIGNATURE ANALYSIS OF BALL BEARINGS

This paper was presented to the eighteenth annual meeting of the Institute of Environmental Sciences on May 2, 1972. It was written by A. S. Babkin and J. J. Anderson. It describes a method of analyzing high speed aircraft engine bearings for potential failures. Repeated frequencies in the bearing signatures can be detected at lower frequencies than the friction and other random noise present. These frequencies are correlated with anomalies in the various parts of the bearing and the condition of the unit evaluated. The method is not directly applicable to laser pointing because of our low speeds, but it does give insight into bearing frequency signatures and what they represent.

2.4 EFFECTS OF THIN OIL FILM ON BEARING TORQUE

This is a 1964 BBRC study which correlated the thickness of lubrication films to the running torque. The method used was to spin the bearings and observe the length of time required to spin down. This gives a measure of the integrated torque but does not give torque versus speed, starting friction, or smoothness data. The method developed can be used in the evaluation of overall friction when parameters such as lubricant choice, preload, and temperature are varied.

2.5 SURVEY OF AEROSPACE REQUIREMENTS FOR BEARINGS (AD439892)

This G.E. report discusses the natural and induced environments

which bearings, lubricants, etc. will experience in earth orbiting satellites. It is relevant to the 405B program as an aid in evaluating the adaptability of the laboratory demonstration hardware to space use.

2.6 ROLLING-CONTACT BEARING REFERENCE SUMMARY (AD692472)

This reference work was prepared by the Batelle Memorial Institute for the Redstone Scientific Information Center in 1969. It is an excellent review and reference for rolling contact bearings and lubrication methods. It contains design data, failure analysis data, and information on space vacuum lubrication. Although it does not address the slow speed and extreme accuracy requirements of laser communications, it has use as a general reference on bearing applications.

2.7 INSTRUMENT FOR MEASURING SMALL FRICTIONAL FORCES

This is a paper delivered in 1969 to the annual meeting of American Society of Lubrication Engineers. It was prepared by B. R. Livesay and R. B. Belser of the Georgia Institute of Technology. It describes a device for measuring the extremely small frictions (2-50 dynes) of crossed textile fibers or crossed wires. The paper is of interest to our bearing tests because the described device is remarkably similar to our bearing test fixture in operating principles. The operating principle of both devices is to drive one element of the test article at a steady rate (one bearing race or one fiber) and use a servo loop to maintain the zero position of the opposite element. In both devices an iron-free galvanometer type torque motor is used to provide rebalance torque and the current through the torque motor measured to indicate friction amplitude. The fiber friction test fixture used a light source, rotating mirror and photo diode for the position sensing system. This was not considered sensitive enough for our test fixture where we used a linear variable differential transformer. Both test fixtures used a worm screw to provide the initial input motion. As in our tests, the factors that limited precision and accuracy in the fiber tests were the room vibration, room disturbances, and extraneous noise. Since this paper had not been reviewed before we designed the bearing fixture, the similarity of the two concepts is unusual. However, the similarity of the limiting test factors lends confidence and support to the concept used and limiting factors found on our tests.

2.8 EVALUATION OF DRY LUBRICANTS AND BEARINGS FOR SPACECRAFT APPLICATIONS

This paper was prepared for the Third Aerospace Mechanisms Symposium by D. L. Kirkpatrick and W. C. Young of the General Electric Company. A number of 1/4 inch bore bearings were tested using ten types of dry lubricants. Slow speed and low torque were not test objectives, so in these areas the paper gives no applicable

data. It does contain life information, bearing torque data at speeds between 480 and 500 rpm, and data on the effects of non-running dwell on the friction thereafter. Its application to the laser pointing task is as a general reference for dry lubrication applications.

2.9 FRICTION TORQUE IN LIGHTLY LOADED BALL BEARINGS WITH VAC KOTE LUBRICANT

A compilation of BBRC test data allowed curves to be drawn from which predictions of torque data could be made. Data was collected on 121 bearings of 19 different sizes and types. The data is given for speeds up to 100 rpm, but is not available for the less than 1 rpm speeds we tested at. All data is for unloaded bearings with either wet or dry Vac Kote.

2.10 MISALIGNED BALL BEARINGS

An article in the February 1970 issue of Tribology was written by E. E. Ellis of the RHP General Bearings Division, Chelmsford, Essex, England. The article defines ball bearing misalignment, discusses its effects on bearing wear and gives guidelines to minimizing the problems. It is most applicable to the laser communications program as a reference work that can be useful in evaluating bearing designs during the demonstration program, as well as a general reference in understanding bearing problems.

2.11 TECHNIQUES FOR INVESTIGATION OF FRICTION AND WEAR IN AEROSPACE BEARINGS

This document (ASD-TDR-63-565) was prepared by the Southwest Research Institute for the Air Force Flight Dynamics Laboratory at Wright Patterson Air Force Base. Emphasis was directed toward the instrumentation and techniques for evaluating aerospace bearings rather than the test results. The bearings considered were larger and tested at much higher speeds than those we tested. It is a good background document for test methods which have been previously developed.

2.12 TORQUE VARIATIONS IN INSTRUMENT BALL BEARINGS

This is a report of a study on bearing torque variations made by E. P. Kingsbury of the MIT Instrumentation Laboratory. It is concerned with small, high speed, gyroscopic bearings, so the data derived is not directly applicable to laser pointing. It is of general use as background information on methods and analysis of bearing tests.

2.13 THE EFFECT OF GEOMETRIC CONFORMITY BETWEEN A BALL AND ITS TRACK ON THE FREE ROLLING RESISTANCE

This is a 1972 article by B. G. Brothers and G. R. Bremble in the

publication Wear. It describes tests to confirm theories on the relationship between rolling friction and the geometric shape of the ball and track. It is of interest to this program in that it illustrates the overwhelming effect that bearing design can have on the rolling friction. Bearings as such were not tested, but rather balls rolling in tracks. The tests and instrumentation are described.

2.14 DEVELOPMENT OF A PNEUMATIC SENSOR FOR MEASURING THE TORQUE OF INSTRUMENT BALL BEARINGS

This 1969 ASME paper by E. G. Edwards and H. H. Mabie describes a pneumatic torque measuring device for instrument ball bearings. The device was used to determine the average running torque of bearings running from 1000 to 40,000 rpm, preloaded at 50, 100, and 200 grams. Although used for average torque of high speed bearings, the design could probably be modified for low speed and instantaneous torque as required on laser communications applications.

2.15 BALL BEARING PERFORMANCE AND SURFACE ENERGY THEORY

This 1964 paper was prepared by P. F. Brown for presentation at the USAF-SwRI Aerospace Bearing Conference. It describes tests on angular contact bearings which correlate the bearing performance to the energy of adhesion between materials in the bearings. Its application to the laser communications task is as a general reference showing the relationship of bearing design to performance.

SECTION III

BEARING TEST EQUIPMENT DESCRIPTION

3.1 INTRODUCTION

The bearing test equipment consists of two major assemblies, the bearing test fixture and the servo control electronics. The method used to measure bearing running friction is to rotate the outer race at a constant rate, servo the inner race to maintain a zero position, and measure the torque required to maintain this zero position. The torque to maintain position is supplied by a brushless dc torque motor and motor current is measured to indicate torque. The outer race rates are generated by a motor-transmission combination driving a worm gear and wheel. The worm wheel is attached to the test bearing outer race which rotates at rates between 0.001 and 1.0 degrees/second.

The method used to measure starting friction is to apply extremely small torque levels to the inner race while holding the outer race stationary, and observing the movement of the inner race in response to the torque. For this, the servo loop is not closed, and only the dc motor and the readout system are used with the bearing test fixture. The bearing fixture and the electronics are described below.

3.2 TEST FIXTURE

The test fixture is shown in Figure 1. It is made up of three major subassemblies: the outer race drive assembly, the inner shaft assembly, and the position readout assembly.

The outer race drive assembly is made up of an Inland dc torque motor, a speed reducing transmission and a worm gear driving a worm wheel. The outer race of the test bearing is fitted to the worm wheel through an interchangeable adapter for the three sizes of bearings. The dc motor was driven at 60 rpm through gear reductions of 1000, 100, 10, or 1 in the transmission. The worm gear is driven through an in-line coupling from the gear box. The worm is a 48 pitch, single thread gear which mates with a 48 pitch, single thread wheel, with 360 teeth. The worm combination is an ACMA standard class 10, lubricated with a $M_{O}S_{2}$ type commercial lubricant.

The original design incorporated a synchronous motor rather than the dc motor to drive the outer race. During the fixture check-out, this motor exhibited excessive vibration at 60 and 120 Hz. To eliminate the jitter we replaced the synchronous motor with the dc motor and mounted the dc motor and transmission on an adjacent bench rather than on the test fixture. In the final configuration, the only connection between the fixture and the motor/transmission is via the shaft which connects the transmission to the worm gear.

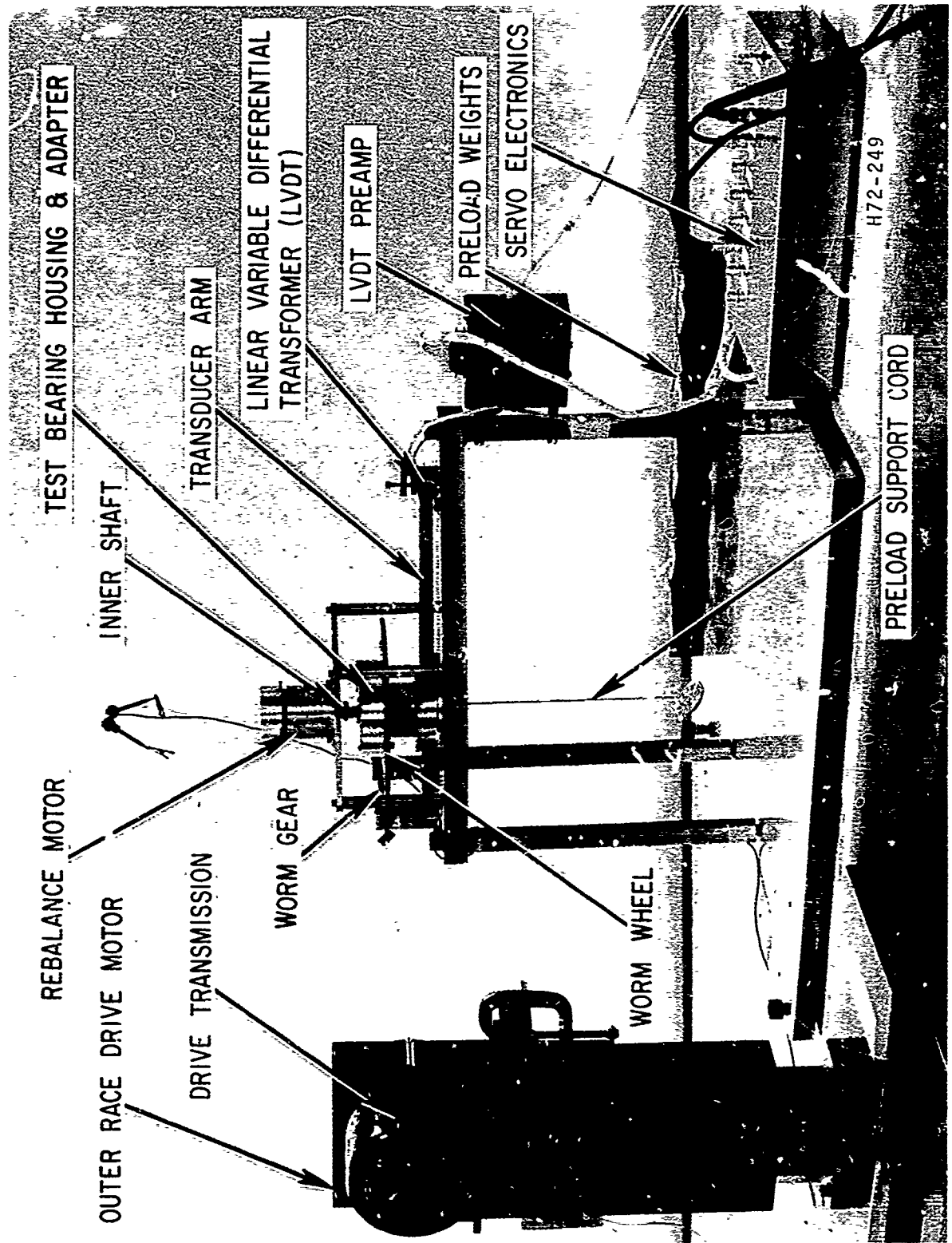


Figure 1 Bearing Test Fixture

The inner shaft assembly runs through and is attached to the inner race of the test bearing. At opposite ends of the shaft the rotor of the rebalance torque motor and the arm which supports the core of the position transducer are mounted. The dc rebalance motor is used to provide the torque to maintain the inner race at a steady position. It is an Aeroflex model TMC20-1P brushless motor which has no contact or friction between the rotor and stator which would degrade our ability to detect the bearing friction. The rotor is a moving coil device without any iron or soft magnetic materials. For this reason it has no hysteresis effects and no null uncertainty or dead zone.

The position transducer-core support arm is a single machined piece of magnesium which incorporates stiffness and light weight. These characteristics allow a high servo bandpass without an excessively large motor or an unreasonably sensitive position transducer. Weights to produce bearing preloads are hung from the lower end of the shaft. They are hung via a nylon cord so that there is negligible torsional resistance that would appear as bearing friction.

In the original fixture design the shafts for each size bearing were fabricated of a magnesium alloy. The shaft for the small bearing test was not stiff enough torsionally, and caused an undamped spring effect in the servo. To correct the servo problem we made another shaft, somewhat larger and of steel. This raised the resonant frequency enough above the servo control range that the problem was eliminated.

The angular position transducer is a linear variable differential transformer (LVDT). It is a linear device which is placed at a 10 inch lever arm to measure the angular movement of the inner race. It has resolution that is theoretically infinite and in practice detects movements of less than 1 microinch. At the end of the 10 inch radius arm, this is equivalent to an angle of 0.1 micro rad. It is a torroidally wound transformer that has one primary winding and two secondary windings wound opposing each other as shown schematically in Figure 2. The core is placed in the hole of the torroid, but not touching the walls. As the core is translated in the cavity the magnetic reluctance is changed between the primary and the secondaries. The flux coupling is thus changed and the secondary output varies linearly with the core movement. In the bearing test fixture the LVDT core is mounted on the arm which is attached to test bearing inner race. As the inner race rotates, the core translates inside the LVDT winding, producing an ac output proportional to the amount of travel. This signal is demodulated and used by the control servo as the position error signal. The servo then drives the rebalance torque motor to keep the LVDT output nulled.

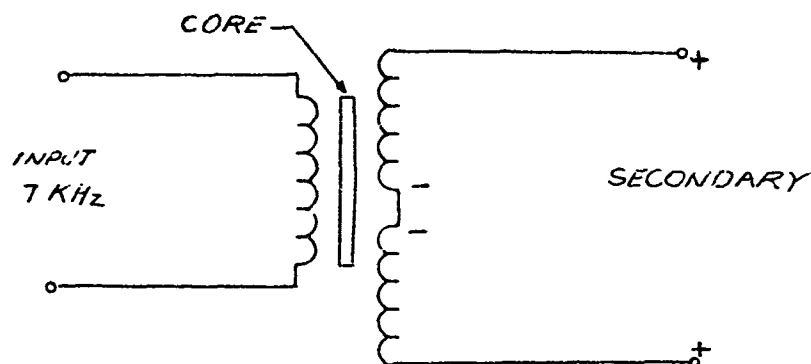


Figure 2 LVDT Schematic

3.3 ELECTRONICS

The Space bearing test electronics are illustrated in block diagram form in Figure 3. The schematics are shown in Appendix B.

A Wien Bridge oscillator with constant amplitude control is used to provide the 9V RMS, 7 KHz excitation for the LVDT. This circuit meets the desired +0.05 percent amplitude control and +0.3 percent harmonic distortion requirements set as design goals.

The preamp uses a high slew rate, low noise Signetics 531 operational amplifier operated as an ac amplifier (1 decade above and below the 7 KHz excitation frequency) with a gain of 86.6 (38.8 db). The gain of 86.6 was chosen to provide 1 mV of output signal per microinch of LVDT travel (0.02 arc second at 10 inches), which was the desired system resolution. Any higher preamp gain would have limited the dynamic range of the system.

The noise output of the preamp was measured and found to be 0.65 mV RMS or $2.46 \mu\text{V}/\sqrt{\text{Hz}}$, which compares very favorably with the desired resolution of one millivolt. The preamp circuit was constructed on brass vectorboard to improve the high frequency characteristics.

The demodulator uses a Harris 2515 high slew rate amplifier in a balanced phase shift configuration, providing a gain of +1.00. Zero detection is also accomplished by a Harris 2515, providing the fastest switching at zero for minimum distortion in the demodulator output. A 2N3677 chopper transistor was used as the demodulator chopper stage, rather than FET switches, which exhibited unequal on and off times.

Due to a relatively large LVDT quadrature component (approximately 50 mV peak to peak) at null, resulting in 7 KHz and 14 KHz components throughout the loop, it was found necessary to incorporate a notch filter at each frequency, to effectively eliminate these frequencies from the output. This was implemented by two

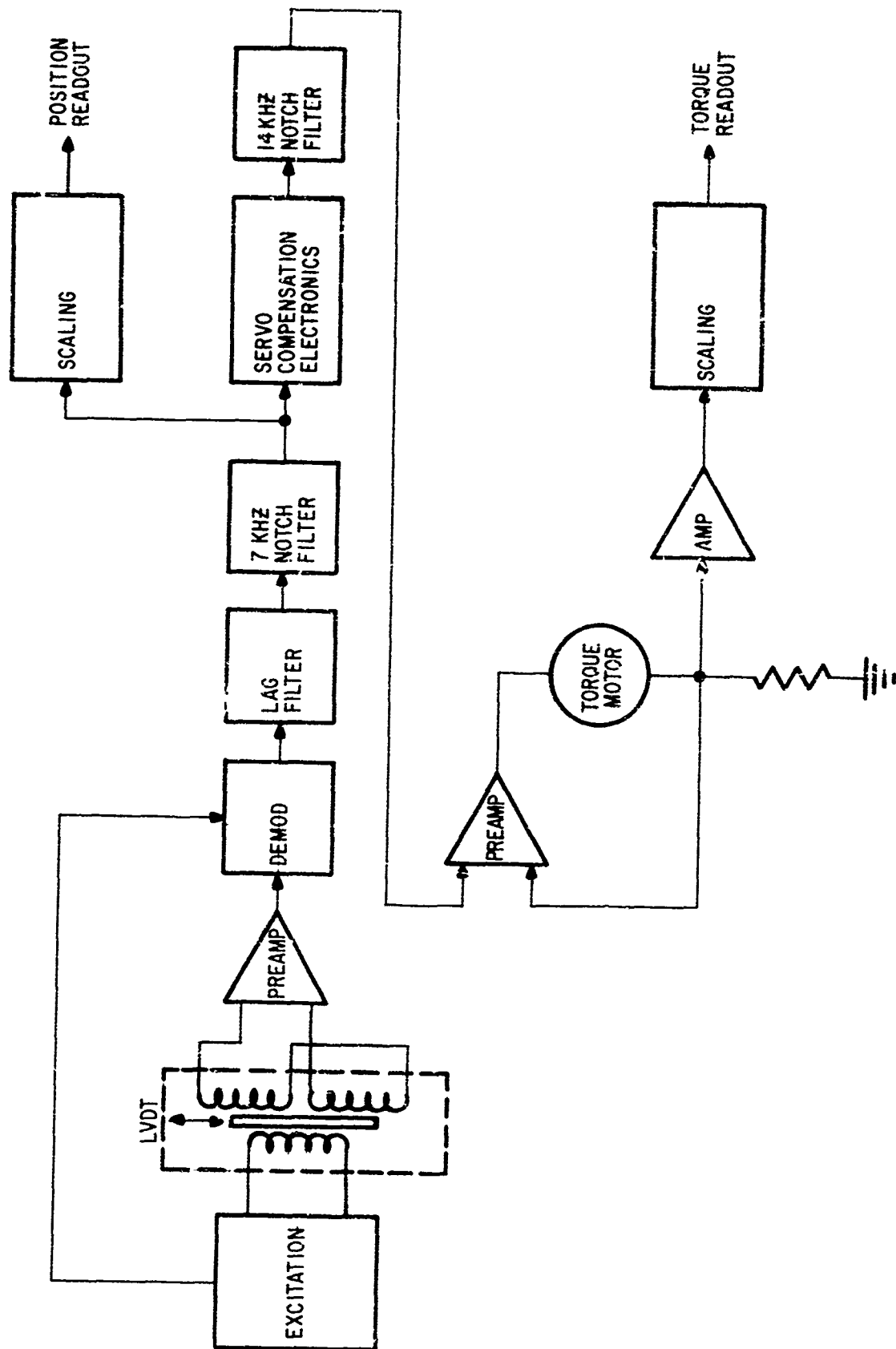


Figure 3 Bearing Test Electronics

active twin-T networks, each precisely tuned to its respective frequency. Attenuation for each was -34db (50:1) with unity pass-band gain. Comparison tests showed no effect upon the servo loop except the elimination of the undesired frequencies.

The servo electronics uses straightforward active filters as discussed below. LM101A amplifiers were used throughout to provide wide bandwidths that would introduce negligible high frequency poles.

A Motorola MC1438R class A booster amplifier and an LM101A make up the torque motor power amplifier, operated as a feedback current driver, with bipolar current limiting set at +200 mA. Tests showed the pair to be truly class A and linear, with a bandwidth of 50 KHz.

3.4 CONTROL SYSTEM

The control servo is a closed loop feedback system as shown in Figure 4. The intent of the servo analysis was to get the control frequency as high as 200 Hz, if possible. We originally assumed that the fixture was a rigid body with no bending modes below 200 Hz. The rigid body servo compensation derived was

$$\left(\frac{S+1255}{S+6280} \right)^2$$

The LVDT demodulator requires an output filter which we viewed as an integral part of the plant to be controlled. We limited the filter to a single pole lag and adjusted its frequency on the basis of the servo compensation as well as for filtering purposes. For the rigid body servo we set the filter break frequency at 500 Hz. Since the LVDT carrier frequency is 7000 Hz the filter gave attenuation of approximately 23db. This loop has very high frequency response which is practically limited only by the noise in the system if the plant is truly rigid. A computer simulation showed the loop would operate at frequencies up to 200 Hz.

Structural tests on the test fixture showed that it was not sufficiently rigid. We found a torsional bending mode in the inner shaft which led to a system resonant frequency of approximately 100 Hz. Two solutions were applied to the resonance problem. The inner shaft was reconstructed of steel, rather than magnesium, to gain added stiffness and raise the resonant frequency well above 200 Hz. In addition, the control compensation was changed to lower the bandpass below the 200 Hz resonant point and to make the servo less sensitive to the resonance by adding some closed loop electronic damping. The compensation was changed from a double to a single lead-lag

$$\left(\frac{S+750}{S+3140} \right)$$

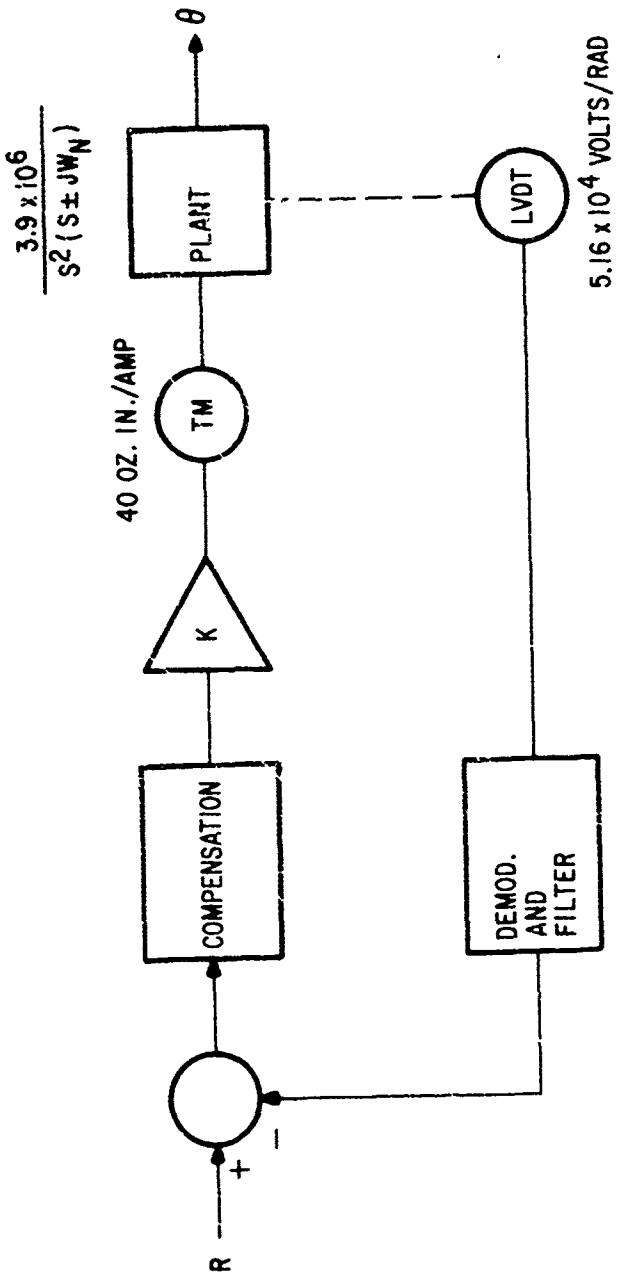


Figure 4 Servo Block Diagram

The demodulator filter was kept at 500 Hz. This servo control was checked out and worked well with the intermediate sized (33267) bearings.

Since the inner shaft must fit through the inner race of each test bearing, separate shafts were constructed to mate with the different size bearings. Each shaft established the bending mode for a different resonant frequency point so each bearing size required some modification of the control system. A servo compensation was designed which accommodated all 3 bearing sizes by lowering the servo bandpass well below that of the lowest resonant point. The compensation used was

$$\frac{(s+150)^2}{s+750}$$

With this compensation we were able to decrease the break frequency of the demodulator filter to 120 Hz. This system was used on the speed-torque tests for all of the bearings tested.

SECTION IV
BEARING TESTS

4.1 INTRODUCTION

This section describes the bearing tests performed in Phase I. The section is arranged to cover three points chronologically.

- Test bearing descriptions - Types and sizes of bearings, procurement sources, reasons for the choices and a review of the lubricants used.
- Bearing tests - Description of the tests run and the results obtained.
- Test conclusions - Applicability of bearings to 405B laser pointing.

4.2 DESCRIPTION OF TEST BEARINGS AND LUBRICANTS

Three sizes of bearings were tested to obtain comparative running and starting friction characteristics of bearings in the size range considered for use on Project 405B laser pointing. The bearings tested have pitch diameters of 2.59, 1.417, and 0.250 inches and are all of ABEC class 7 quality. They were lubricated with either liquid or dry Vac Kote, a BBRC space lubricant. A description of each bearing follows.

4.2.1 Bearing 33267

This bearing is the intermediate size of the three sizes tested. It was chosen primarily on the basis of availability and known past test and flight history. The bearing was produced to BBRC specification by Industrial Techtonics, Incorporated for the OSO-7 satellite. The satellite was launched in September, 1971 and has operated properly since. Flight spare bearings were available so they were the first bearings tested while the other sizes were being procured.

The 33267 units are matched duplex pairs of ABEC class 7 angular contact bearings having a normal axial preload of 10 to 20 pounds when assembled and mounted in a back to back manner. Each bearing has passivated 440C consumable electrode vacuum melt stainless steel rings and balls which have been hardened to Rockwell C58 (Min.), and Nema grade LE phenolic separators with a porosity of 3 to 7 percent. Bearing dimensions are as follows:

bore	.7874"
outside diameter	2.0472"
pitch diameter	1.417"
ball diameter	13/32"
no. of balls/bearing	5
no load contact angle	16.5 deg.

The duplex pairs were separated into individual bearings for test. One set of four bearings was lubricated with liquid Vac Kote and was thus identical to those flown on OSO-7. On the other set of four, the original phenolic separators were replaced with identical separators made of Rulon A material and the races and balls were cleaned and lubricated with dry Vac Kote.

4.2.2 Bearing SR156SSW3-0-11

This Barden bearing was chosen for test because it is similar to that specified by LMSC in SAMSO report TR71-252 and used by LMSC in the coarse mirror gimbal of their laser pointing demonstration model. The bearing originally called for was a SR156SSW5-0-11 which differs from the bearing tested only in that its contact angle is nominally 11 degrees compared to 16 degrees for the bearing used. This choice was due to delays in the procurement time of the specified bearing which would have unacceptably delayed the program schedule.

The .156 is a deep groove double shielded ball bearing constructed of 440C stainless steel shields, races, and balls and with a two piece pressed stainless steel anti-windup separator. The bearing dimensions are:

bore	.1875"
outside diameter	.3125"
pitch diameter	.250"
width	.1250"
ball diameter	1 mm
no. of balls	11

Eight bearings were tested; four lubricated with liquid Vac Kote and four with dry.

4.2.3 Bearing 36563

This bearing is similar to that chosen by McDonnell Douglas for use in their laser pointing demonstration. It was selected for test after the test program on the other bearings was underway and for this reason introduced a procurement problem. Because of this we used a pair already available in-house. The bearings tested were manufactured by the Fafnir Bearing Company to a BBRC specification and were used in the design of a biaxial antenna pointing gimbal to be flown on the Nimbus-F spacecraft. The flight hardware has been qualified and delivered to General Electric, the Nimbus prime contractor, so previous test history existed on these bearings. Since only one pair was available the tests were limited to these bearings.

The bearings tested have external dimensions, i.e., bore, outside diameter, and width, identical to those specified by a McDonnell Douglas drawing. Other dimensions may be identical; however, not

enough information could be obtained from the drawing to make a valid comparison.

The 36563 bearings are a matched duplex pair of ABEC class 7T angular contact bearings. When assembled and mounted in a face-to-face manner an axial preload of 30 to 40 lbs. is obtained. The balls and races are made of passivated air melt 440C stainless steel which has been hardened to Rockwell C58 (min). The separators are made of Rulon A which also contains 5% $M_{O}S_{2}$. The bearings were tested individually, not as a pair. One bearing was lubricated with dry Vac Kote, as were the bearings on the Nimbus gimbal. The other was lubricated with liquid Vac Kote. The Rulon A separator was retained with the liquid lubricant, unlike normal practice. Bearings with liquid Vac Kote normally use phenolic ball separators because the phenolic can be impregnated with lubricant and form a lubricant reservoir. No significant differences between the torque characteristics of the two retainer materials was predicted and none was found in the test. The bearing dimensions are:

bore	2.3125"
outside diameter	2.8750"
pitch diameter	2.594"
ball diameter	.18"
no. of balls/bearing	.48
nominal no-load contact angle	15 deg.

4.3 DESCRIPTION OF VAC KOTE

Vac Kote is the generic name for several proprietary lubricant formulations and application processes developed by BBRC for use in hard vacuum. Vac Kote development was begun in 1959 when the first Orbiting Solar Observatory was being designed. At that time, it was discovered that the available lubricants for vacuum service were not effective at the hard vacuum levels of outer space. Two basic systems resulted from this early work, one based on a liquid and one based on a dry lubricant. Subsequently, combinations of the original systems and greases were developed.

The liquid system has been most widely used. The lubricant consists of a long-chain hydrocarbon fluid with metallo-organic additives which reduce adhesive wear. The base fluid is selected for chemical stability and low vapor pressure. The additive is chosen for its effectiveness in reducing wear.

The liquid lubricant is the one best suited for long life applications or heavy load applications because there is a replenishment mechanism available for it. As with any fluid, evaporation of the lubricant takes place, although at a low rate. When a source of lubricant is placed near the bearings or other lubricated

components, lubricant lost by evaporation from the component is replaced by lubricant evaporated from the adjacent source that strikes and adheres to the bearing surface. In liquid system designs, reservoirs of liquid Vac Kote are placed near the bearings and inside the labyrinth seal which keeps the evaporation loss to a minimum. These reservoirs are made of an impregnated porous material such as Nylasint.

The dry lubricants are high purity hexagonal crystal compounds such as molybdenum disulfide, applied with a proprietary process. Submicron sized lubricating particles are applied by a mechanical method that deposits approximately 0.000010 of an inch. The lubricating particles strongly adhere to substrate surfaces without the use of bonding agents.

The dry lubricants are most applicable in areas of temperature extremes or severe cleanliness requirements. The dry Vac Kote does not evaporate at high temperatures or increase the bearing torques at low temperatures as does the liquid. For applications such as the Apollo Telescope Mount experiments, BBRC used the dry Vac Kote lubricant to ensure that lubrication contamination would not occur on precise optical components. The dry lubricants are not usually recommended where the bearings must carry heavy loads for a long life. This is because the thin lubricant layer could be worn off and there is no replenishment mechanism with the dry lubricants.

4.4 DESCRIPTION OF BEARING TESTS

Two types of tests were run on each bearing, starting friction and speed-torque running friction. The starting friction tests were run by holding the outer bearing race stationary, applying a small torque increment to the inner race, and observing the corresponding angular movement of the inner race. The torque increments were applied with the brushless rebalance motor and the movement detected with the LVDT position transducer. The torque steps were applied at two levels, 0.0005 and 0.005 oz.in./step. Ten steps were usually taken, giving torque peaks of 0.005 and 0.05 oz.in. In each case the torque was reduced stepwise to zero, 10 negative steps of torque applied and again stepped back to zero.

The speed-torque tests were run by rotating the test bearing outer race at speeds of 0.001, 0.01, 0.1 and 1.0 degrees/second and holding the inner race still with the rebalance motor. The inner race was held with the closed loop servo described in Section IV. The motor current supplied by the servo electronics to hold the inner race is a direct measure of the bearing torque.

Table I is a summary of the tests and the conditions under which they were run. The preloads were selected to cover the ranges that would normally apply to the size of bearing and the load it

BEARING S/N	LUBRICATION	APPLIED PRELOAD, LBS, @ TEMPERATURE			
		0°F	32°F	70°F	120°F
<u>BEARING 33267</u>					
33267-501-9A	LIQUID VAC KOTE	10	10	0,10,20,30,40,50	10
33267-501-9B	" "	10	10	0,10,20,30,40,50	
33267-501-13A	" "	0,10,30	0,10,30	0,10,20,30,40,50	0,10,30
33267-501-13B	" "	10	10	0,10,20,30,40	10
33267-501-12A	DRY VAC KOTE	0,10,30	0,10,30	0,10,20,30,40,50	0,10,30
33267-501-12B	" "	10	10	0,10,20,30,40,50	10
33267-501-14A	" "	10	10	0,10,20,30,40,50	10
33267-501-14B	" "	10	10	0,10,20,30,40,50	10
<u>BEARING SR156</u>					
SR156SSW3-A	LIQUID VAC KOTE	5	5	0,2,6,7	5
SR156SSW3-B	" "	5	5	0,2,5,10	5
SR156SSW3-C	" "	5	5	0,2,5,10	5
SR156SSW3-D	" "	5	5	0,2,5,10	5
SR156SSW3-E	DRY VAC KOTE	2	2	0,2,5	2
SR156SSW3-F	" "	0,2	4	0,2,5,10	0,2,4
SR156SSW3-G	" "	2	2	0,2,5	2
SR156SSW3-H	" "	2	2	0,2	2
<u>BEARING 36563</u>					
MD-1	LIQUID VAC KOTE	0,10,30	0,10,30	0,10,20,30,40,50	10
MD-2	DRY VAC KOTE	0,10,30	0,10,30	0,10,20,30,40,50	10

TABLE I
BEARING TEST CONDITIONS

would carry in the laser pointing application. The preloads for the two larger bearings were varied between 0 and 50 pounds in 10 pound steps. The maximum preload for the SR156 bearing was 10 pounds. The entire load carried by each bearing was approximately 8 ounces more than the preloads shown because each bearing also supported the rotor of the rebalance motor, the inner shaft, and the support arm for the LVDT. The choice of optimum bearing preloads for aerospace equipment is not influenced overwhelmingly by any single factor. Among those factors which can affect the choice are the 1-g test requirements, desired rigidity of the system, thermal environments, and the load to be carried by the bearings. The friction torque resulting from preload is also one of the most important factors and this led us to the preload variations during the tests.

Room temperature tests were considered the most significant of those run because the requirements of a laser pointing system would appear to dictate an instrument with tight thermal controls. Since the ground fabrication and test tasks are most easily accomplished at room temperature, the thermal control systems are most often designed to operate here. For this reason the greatest test effort was applied at the 70°F temperature. However, satellites must operate and are qualified over various temperature ranges associated with inaccuracies in the analytical temperature predictions and with potential failure mode operation. For this reason, information on bearing operation at reduced and elevated temperatures is also relevant. The only predictable change of bearing friction with temperature in our test fixture was with the liquid lubricant. Bearing torque is a known function of lubricant viscosity so the low temperature tests with liquid Vac Kote were expected to show increased friction. They did. The torque characteristic of dry film lubricants is essentially independent of temperature.

4.4.1 Overall Test Results

The form of the test results was the same for all three bearings tested, so the general results will be discussed here and each size of bearing reviewed thereafter.

In the starting friction tests, three characteristics stand out in the test results.

- When very small starting torques were applied to the bearings they acted like springs as well as rolling elements.
- The starting or breakaway friction of all 3 bearing sizes was very low; in the cases of the two larger bearings, much lower than expected.
- A peak of starting friction above the low speed running friction was not found.

The spring action of the bearings is shown in Figure 5. When a small step of torque is applied, as shown in Figure 5-a, the bearing race rotates a small amount (5-b), but when the torque is removed the race returns back toward its original position.

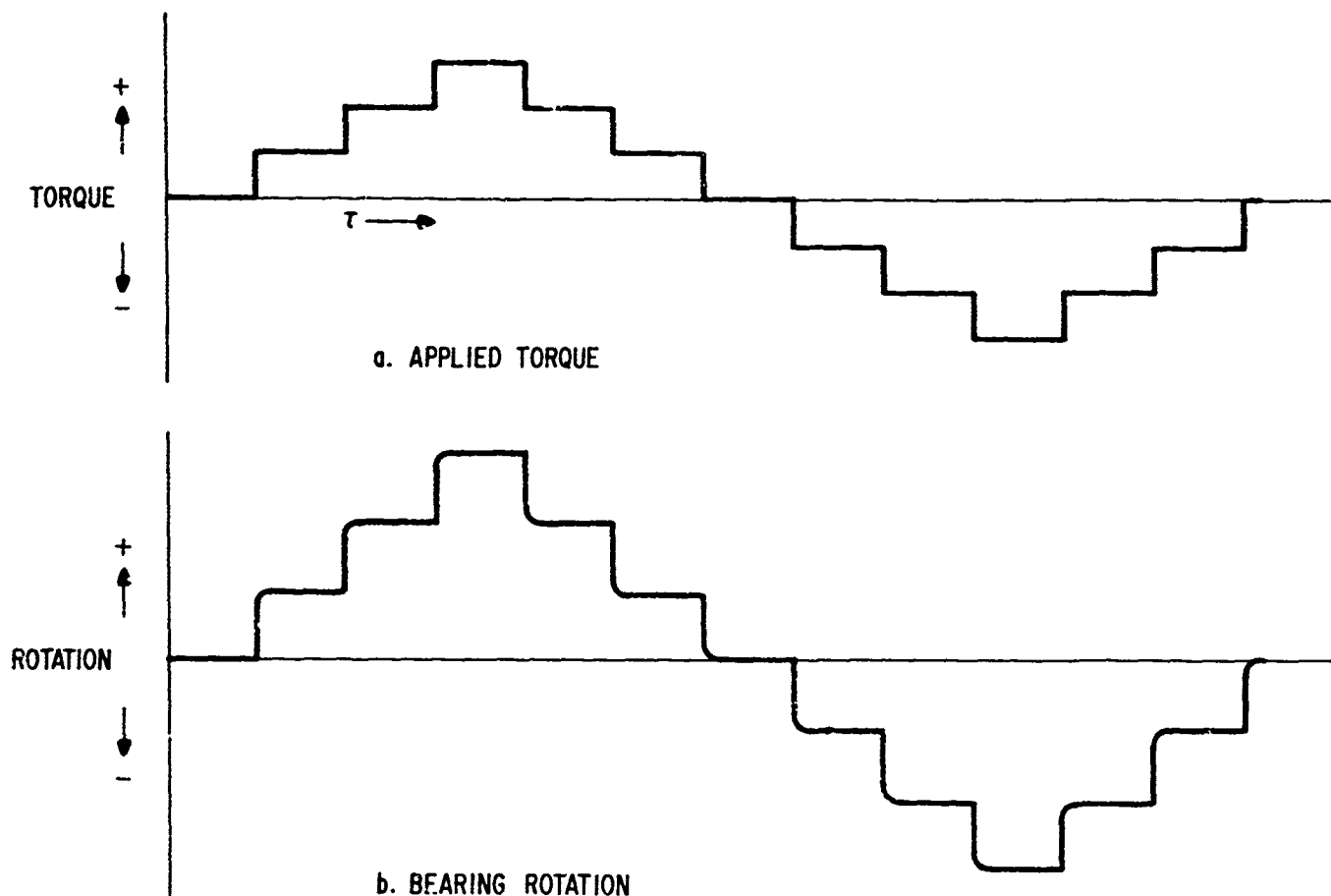


Figure 5 Bearing Spring Effect

Whether several torque steps were applied, as shown, or only a single step, the result was the same; springing to a new position with torque applied and returning to the starting point when torque was removed. Under very low torque steps (0.0005 oz.in.) the bearing does not continue to rotate, but maintains its new position until the torque level is changed. When larger torque steps are applied (.005 to .05 oz.in.), the bearing springs immediately to a new position but from that point continues to roll at a slow rate. This leads to a clarification of our definition of "breakaway" friction. Breakaway as the torque which first causes the bearing to move is insufficient because all the bearings move some amount with infinitesimal levels of applied torque. A better definition of breakaway is that torque level which will

cause continuous rotation after the springing motion has taken place. An example of this is found in Figure 6. When the torque step is applied the bearing moves quickly to a new position corresponding to a spring constant and then continues to rotate indefinitely. Tests were run where the bearing was allowed to run continuously at a very slow speed for as long as 2 hours. Figure 7 is a picture of raw data which illustrates the spring effect and the rolling motion simultaneously. The torque steps applied were each 0.005 oz.in. and resulted in a bearing movement of approximately 3 arc seconds. Each torque level was maintained for about 3 seconds before the next was applied. Inspection of Figure 7 shows that many of the trace sections above zero torque slope upward and those below slope downward. This shows bearing rolling motion which, if allowed to continue, would form a trace similar to Figure 6. Confirmation of the rolling is seen in that the position of the bearing did not return to zero when the torque was returned to zero, on either the positive or negative torque excursions.

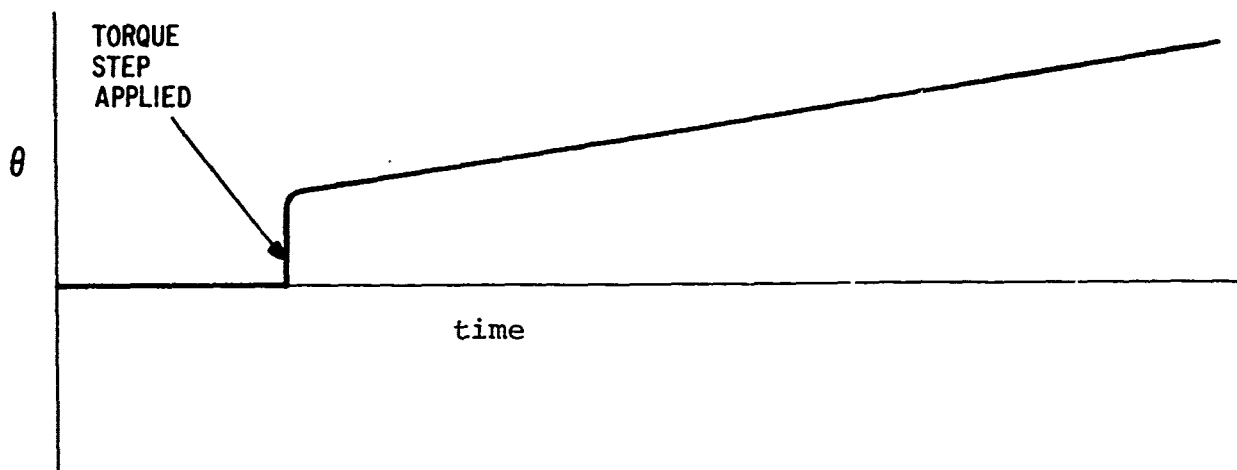


Figure 6 Breakaway Torque

It was not possible to balance the test fixture perfectly and the unbalance gave a steady state offset torque in one direction. This unbalance was measured at levels between 0.0005 and 0.003 oz.in. The result of the unbalance torque was that data traces such as shown in Figure 7 were not always symmetrical about the zero torque line. The unbalance was easily accounted for in interpreting the data.

The breakaway friction in bearings of the size of the larger two tested was expected to be on the order of 1 oz.in. It was found to be less than 0.05 oz.in. in all cases. Estimates of the breakaway friction of small instrument bearings like the SR156's tested had not been previously made. Two possible explanations for the

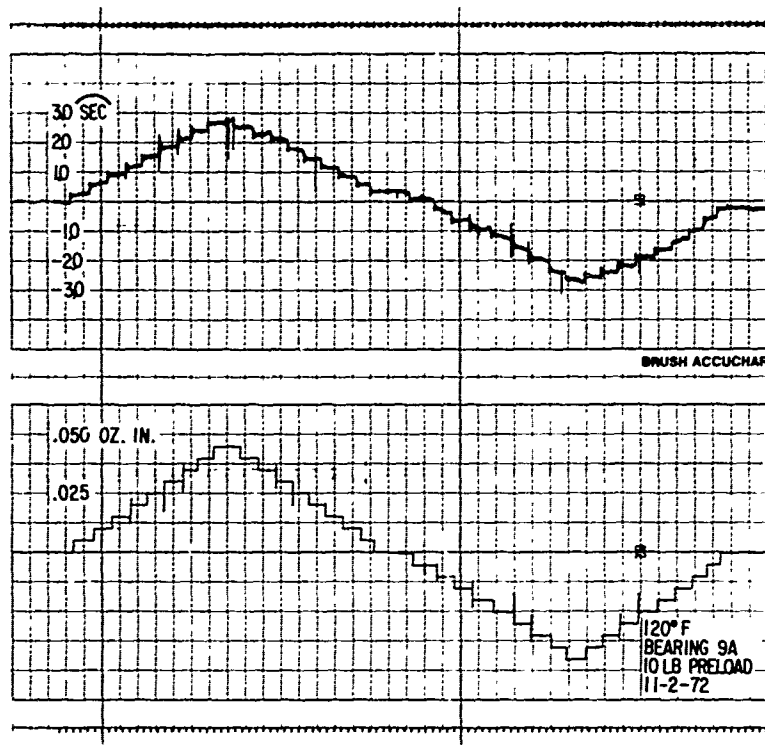


Figure 7 Spring Effect Data

difference between the expected and measured starting friction levels are test techniques and fixture sensitivity. Previous test techniques at BBRC called for an increase in the torque level until the bearing could be seen to move. The rate at which the bearing moved when breakaway occurred in our tests was well below that visually detectable, so we would have undoubtedly had a higher torque level if we had used visual motion indication. In the design of our test fixture we were careful to avoid components that had residual torques themselves. Many test set-ups we reviewed had starting torque associated with the fixture which would be well in excess of 0.05 oz.in. An example of this is a permanent magnet dc motor, most of which have hysteresis or residual torque in the range of 0.1 to 1.0 oz.in.

The third, and possibly most important result found, was the lack of a starting torque peak above the torque level required in order to run at slow speed. Torque-speed relationships such as shown in Figure 8 have been accepted as realistic on many previous designs. Both curves show starting or very low speed friction larger than the low speed running friction, and an increasing viscous friction thereafter as the speed increases. Whether a large torque must be supplied to get any motion (8-a) or whether the torque at some slow speed is higher than at a

higher speed (8-b) was not a known parameter, but that some peak occurred was generally accepted. The tests run on all 3 bearing sizes and with both wet and dry lubricant do not show such a peak. When breakaway torque was applied, the bearings always reacted as shown in Figures 6 and 7. They started moving very slowly and after starting did not move faster unless more torque was applied. In the running torque tests the type of variation shown in Figure 8-b did not occur. Over a speed range of 0.001 to 1.0 degrees per second, the torque always increased as the speed increased. Two possible reasons suggested for the difference between the previously accepted models and the test results are those given above.

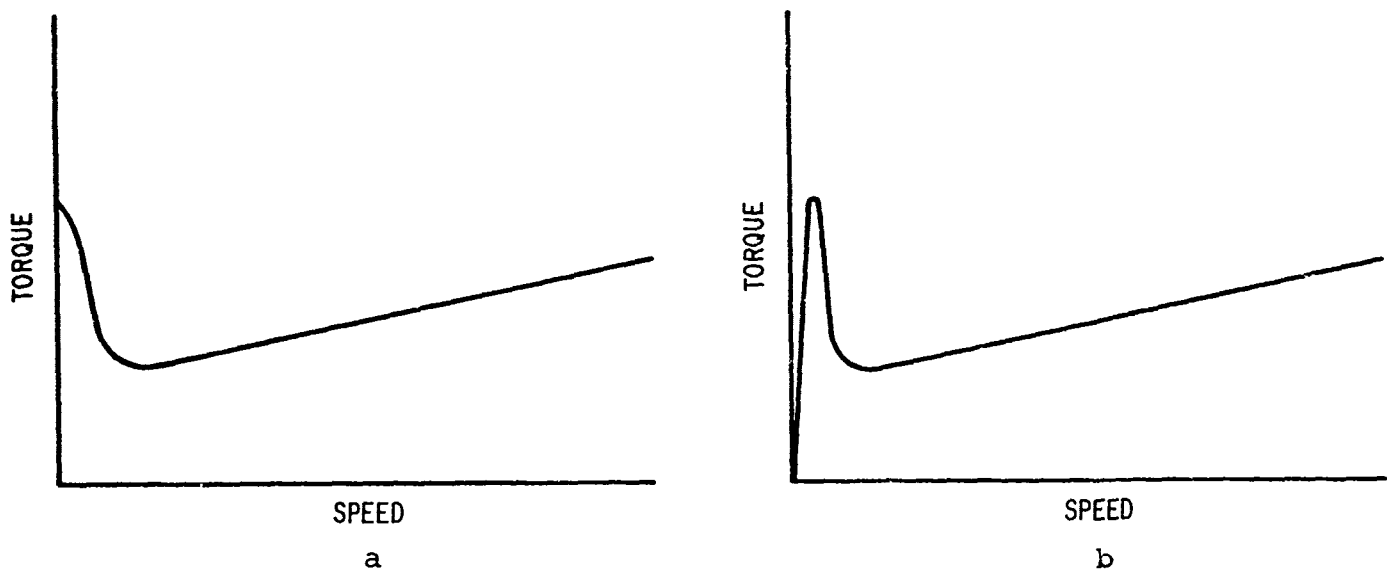


Figure 8 Speed-Torque Models

The running friction test results were approximately as expected, with none that were startling or highly unusual. The magnitude of the friction was smaller than previously calculated on the two larger bearings, but the speeds are enough lower than those in the calculated cases that the differences are not unreasonable. Comparisons for each bearing are drawn in the individual bearing reviews below. The running torque was not found to be a constant, but varied by as much as 50-75% as the bearing turned. This is seen as due to the slow speeds of the test. At high speeds, the bearings make many complete revolutions (and the balls still more) during a short test period. The ball frictions are repeated and averaged out so that to most instrumentation they appear as a constant with superimposed noise. At the slow speeds of our tests, the bearings moved so slowly that the averaging effects did not dominate and the torque variations were clearly evident. The torque variations appeared random, but statistical analysis

of the raw data was not within the scope of the program, so was not attempted.

The slow speeds also led to a difficulty in data taking. Since the running friction varied, we recorded and plotted only the peak torque during a run. We could not, however, make each run for a complete bearing revolution because the slow bearing speeds made the time required prohibitive. For example, Table I shows 163 runs which were made at each of four speeds (1.0, 0.1, 0.01, and 0.001 deg/sec.). A single bearing revolution at 0.001 degree/second would require 100 hours, so obviously each bearing was exercised for less than 360 degrees. Since we plotted the peak measured torque, but did not go a full revolution, there is a chance that the torque would have gone higher at a different rotation angle.

The friction increased with preload in an approximately linear fashion as shown in Figures 9, 10, and 11. This is predictable according to equations published by bearing manufacturers. In Figure 11, the dry lubrication figures are not the same as those with liquid lubricant, but neither are they consistent from bearing to bearing with dry lubricant. This is seen as peculiar to the combination of this bearing and dry Vac Kote, but not in disagreement with the friction increase with preload. The characteristics are discussed more fully under the review of the SR156 bearing below.

At the operating test speeds, the relationship of bearing friction torque to speed was not entirely predictable. An increase of torque with speed is normally expected, i.e., a viscous component of the total friction, but at extremely slow speeds the bearing manufacturers equations do not predict this. For example, the SKF Industries equation for bearing torque is:

$$M = 0.083 f_1 P_B d_M + 1.183 \times 10^{-6} f_o (\mu N)^{2/3} d_M^3$$

Where M = friction torque in foot pounds

f_1, f_o, P_B are constants which depend on bearing geometry and bearing loads.

d_M = the bearing pitch diameter

μ = the lubricant kinematic viscosity in centistokes

N = the speed in r.p.m.

Under conditions where parameters other than speed are constant, the graph of speed versus torque is thus predicted to be an $N^{2/3}$ relationship, which is shown in figure 12. However, the SKF engineering data states that when the product (μN) drops below 2000 it is kept at that constant. The viscosity of liquid Vac Kote is approximately 125 centistokes, which says that for Vac Kote the constant range starts at 16 rpm. Below this speed the

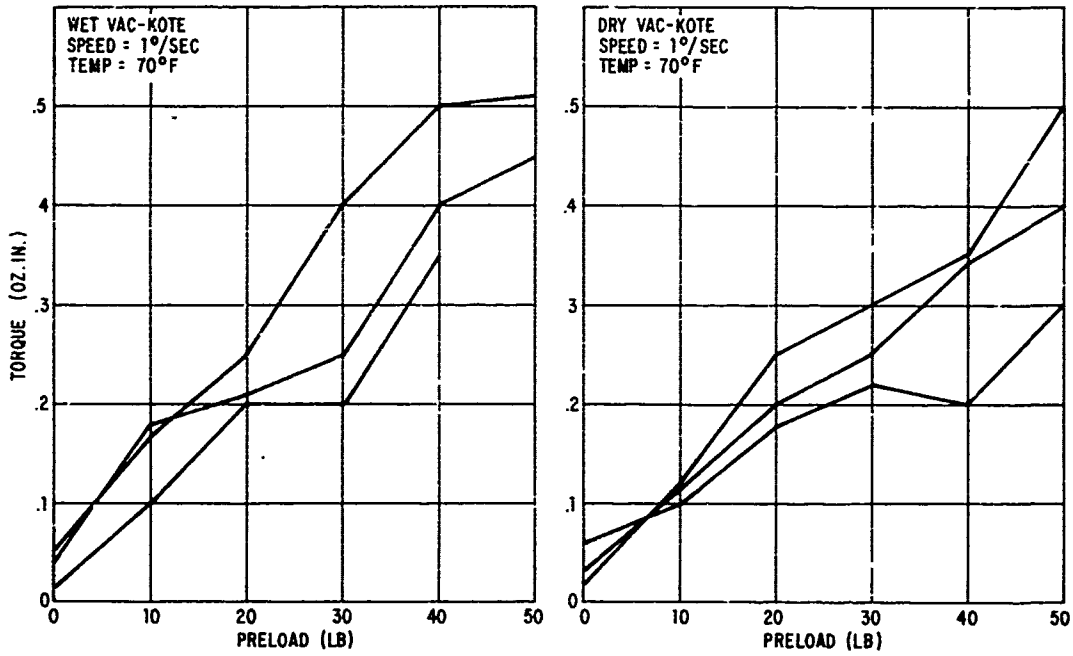


Figure 9 Torque Vs. Preload for Bearing 33267

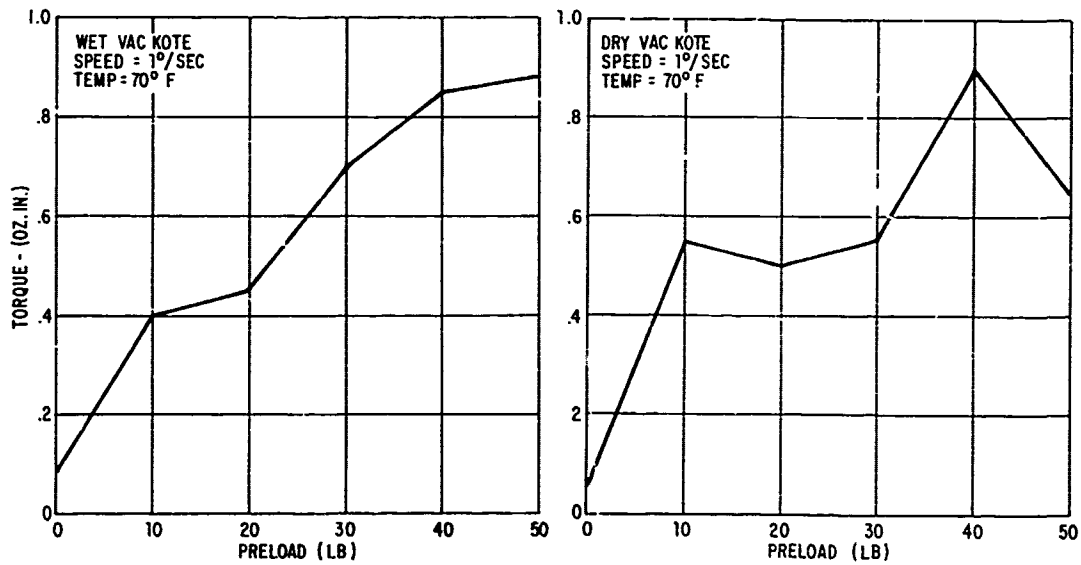


Figure 10 Torque Vs. Preload for Bearing 36563

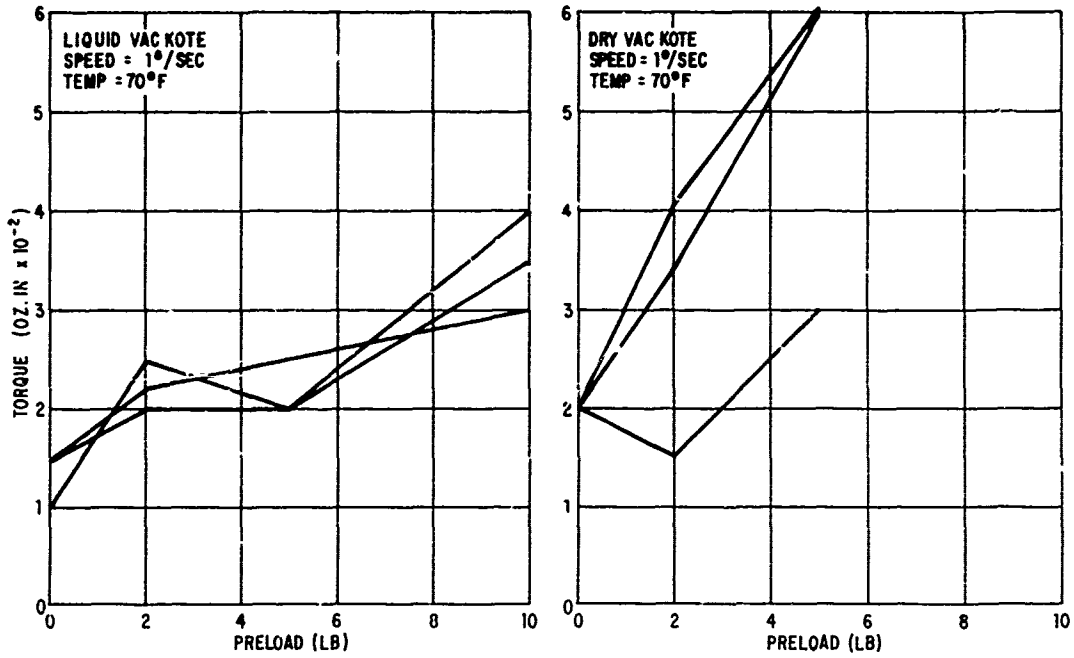


Figure 11 Torque Vs. Preload for SR156

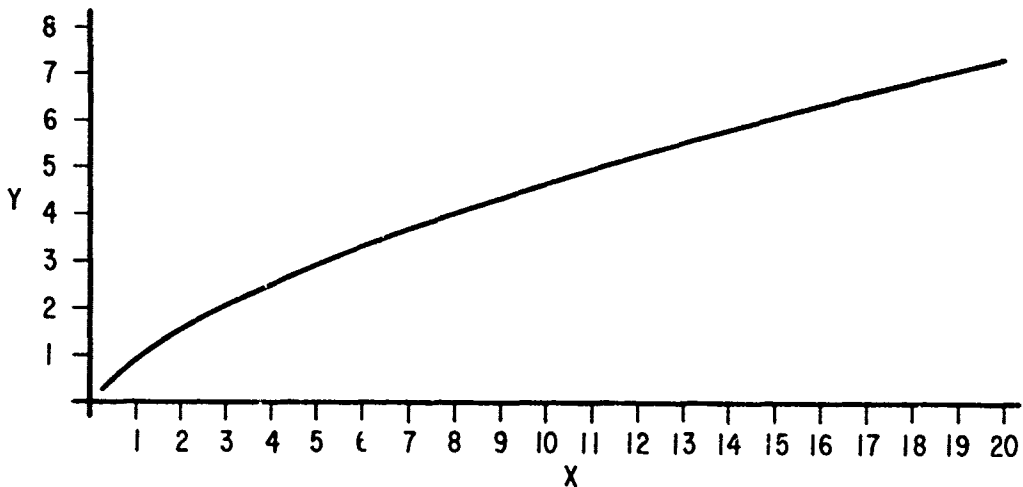


Figure 12 $Y = X^{2/3}$

predicted form of the curve is a constant. We did not find the constant to be the case. Rather, the exponential curves (X^a where a is less than 1) continue to be present. Figures 13, 14, and 15 are representative curves for each size of bearing and show the exponential relationship. It is conjectured that the type of tests which would show the exponential speed torque relationship at low as well as high speeds have not been previously done, or done with less sensitive equipment. The viscosity of dry Vac Kote is not listed because the dry lubricant is a solid and not viscous. The fact that the exponential curve was found on both liquid and dry Vac Koted bearings suggests that the speed-torque characteristic is a function of the bearings rather than the lubricants.

Figures 12 through 15 are plotted linearly. In the tests, the speed range covered four orders of magnitude (10^4) so the data was plotted on semi-log paper. The curve of $y = x^{2/3}$ is plotted piece-wise linear on semi-log paper in Figure 16, as a reference to the predicted form of the speed-torque relationship.

Plots of this form predominate the individual bearing reviews to follow.

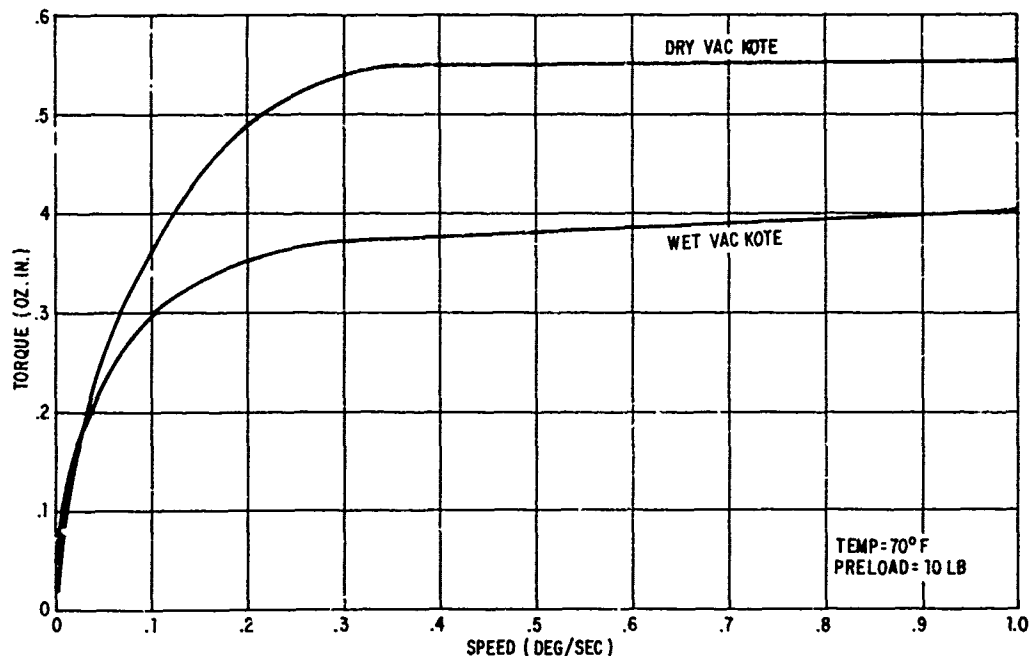


Figure 13 Speed-Torque of Bearing 36563

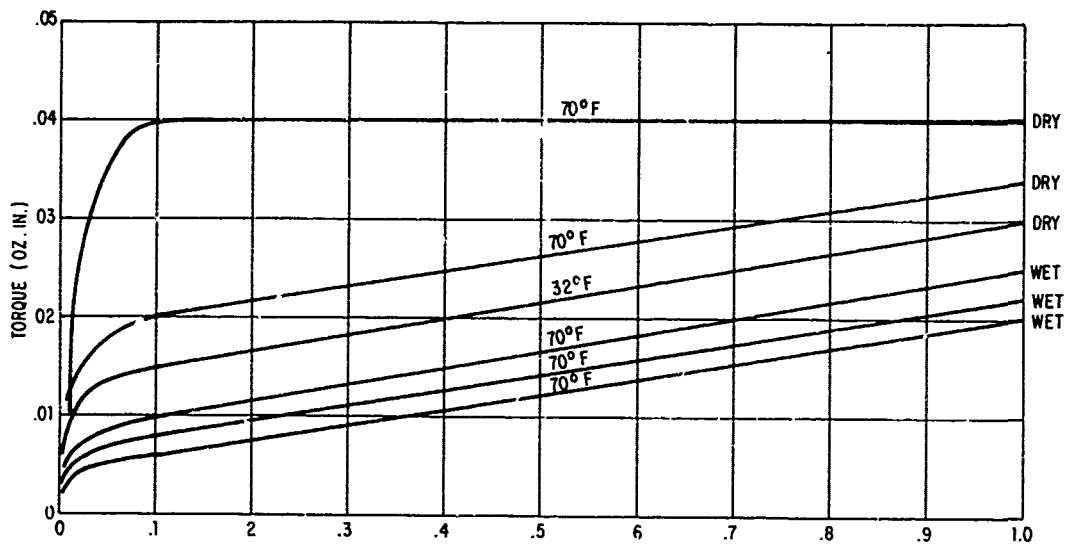


Figure 14 Speed-Torque of Bearing SR156

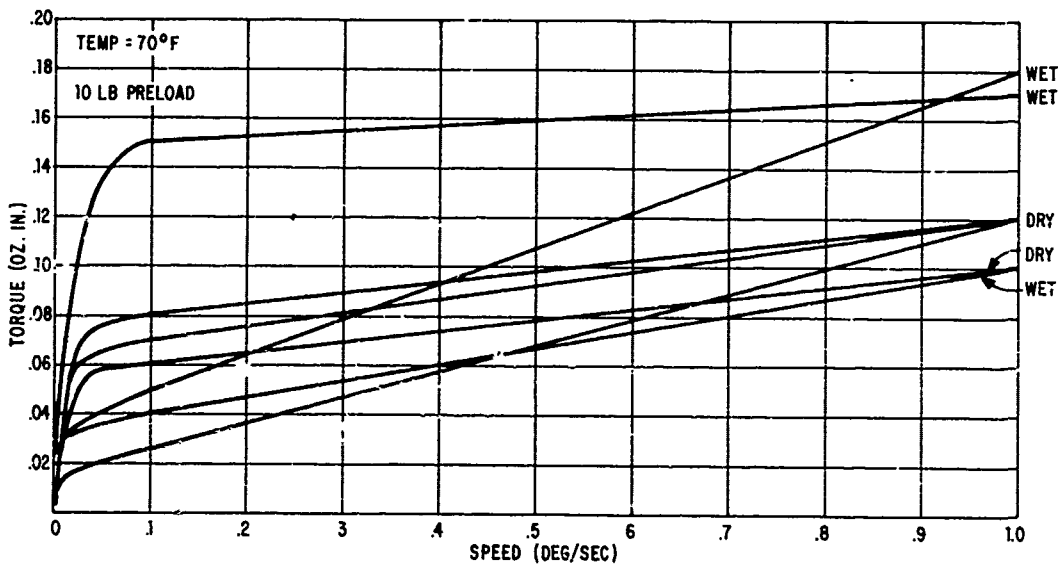


Figure 15 Speed-Torque of Bearing 33267

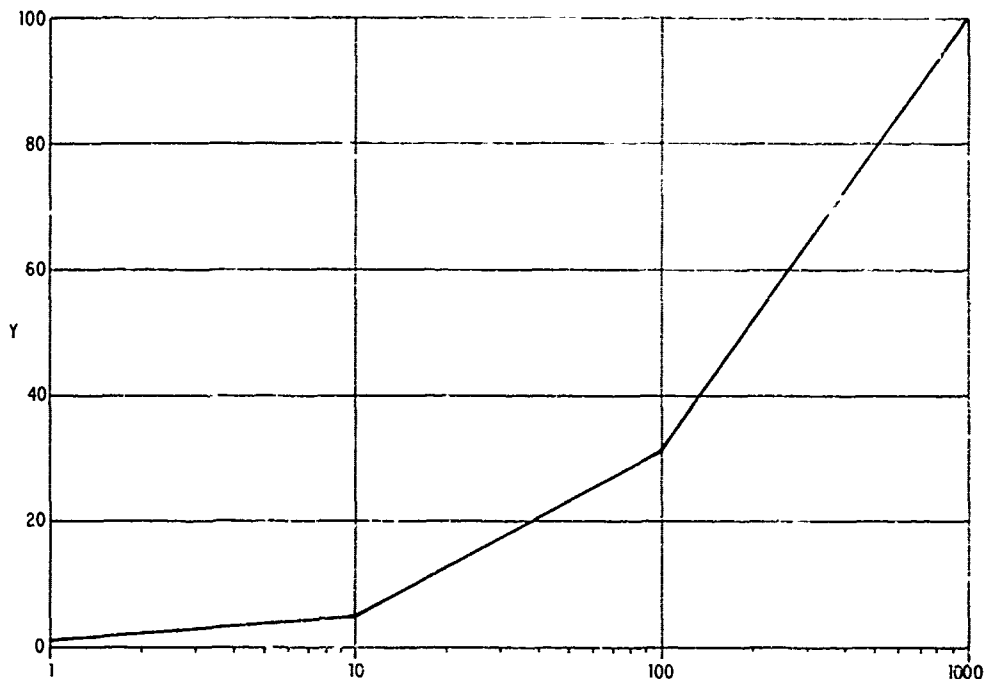


Figure 16 $Y = X^{2/3}$ Piece-wise Linear

4.4.2 Bearing 33267

Four bearings were tested with liquid lubricant (9A and B, 13A and B) and four with dry (12A and B, 14A and B). Ambient temperature speed-torque plots for the liquid lubricated set are given in Figures 17 through 20 and for the dry set in Figures 21 through 24. The plots show that the torque increases with speed and with preload as previously discussed and that the general shape of the curves conforms to that of Figure 16. The running torque for the ambient temperature tests varied from near zero to 0.2 oz.in. at 0.001 degree/second and from 0.017 to 0.5 oz.in. at 1.0 degree/second, as the preloads were varied from zero to 50 pounds. Comparison of the liquid and dry lubricant plots shows little discernible difference in the torque performance on either. This is reasonable, since viscosity is not a significant factor at our test speeds, and other than the lubrication systems the bearings were identical.

The results of our tests were compared to the results of the Barden tests reviewed in Section II. At 10 and 20 pounds preload Barden measured 0.24 and 0.42 oz.in. of torque respectively. This compares to our average figures of 0.15 and 0.22 oz.in. at the same preloads. However, the equation for bearing torque shows that torque is proportional to the pitch diameter. Since the pitch diameter of the Barden bearing was 1.8 inches and that of the 33267 bearing 1.4 inches, a corrective factor to account for

this brings the measured torques to approximately the same values. Since the respective bearing geometries and the test equipment were not compared there could still be some variation, but the results do generally agree.

For the application on OSO the 33267 bearing torque averaged .65 oz.in. during test, compared to a calculated torque of 0.6 oz.in. The tests and calculations were both at 30 rpm. We made further calculations for the torque at our test speeds. At 10 - 20 pounds preload the calculated torque was in the 0.15 - 0.25 oz.in. range which corresponds to the 0.15 - 0.22 average we measured.

The temperature tests were run at three preload values on one bearing of each set of four, while the remaining three bearings were run at the one most likely preload value for space application. Figures 25 through 30 are the graphs of the liquid lubricated bearings. Serial number 13A was preloaded at 0, 10, and 30 pounds while serial numbers 9A, 9B, and 13B were preloaded at 10 pounds. Figures 31 through 36 are the graphs of the dry lubricated bearings. Serial number 12A was preloaded at 0, 10, and 30 pounds while serial numbers 12B, 14A, and 14B were preloaded at 10 pounds. No significant differences between the room temperatures and extended temperature results were expected or found. As predicted, on the bearings lubricated with liquid Vac Kote, the run at 0°F exhibited higher torque because of the stiffness of the lubricant. The test runs with dry Vac Kote do not show a correlation between friction torque and temperature. We believe that the torque variations were more a function of the bearing geometry than of temperature.

One phenomenon which was found in previous tests on a number of bearings, including OSO azimuth drive bearings, can be detected by an examination of Figures 25, 26, and 27. At temperatures near or below 0°F a decrease of friction torque accompanies an increase in preload over the normal preload range of the bearings. As the preload is increased further the friction torque again increases, giving a dip at the low end of a preload vs. torque curve. This is explained by the fact that the pour point of liquid Vac Kote is 15°F and at temperatures below this the lubricant becomes very viscous and must be channeled out of the path of the rolling balls. This phenomenon does not take place with dry lubricated bearings at low temperatures because no viscosity problem exists. Figures 31, 32, and 33 show that at 0°F the running friction does increase with preload on dry lubricated bearings.

The starting tests showed that starting torque values were extremely low and were not above the values found in the running torque data of Figures 17 through 36. Using the continuous motion definition of breakaway, the data was examined to produce Figure 37. This indicates that the starting friction is approximately linear with preload and is much lower than previously thought.

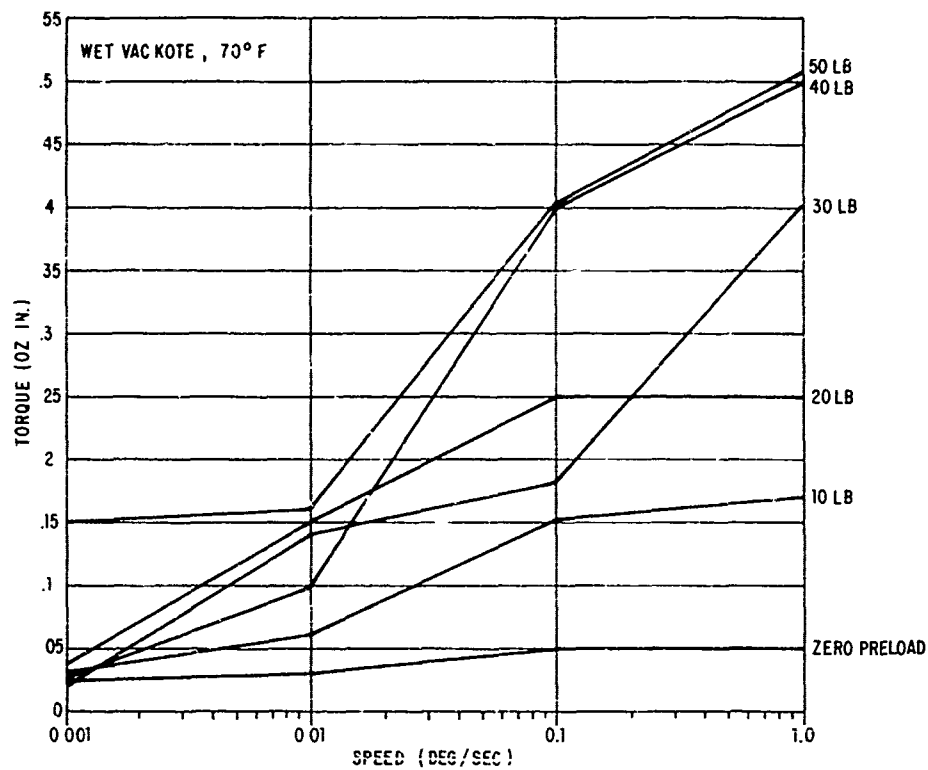


Figure 17 Bearing 9A Speed-Torque

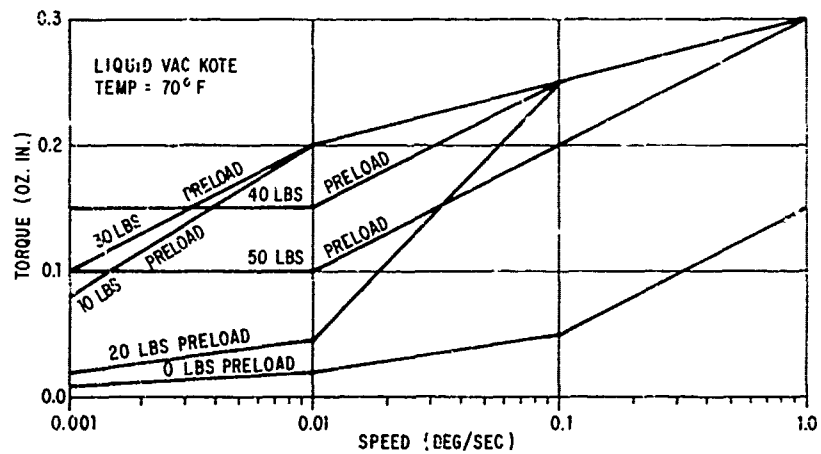


Figure 18 Bearing 9B Speed-Torque

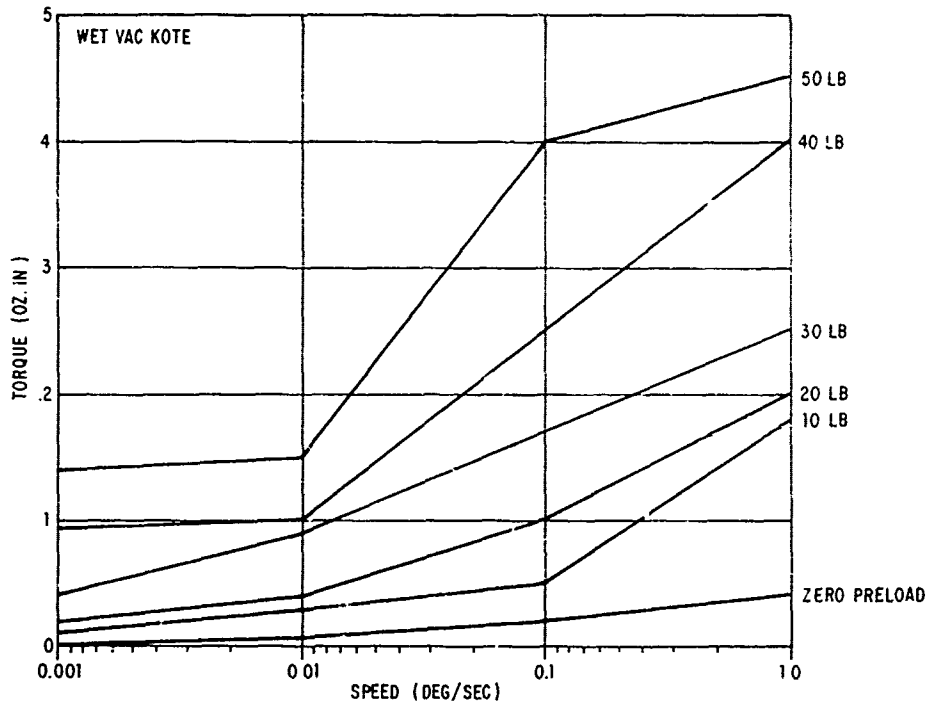


Figure 19 Bearing 13A Speed-Torque

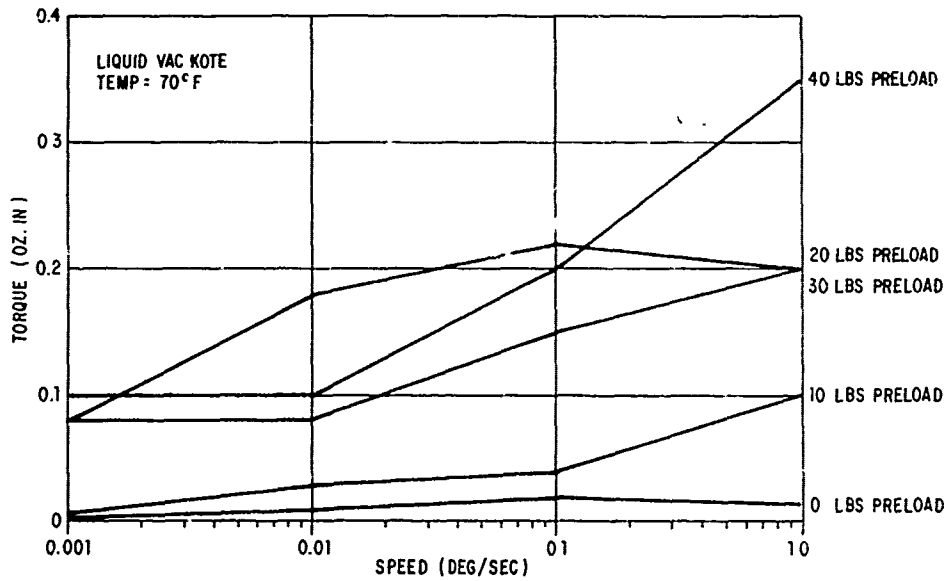


Figure 20 Bearing 13B Speed-Torque

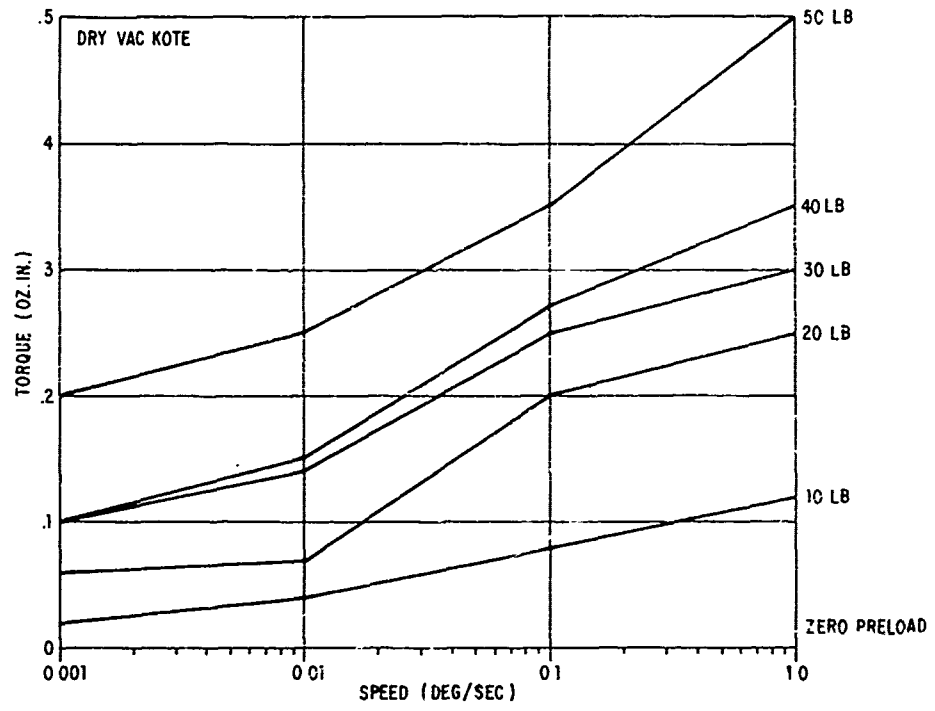


Figure 21 Bearing 12A Speed-Torque

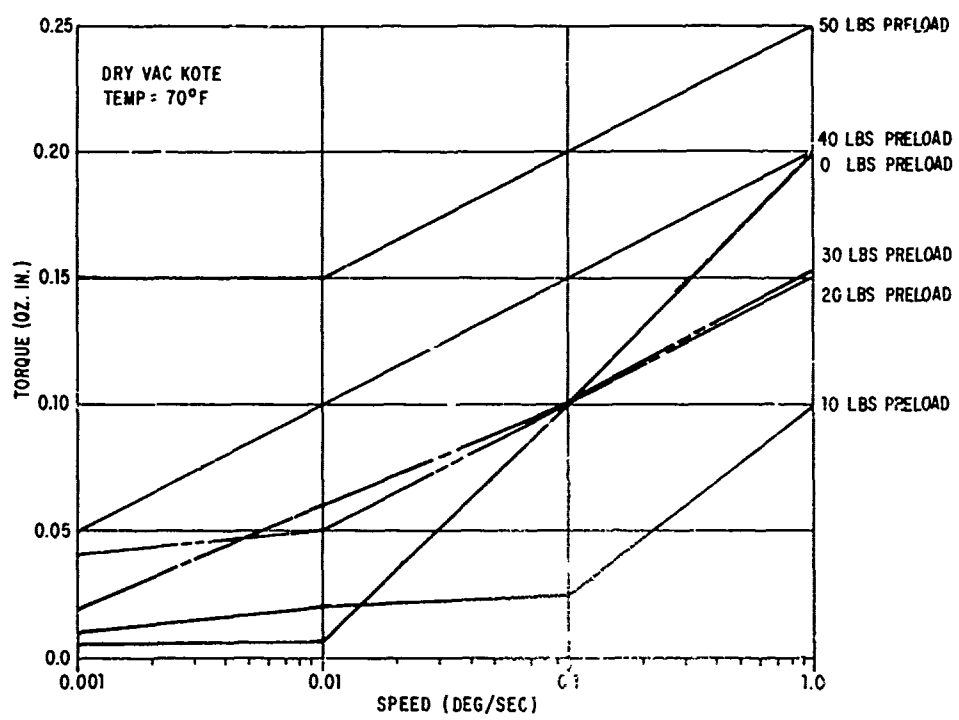


Figure 22 Bearing 12B Speed-Torque

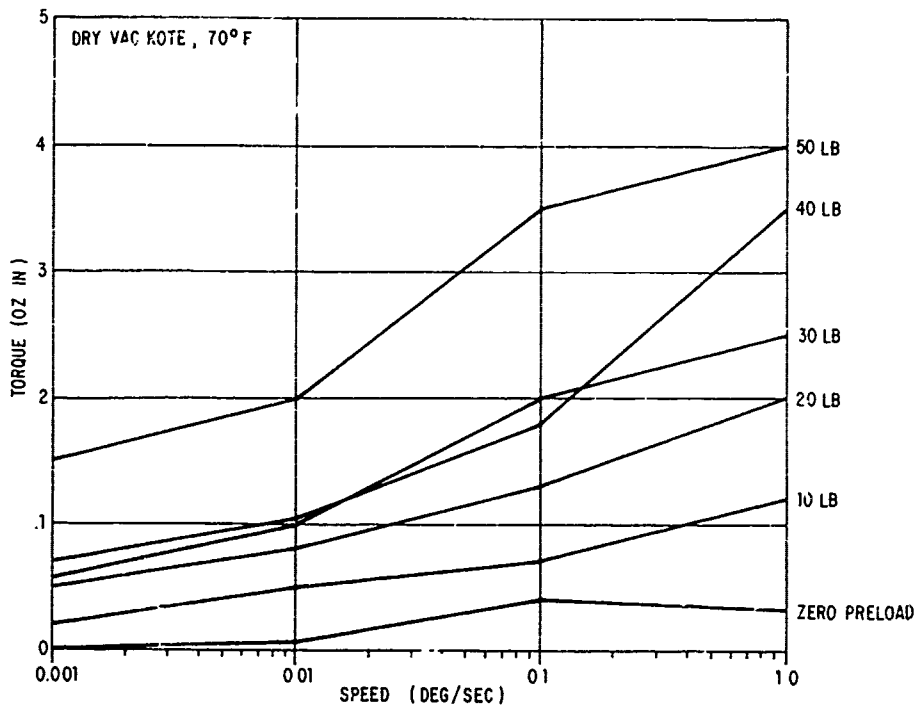


Figure 23 Bearing 14A Speed-Torque

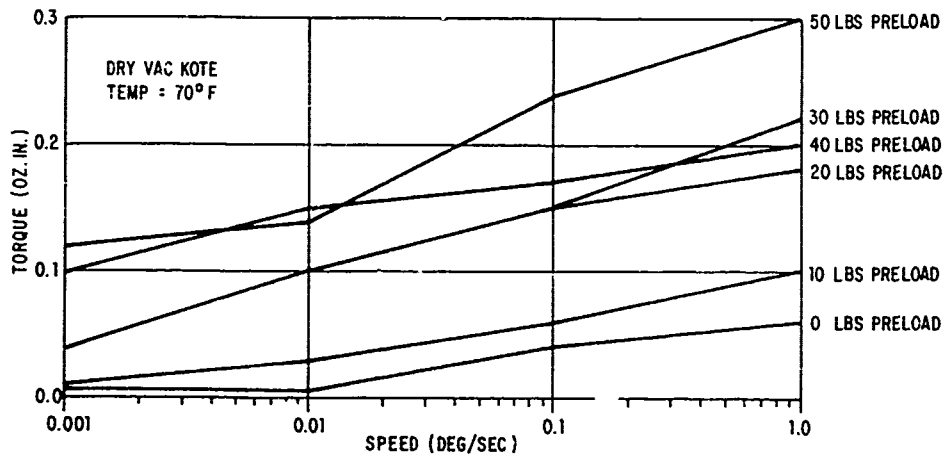


Figure 24 Bearing 14B Speed-Torque

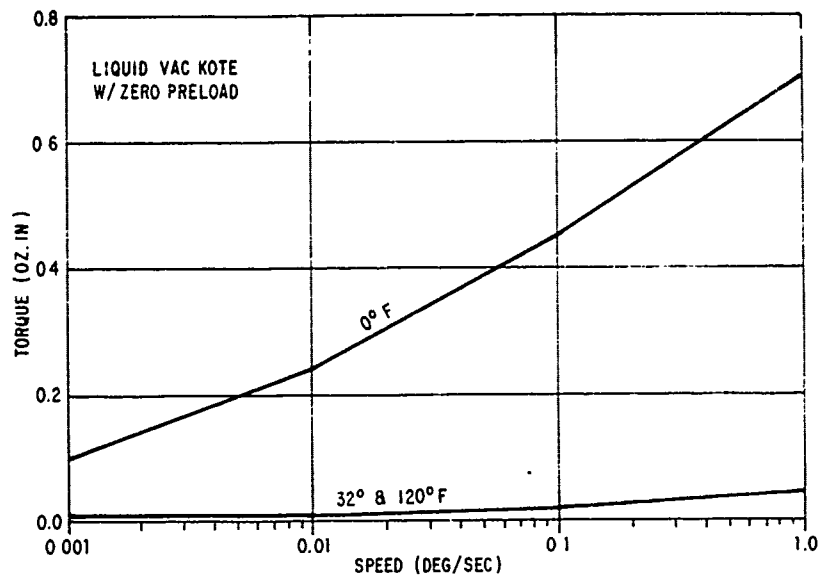


Figure 25 Bearing 13A Temp. Test at Zero Preload

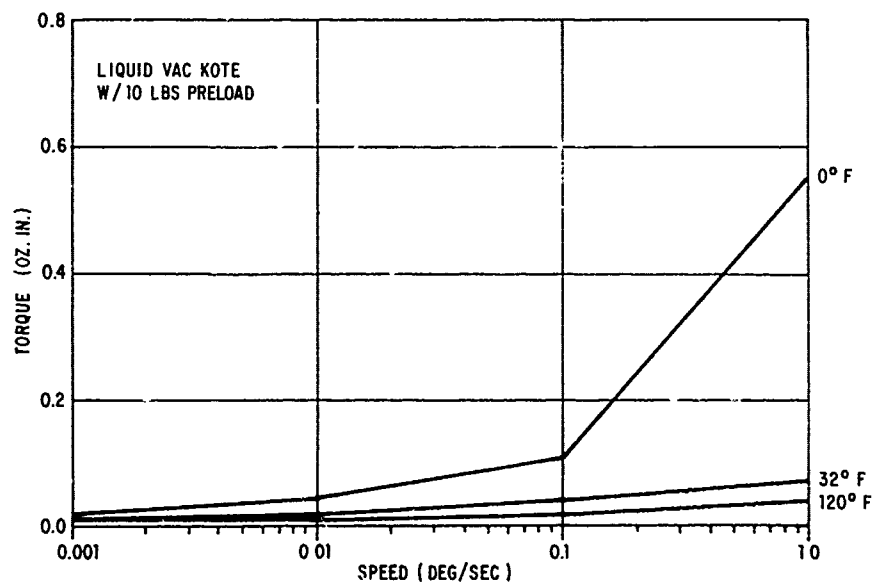


Figure 26 Bearing 13A Temp. Test at 10 Lb. Preload

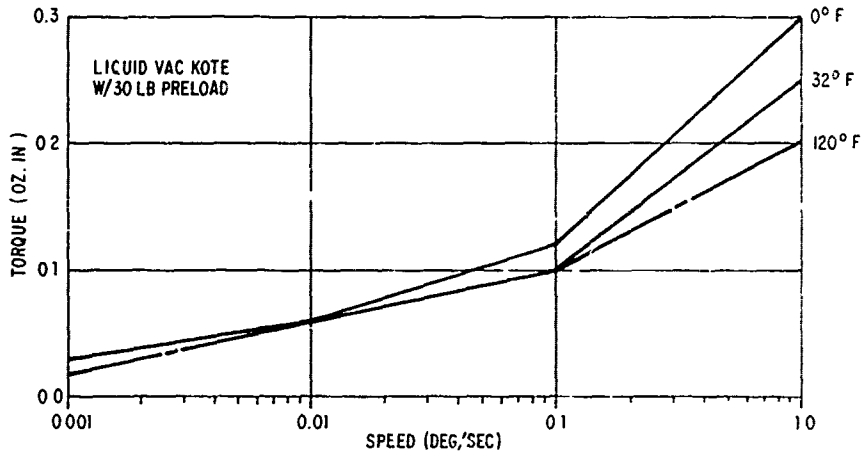


Figure 27 Bearing 13A Temp. Test at 30 Lb. Preload

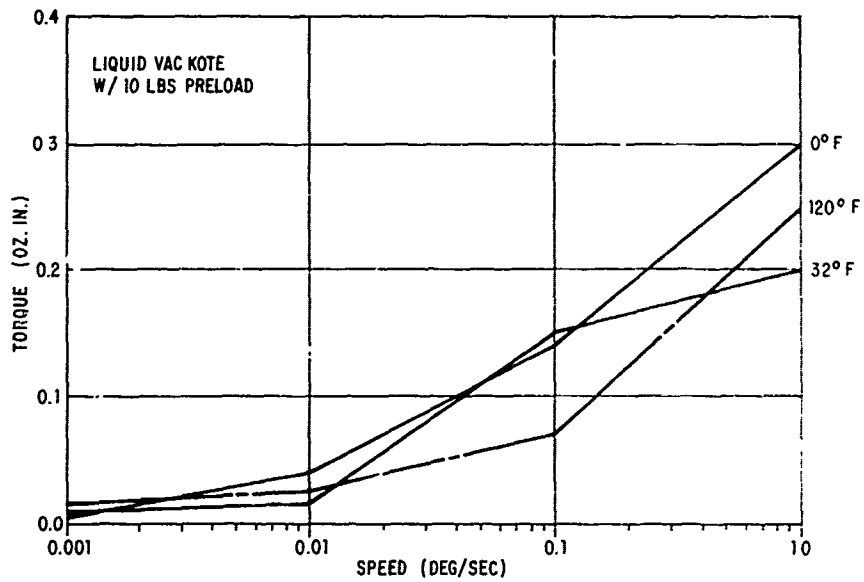


Figure 28 Bearing 9A Temperature Test

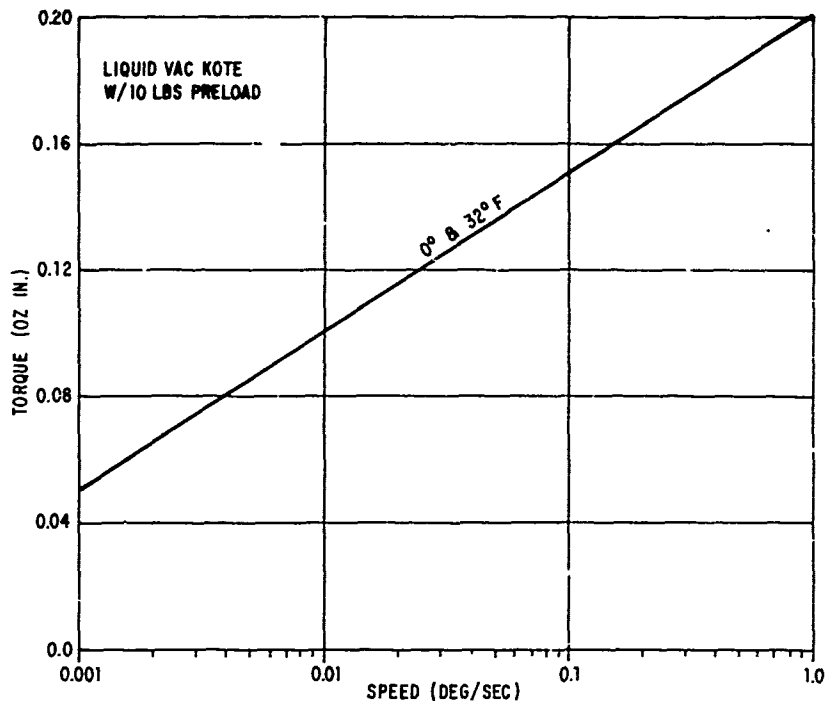


Figure 29 Bearing 9B Temperature Test

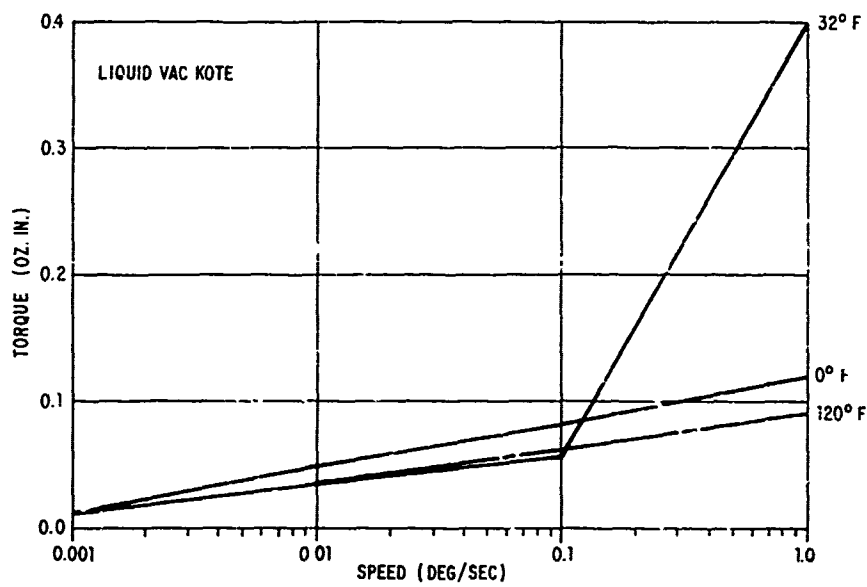


Figure 30 Bearing 13B Temperature Test at 10 Lb. Preload

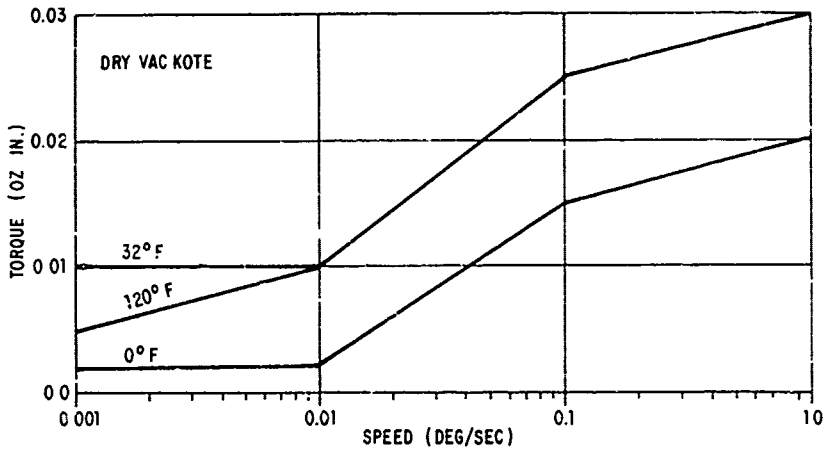


Figure 31 Bearing A Temp. Test at Zero Preload

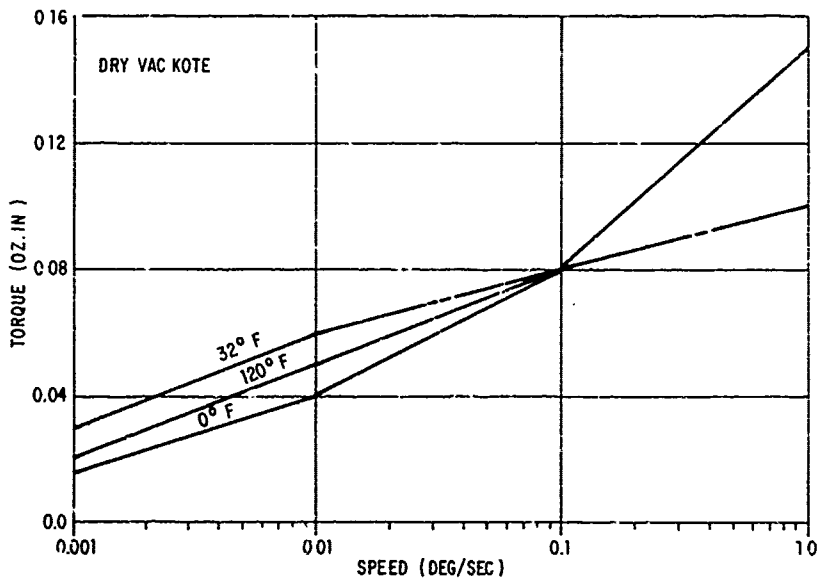


Figure 32 Bearing 12A Temp. Test at 10 Lb. Preload

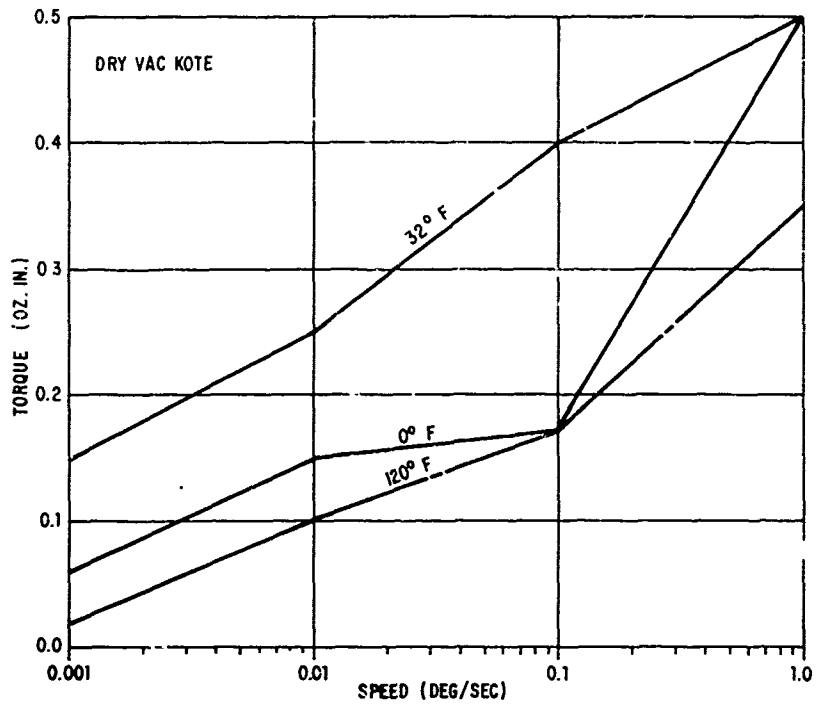


Figure 33 Bearing 12A Temp. Test at 30 Lb. Preload

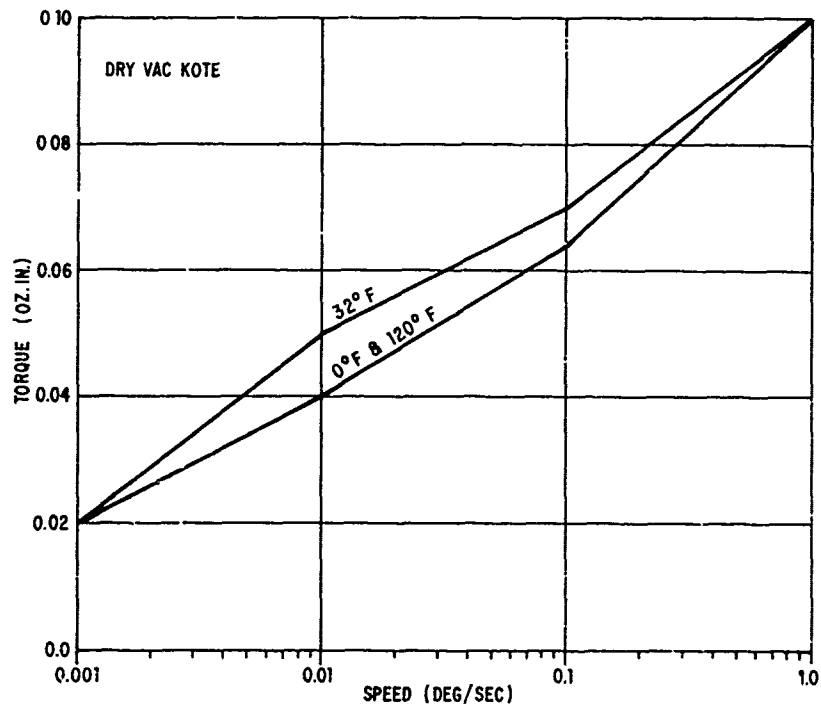


Figure 34 Bearing 12B Temp. Test at 10 Lbs. Preload

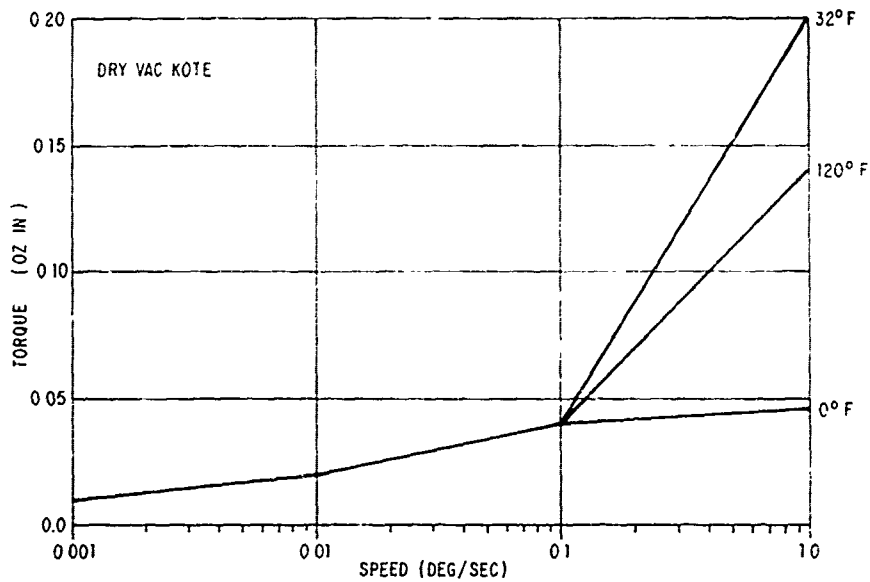


Figure 35 Bearing 14A Temp. Test at 10 Lbs. Preload

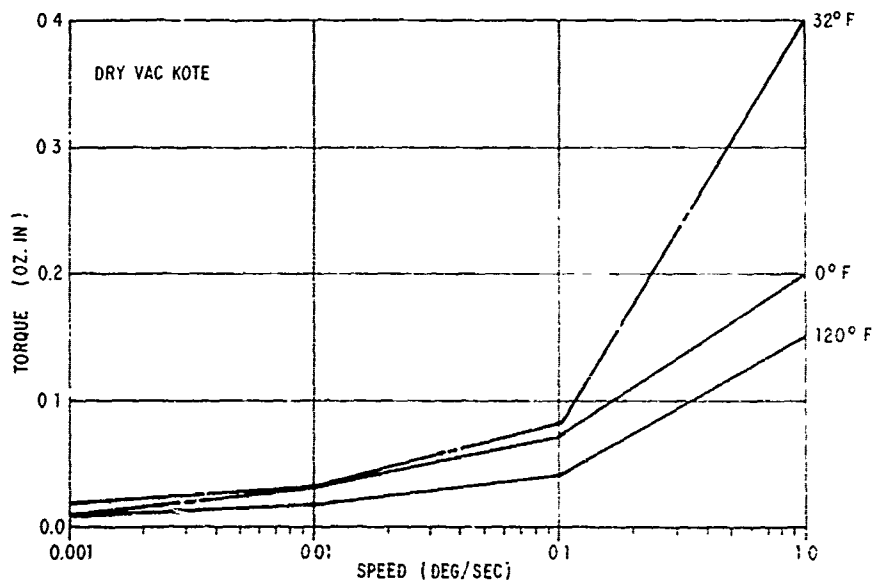


Figure 36 Bearing 14B Temp. Test at 10 Lbs. Preload

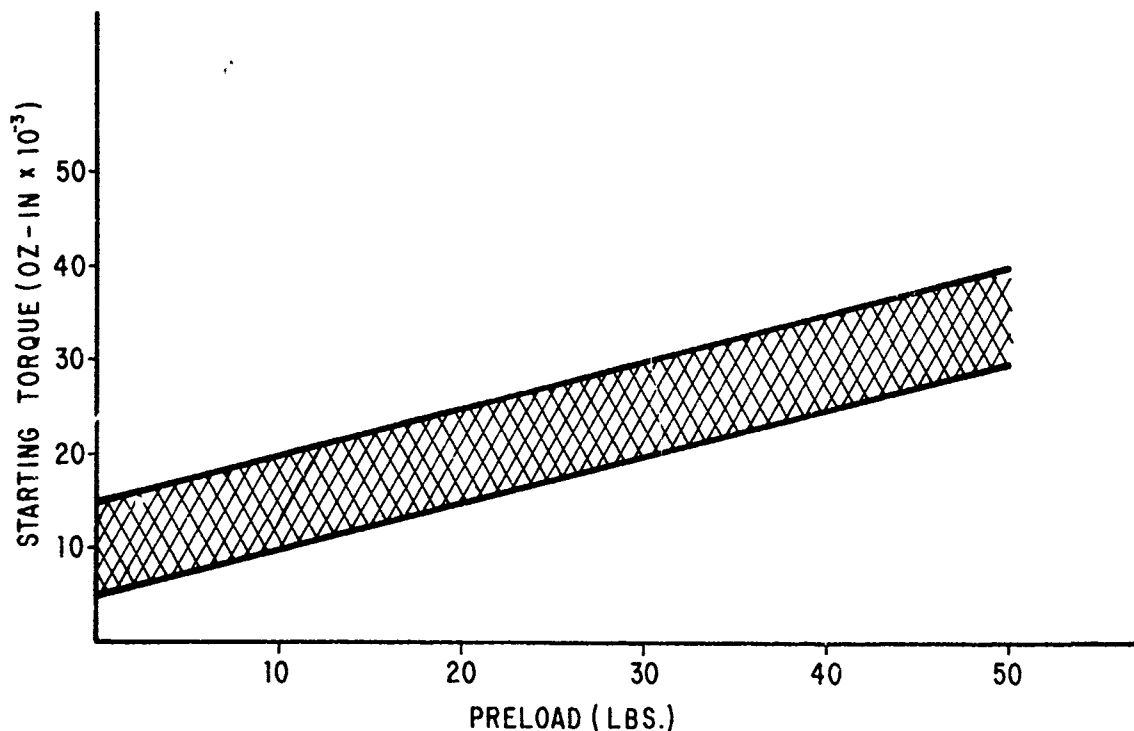


Figure 37 Breakaway Torque Vs. Preload

The starting torque requirement for this bearing was listed at 1.25 oz.in. and acceptance tests showed starting torques in the range of 0.5 oz.in. when preloaded to 10-20 pounds. The accuracy and sensitivity of the previous tests were obviously much less than those of our project 405B tests. No significant differences were detected between the room temperature starting test results and those at the high and low temperatures.

A number of representative plots of raw data are shown in Figures 38, 39, and 40. Both liquid and dry lubricant plots are shown for reference and comparison.

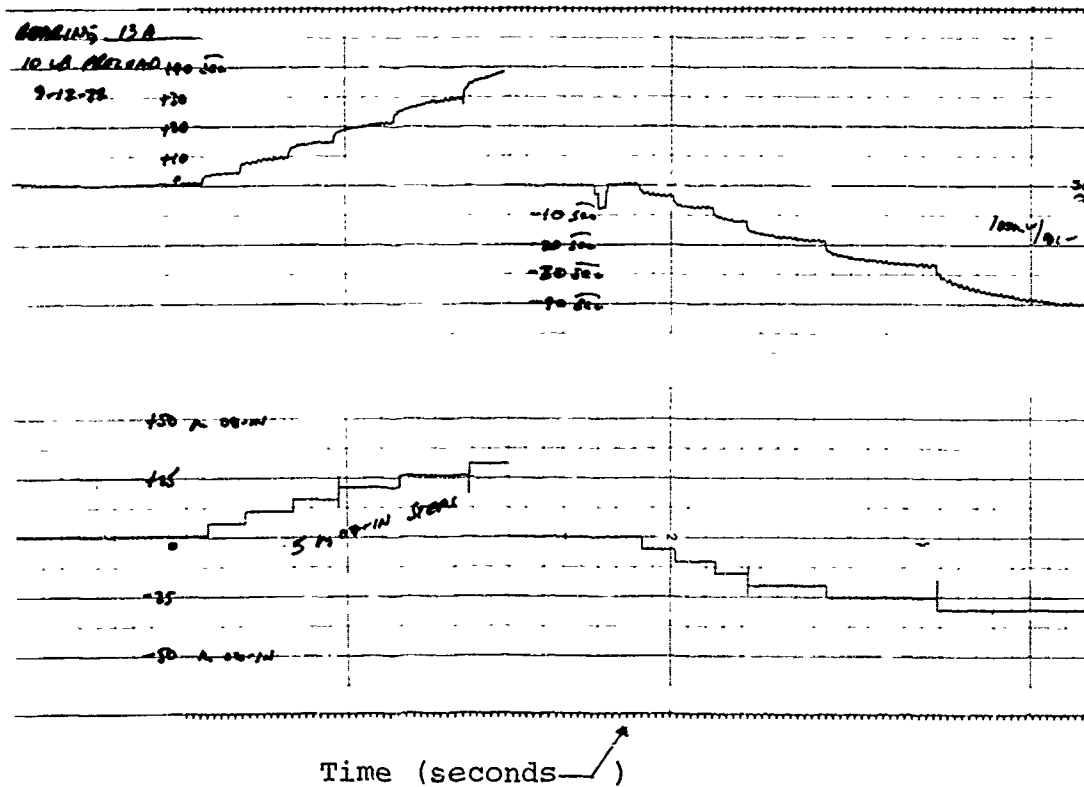
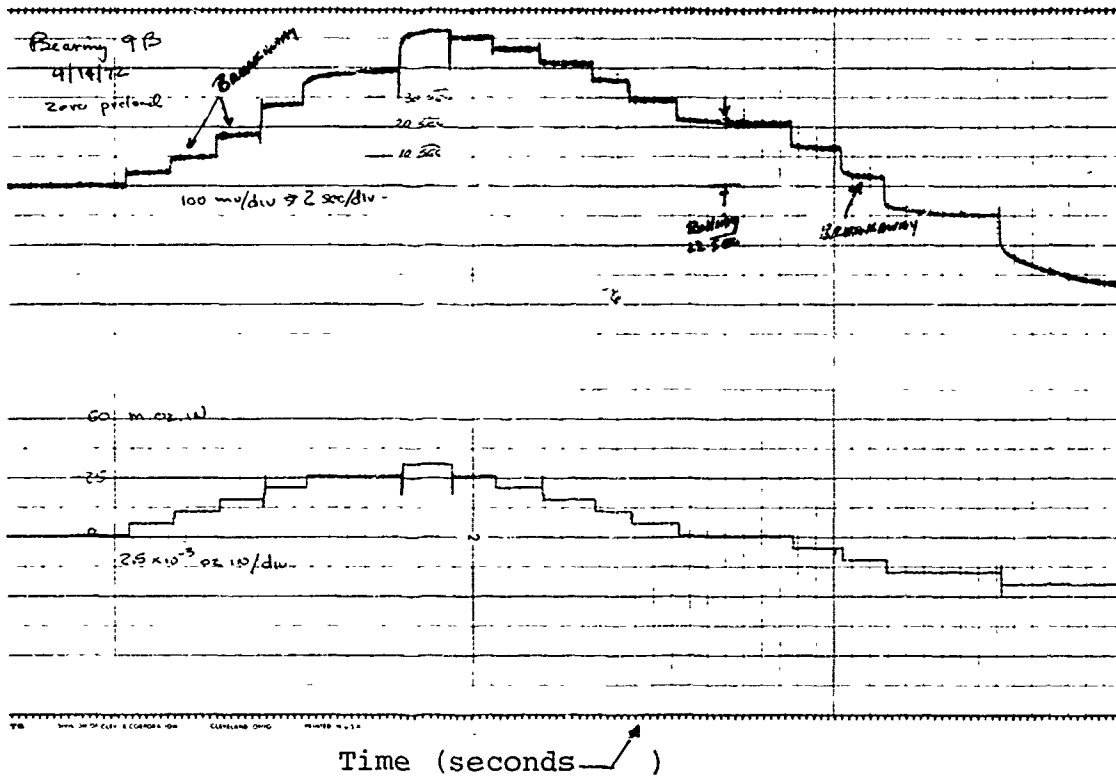


Figure 38 Brg. 33267 - Starting Data - 0 & 10 Lb. Preload

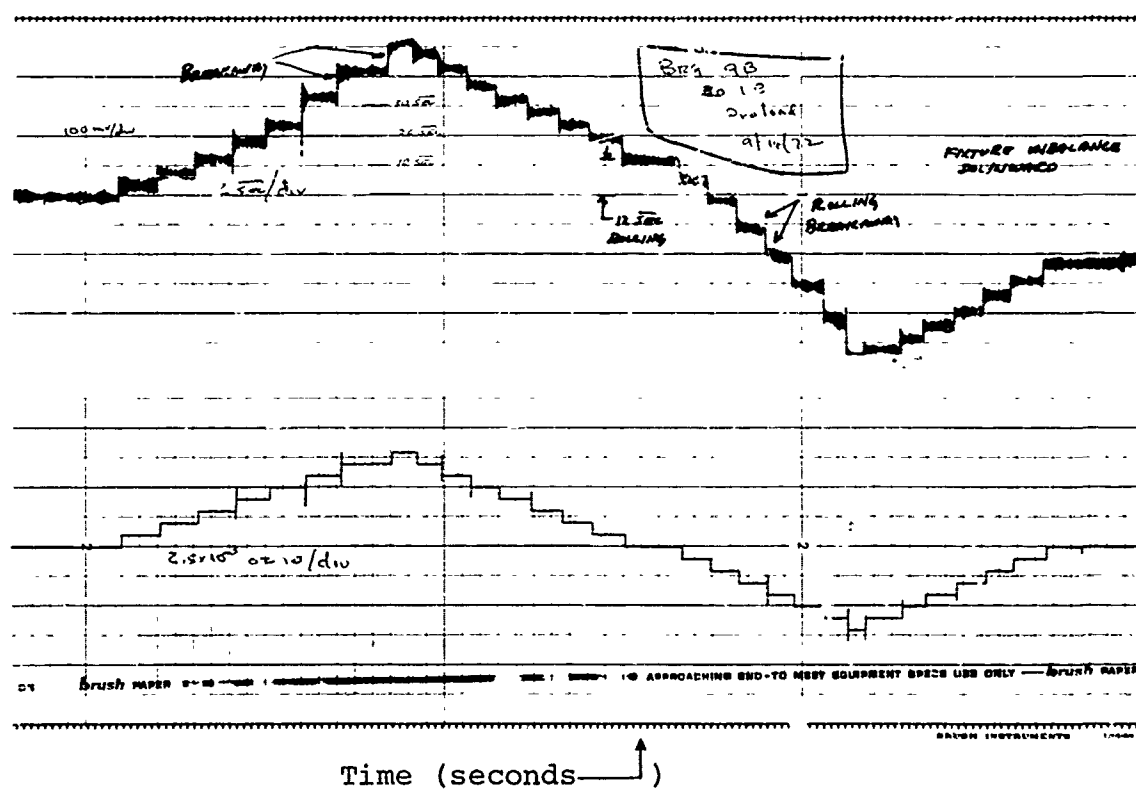
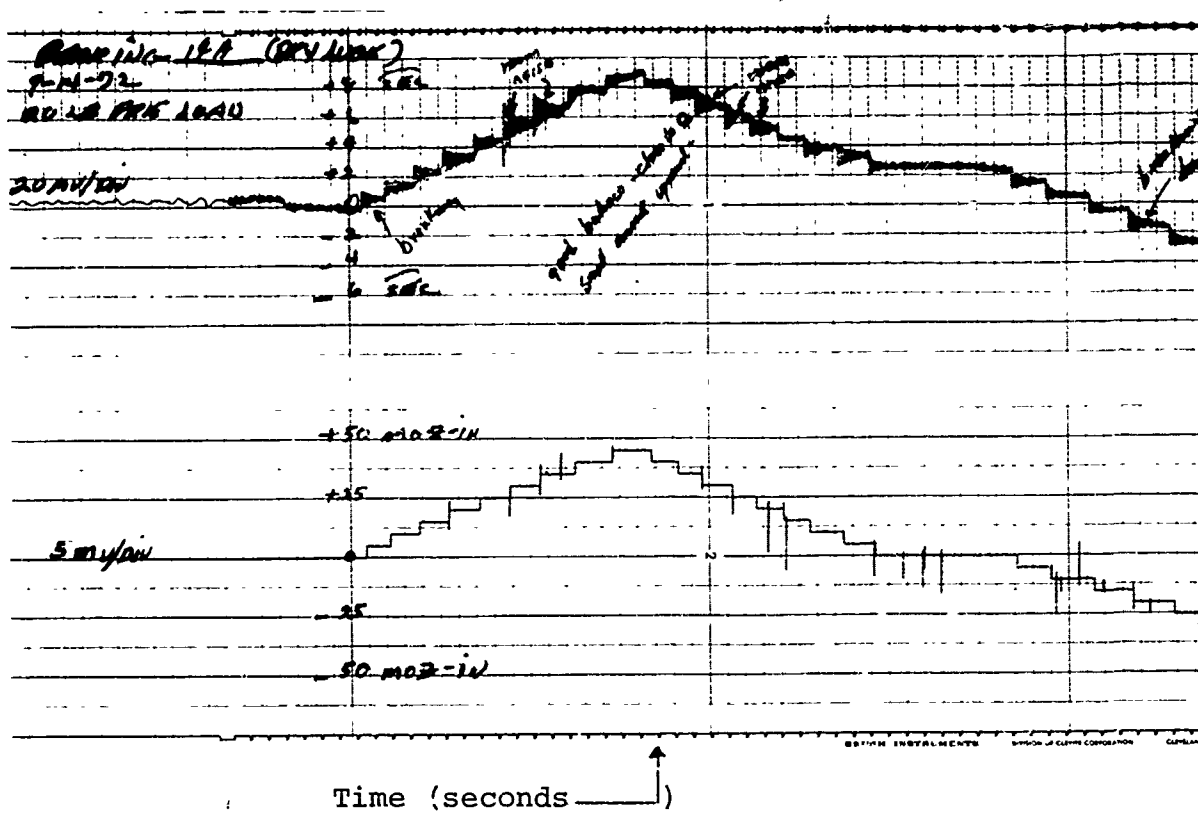


Figure 39 Brg. 33267 - Starting Data - 20 & 30 Lb. Preload

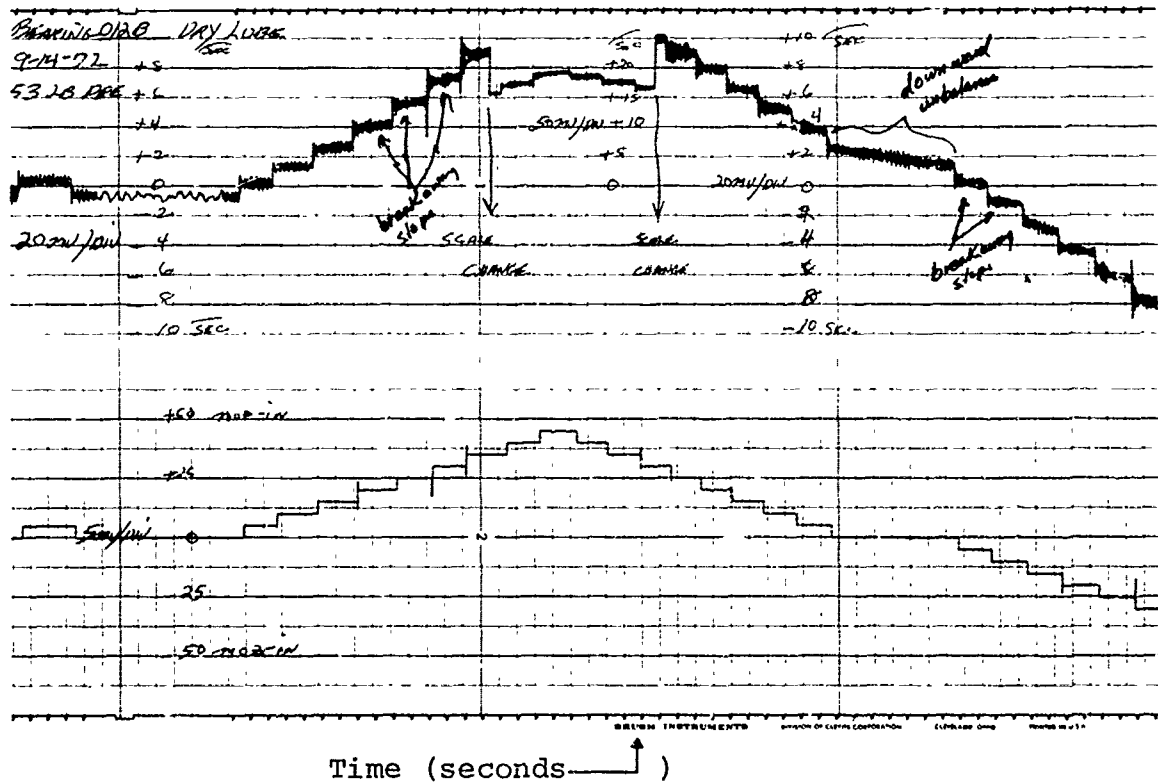
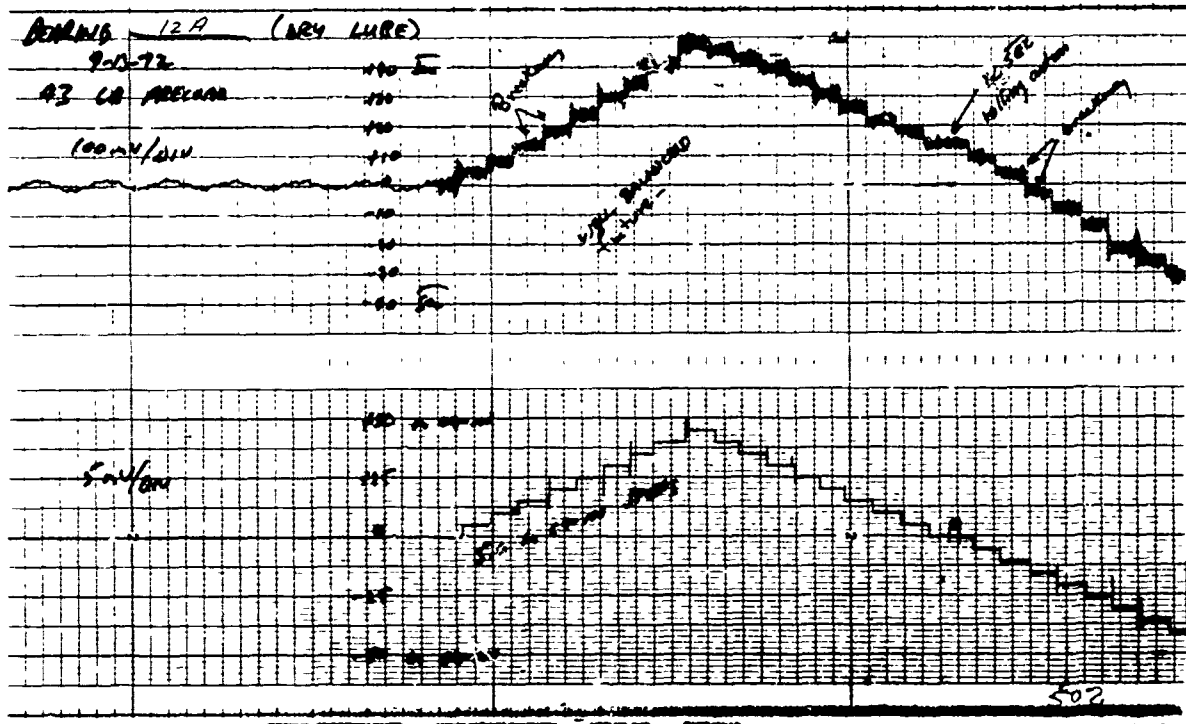


Figure 40 Brg. 33267 - Starting Data - 43 & 53 Lb. Preload

4.4.3 Bearing 36563

Two bearings, originally members of a duplex pair, were tested; one lubricated with liquid and one with dry Vac Kote. The graphs of the liquid lubricated bearing are given in Figures 41 through 44 and for the dry lubricated bearing in Figures 45 through 48. Each bearing was tested at room temperature with preloads of 0, 10, 20, 30, 40, and 50 pounds and at 0°F and 32°F with preloads of 0, 10, and 30 pounds.

As with other bearings tested, the running friction torque increased with speed and with preload. The maximum torques measured were .8 - .9 oz.in. at a speed of 1.0 degree/second and when preloaded at 40 - 50 pounds. The calculated torque values were 0.5 oz.in. when preloaded at 10 pounds and 2.0 oz.in. when preloaded at 40 pounds. This compares to average measured values of 0.41 oz.in. with 10 pounds preload and .87 oz.in. with 40 pound preload. Since our data did show a torque dependence on speed, we attribute the difference between measured and calculated values to the very low test speeds. The Nimbus pointing system on which these bearings were used runs very slowly on the output of a large gear train. The gear train assures that the drive has so much output torque that the bearing torque is negligible. Because of this, bearing torque tests were not performed as a part of the design program and torque data does not exist.

Early room temperature tests gave the results shown in Figures 41 and 45. Later, we repeated the room temperature tests, in addition to the low temperature tests, at preloads of 0, 10, and 30 pounds. Generally, the second series of tests gave lower torque values than the first series. There is no known reason for the difference, but it is possible that some fixture torques were present in the first tests that were not present in the later tests.

No significant difference is seen between the torque values of the liquid and dry lubricated bearing. As expected, on each test of the liquid lubricated bearing the highest friction was measured at 0°F and the results at 0 and 32°F were very close to each other. The same phenomenon of decreasing friction with increasing preload (at 0°F) that was found on the 33267 bearings was also found here. Figures 42, 43, and 44 show that the friction torque is highest at zero preload, dips at 10 pounds preload and is beginning to rise again with 30 pounds preload. No such correlation is found in the dry lubricated bearing.

The running torque of this bearing was compared to that of the 33267 (OSO) bearing. The peak torque was 0.5 oz.in. on the 33267 bearing compared to .9 oz.in. on the 36563 bearing. The ratio of the bearing pitch diameters is 1.83:1. When the lower torque figure is multiplied by this ratio the comparable torque is 0.915 oz.in. The bearing torque formula shown above has a coulomb

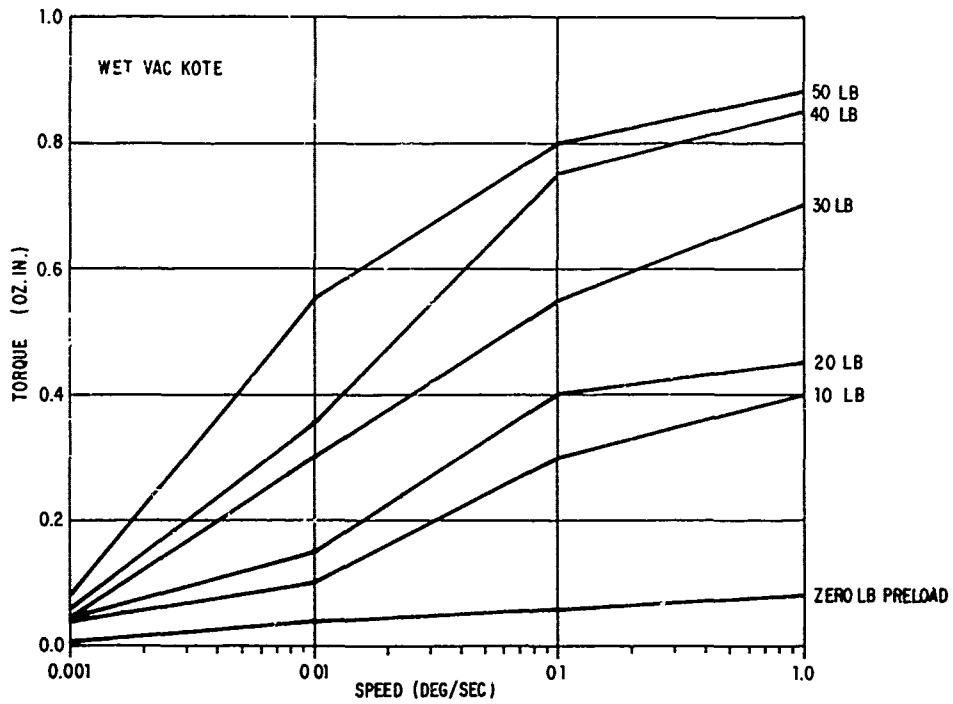


Figure 41 Bearing 36563 Speed-Torque

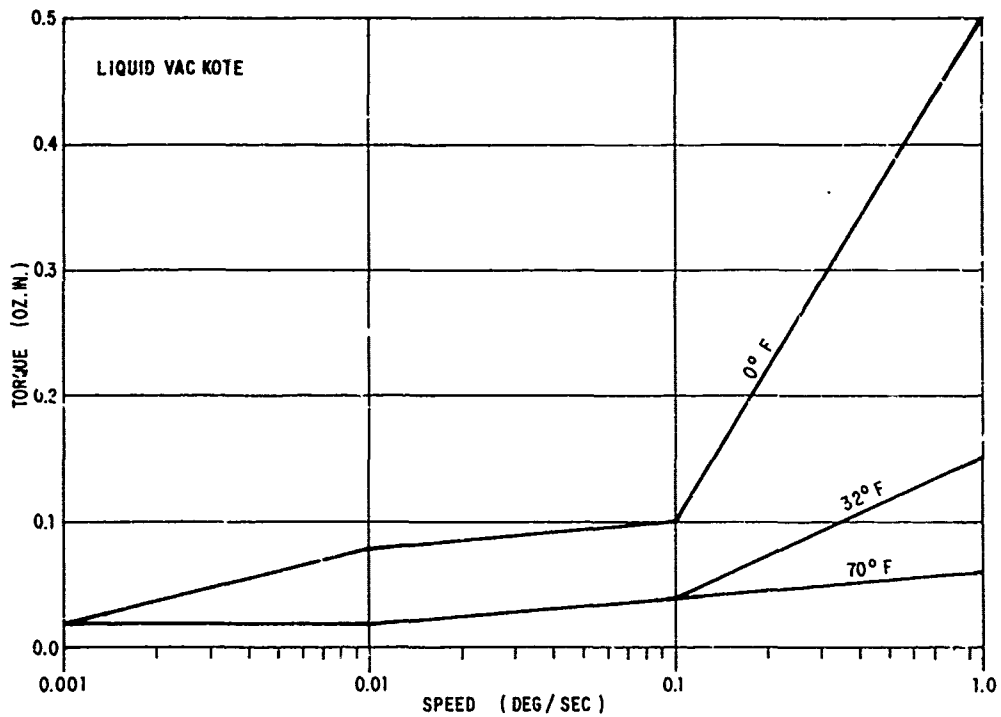


Figure 42 Bearing 36563 Temp. Test at 0 Lbs. Preload

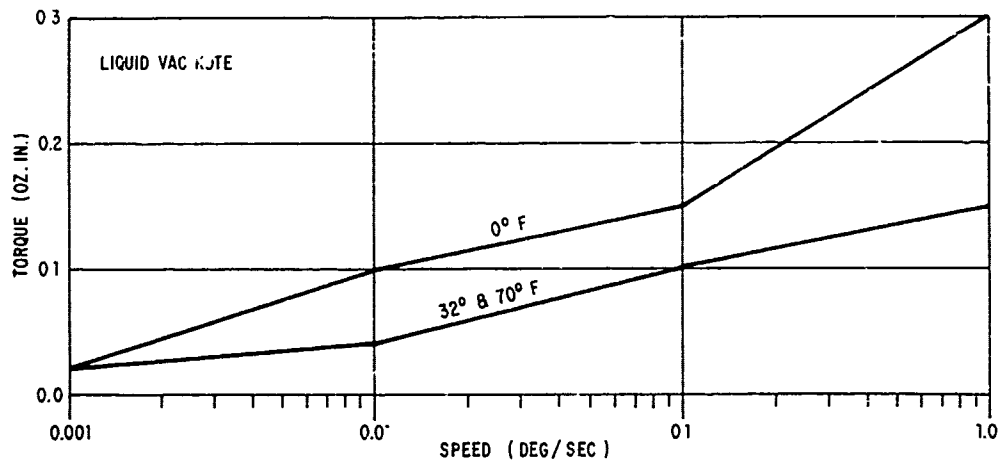


Figure 43 Bearing 56563 Temp. Test at 10 Lb. Preload

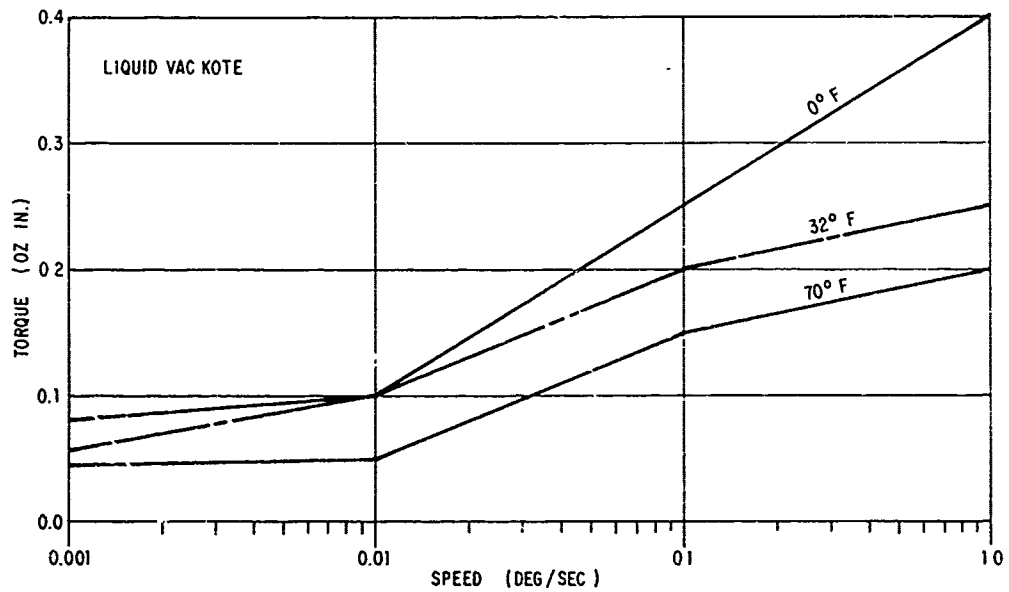


Figure 44 Bearing 36563 Temp. Test, 30 Lb. Preload

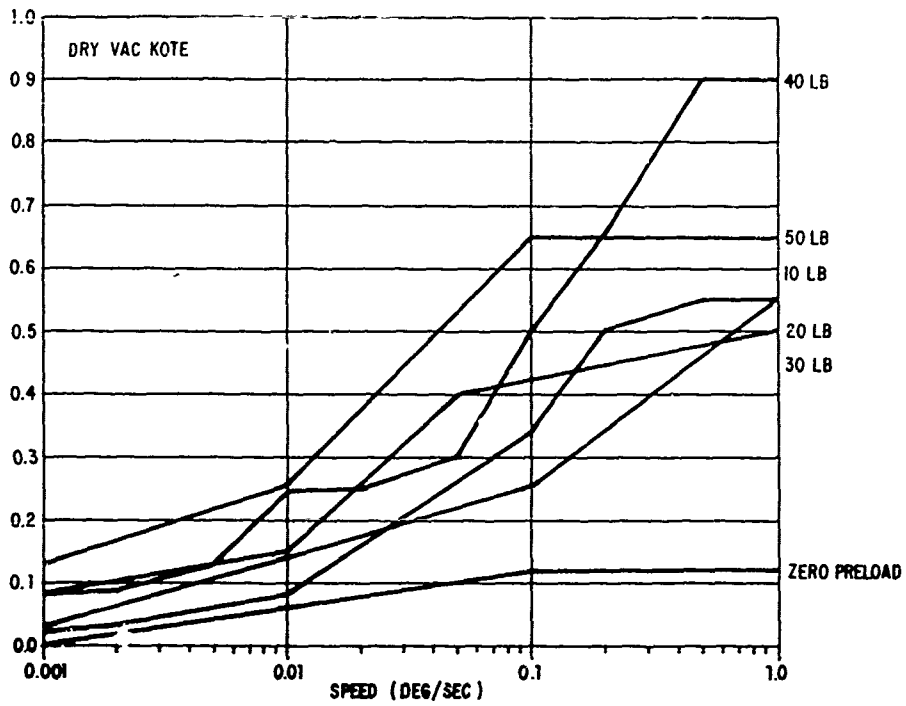


Figure 45 Bearing 36563 Speed-Torque

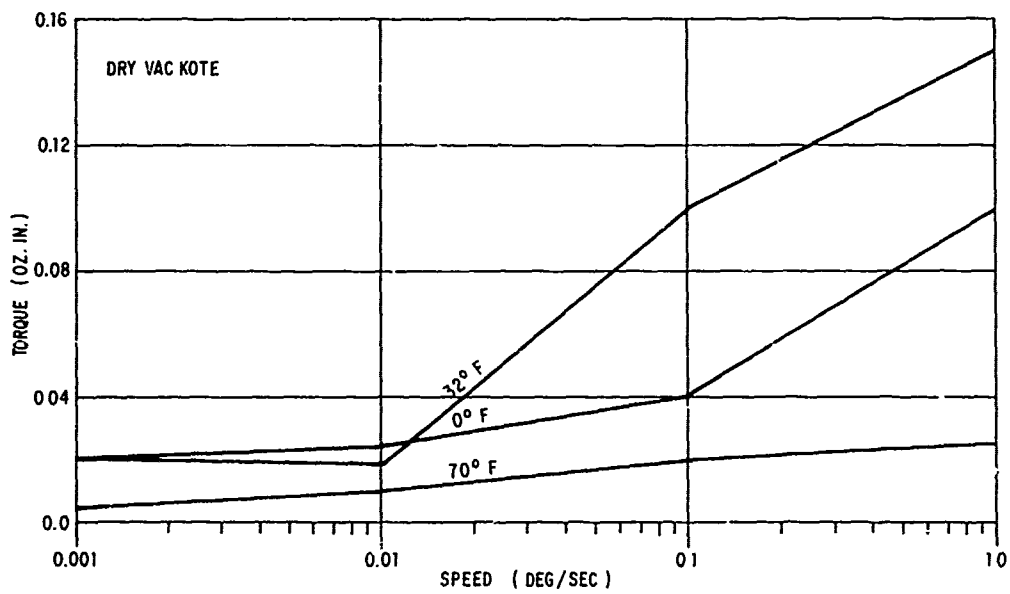


Figure 46 Bearing 36563 Temp. Test at 0 Lb. Preload

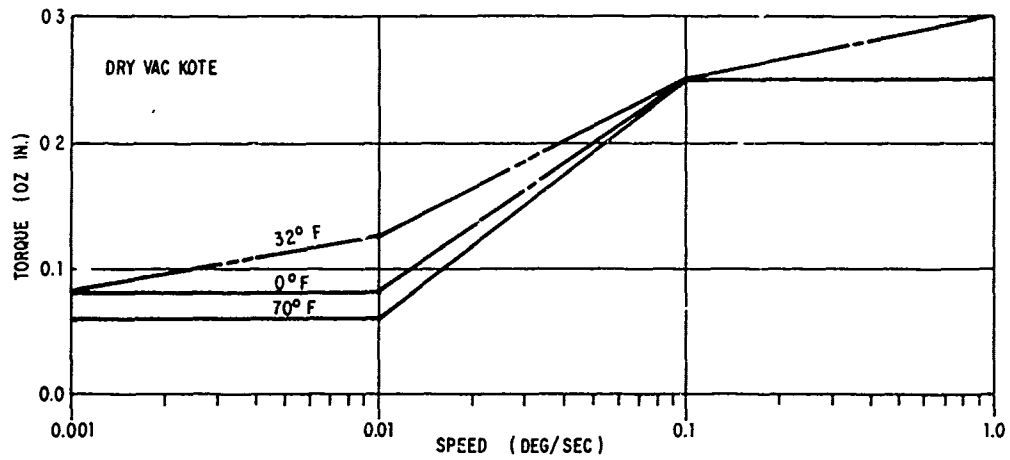


Figure 47 Bearing 36563 Temp. Test at 10 Lbs. Preload

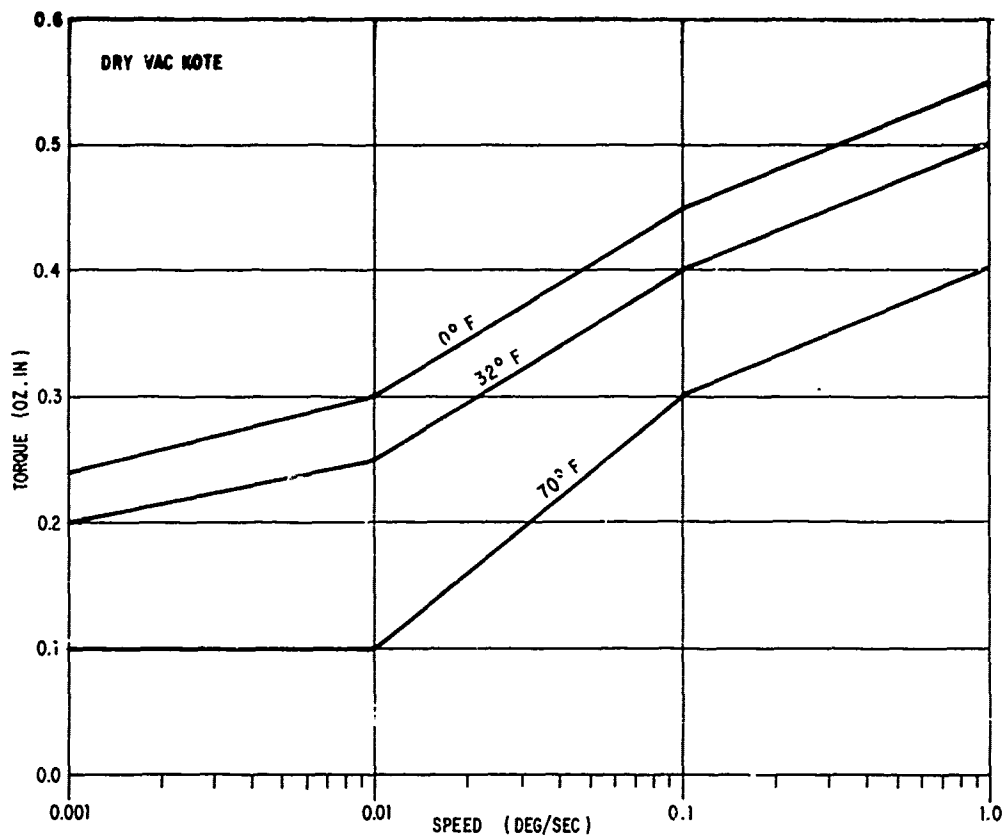


Figure 48 Bearing 36563 Temp. Test at 30 Lbs. Preload

friction component which is proportional to the pitch diameter and a viscous friction component proportional to the pitch diameter cubed. This test data tends to confirm that at these speeds the coulomb friction component outweighs the viscous component.

The results of the starting tests were surprising in that the starting torque of the 36563 bearing was not greater than that of the 33267 bearing as might have been expected from the running torque data. It was, in fact, lower and always broke away at less than 0.03 oz.in., even when preloaded to 50 pounds. The reason for this may be that the 36563 bearing has 48 balls of 0.18 inch diameter while the 33267 bearing has only 9 balls of 0.406 diameter. On previous tests we have seen that a bearing with a large number of small balls often has less starting torque than a bearing with fewer large balls. Breakaway tests were run at 0, 32, and 70 degrees F, but there were no discernable differences in the results, even at 0°F with liquid Vac Kote. Neither were there any significant differences between the results of the liquid and dry lubricated bearings. Figures 49 and 50 are representative runs of the liquid lubricated bearing at different preloads.

4.4.4 Bearing SR156

Eight bearings were tested, four with liquid lubricant and four with dry. For convenience we lettered the four liquid A, B, C, and D and the four dry E, F, G, and H. Figures 51 through 58 graph the torque data for the liquid lubricated bearings while Figures 59 through 68 cover the dry. All eight bearings were tested with a number of preloads (see Table I) at room temperature. For high and low temperature testing one dry lubricated bearing was tested at 0, 2, and 4 pounds preload while the remaining 3 were tested at 2 pounds preload. All four liquid lubricated bearings were temperature tested at 5 pounds preload because the wet lubricant can normally be used at higher preloads than the dry. In addition, since most of the room temperature liquid and dry data was similar, this was a good way to more extensively compare the operation at different preloads.

The tests on the SR156 bearings were the most difficult and have the highest probability of excessively high torque readings. This is because the bearings are so small and their torque so small that the fixture unbalances, room noise, and electrical noise are all a much larger portion of the total torque than on the other bearings. This also gives data which is not as clearly correlated as that on the previous bearings. The torque vs. preload data of Figure 11 shows a larger variance between the wet and dry lubricated bearings than we feel is reasonable, particularly when viewing Figures 51 through 68. The inability to distinguish bearing torque from disturbance torque in the 0.01 - 0.04 oz.in. range is the cause of these variations. No previous test data

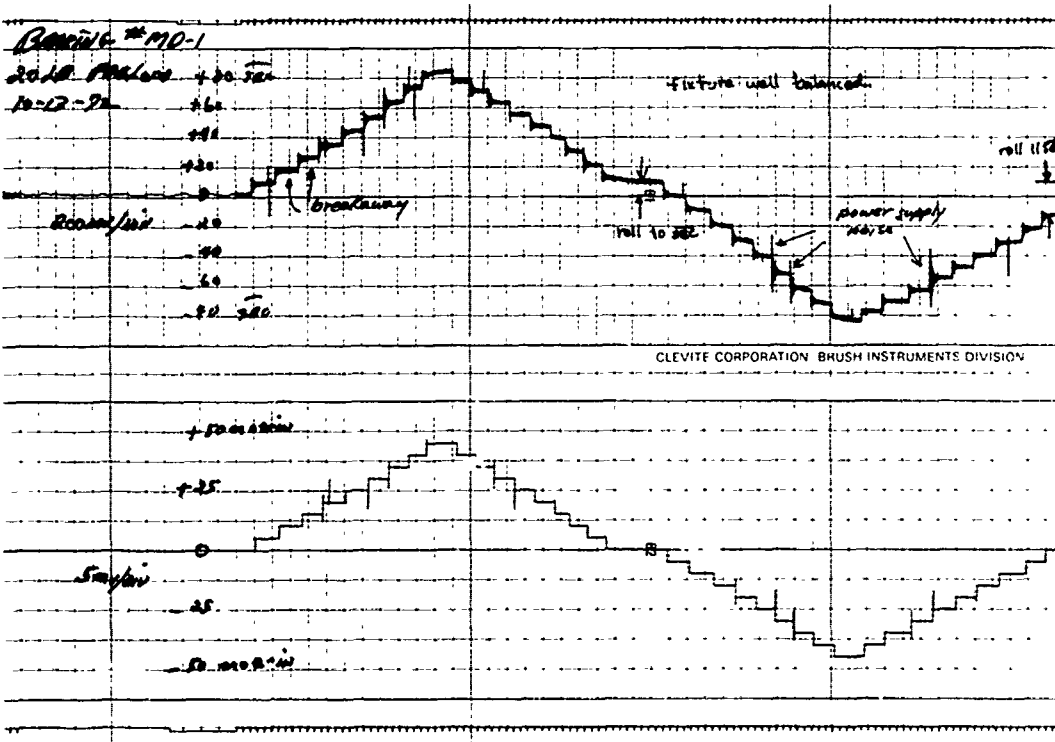
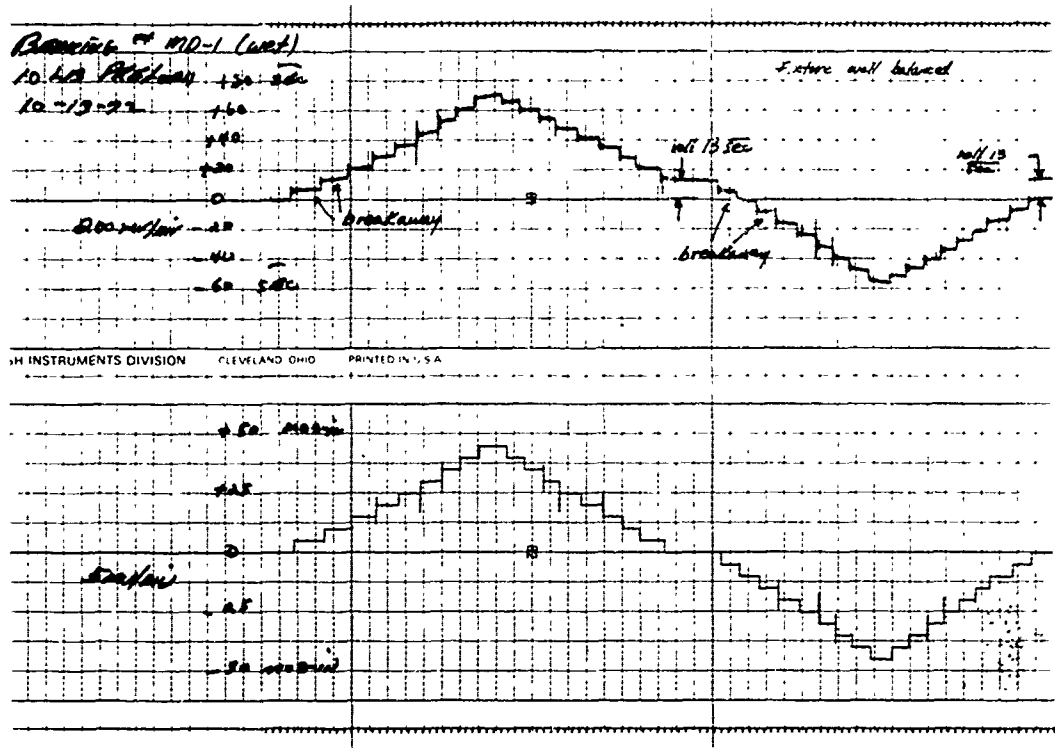


Figure 49 Brg. 36563 - Starting Data - 10 & 20 Lb. Preload

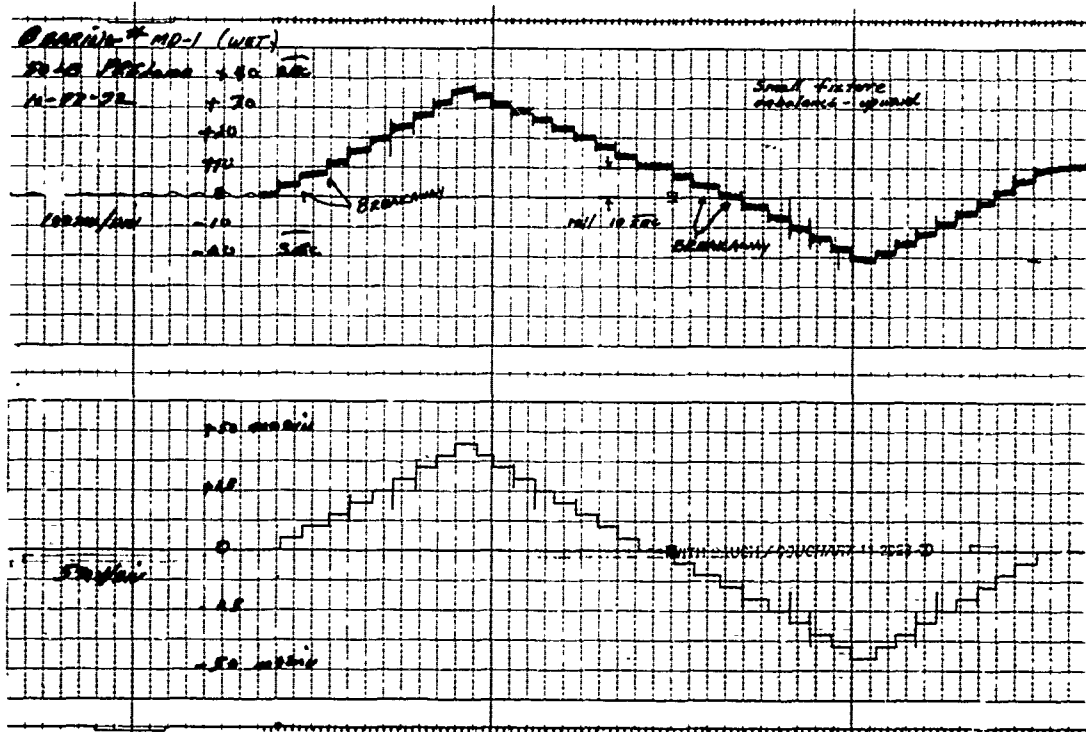
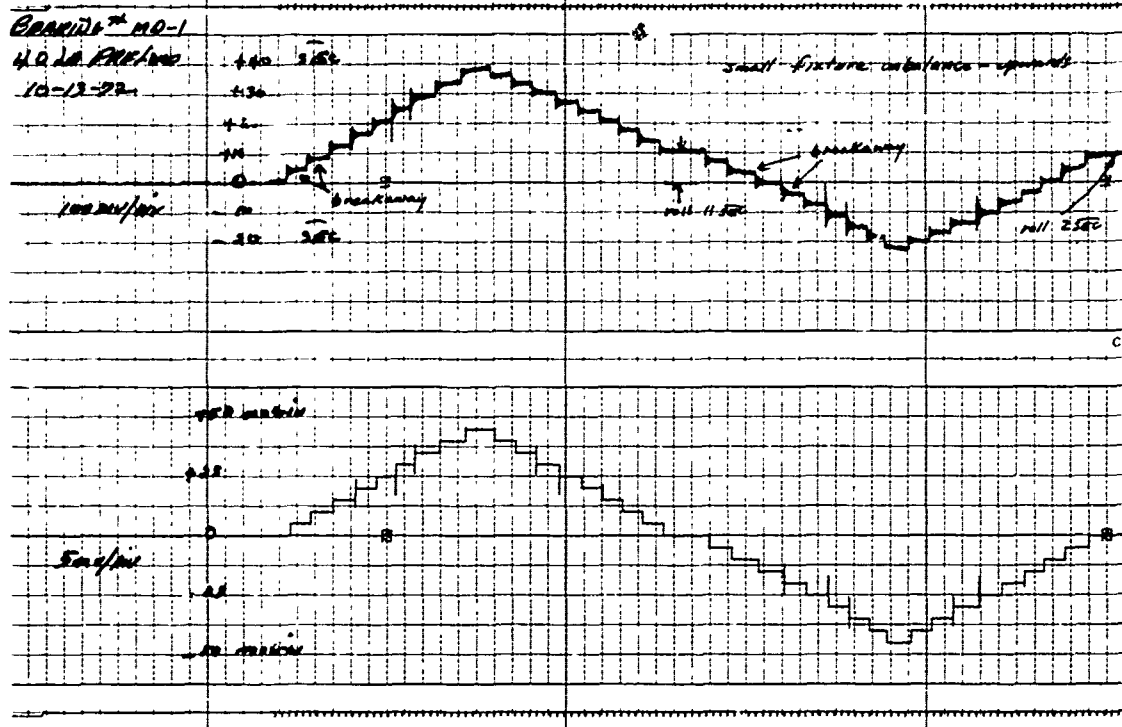


Figure 50 Brg. 36563 - Starting Data - 40 & 50 Lb. Preload

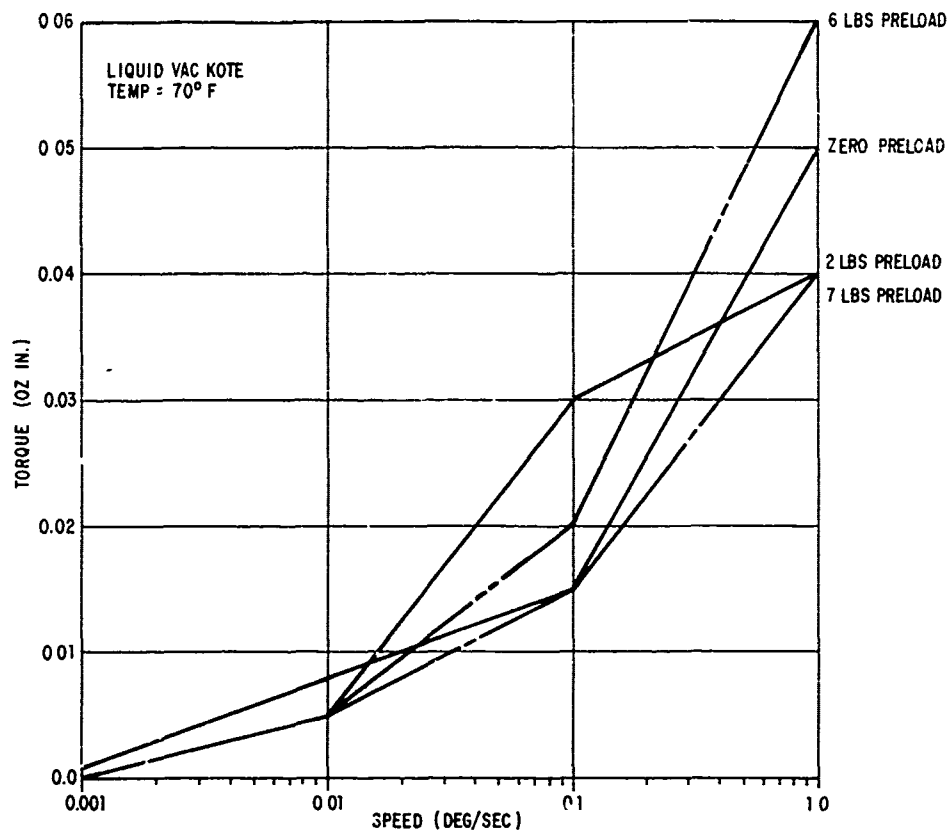


Figure 51 Bearing SR156-A Speed Vs. Torque

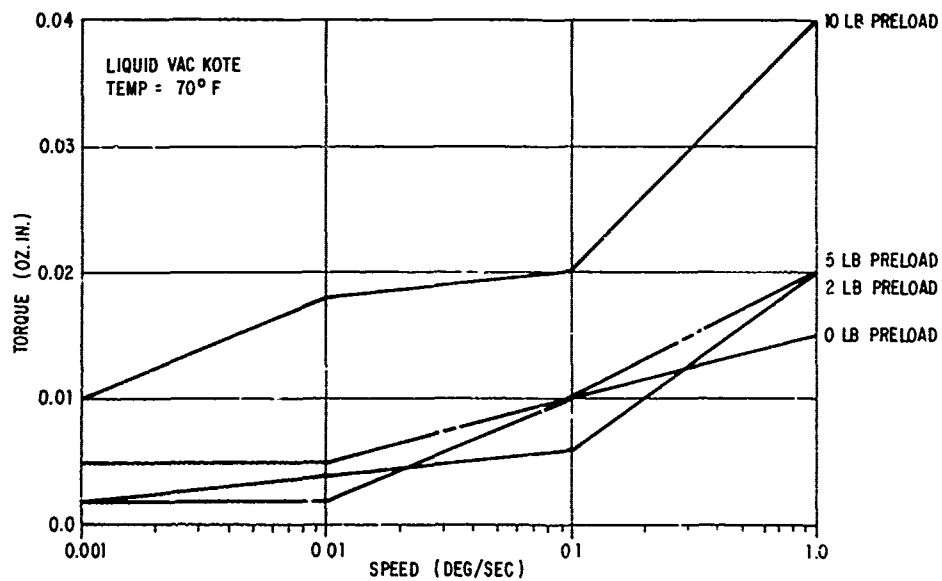


Figure 52 Bearing SR156-B Speed Vs. Torque

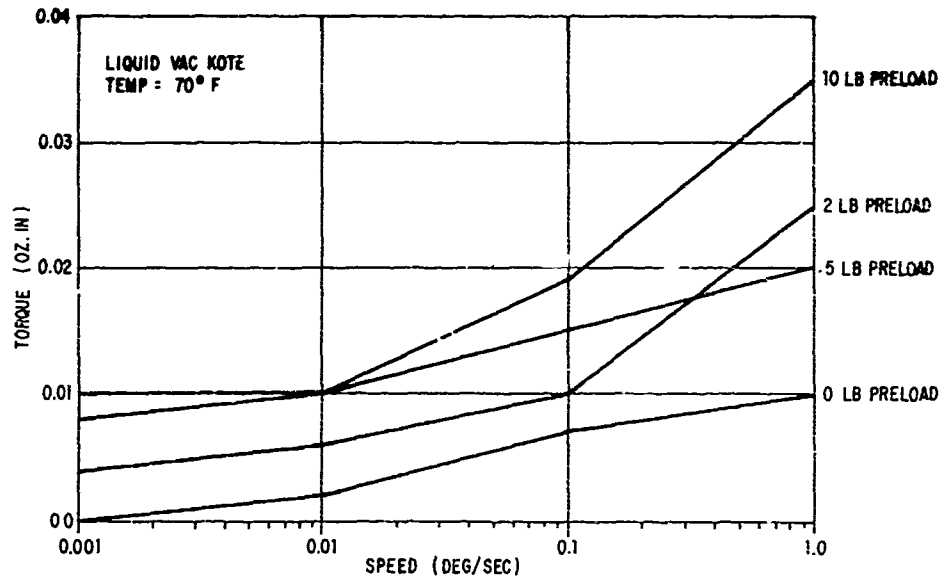


Figure 53 Bearing SR156-C Speed Vs. Torque

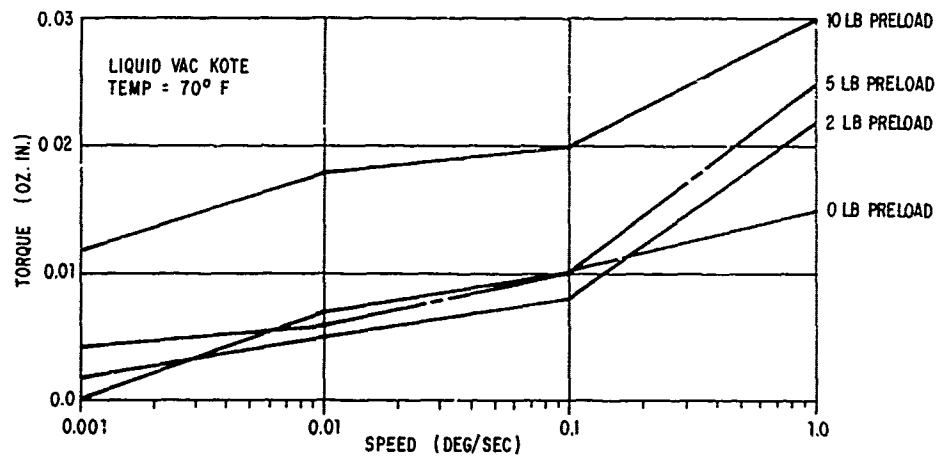


Figure 54 Bearing SR156-D Speed Vs. Torque

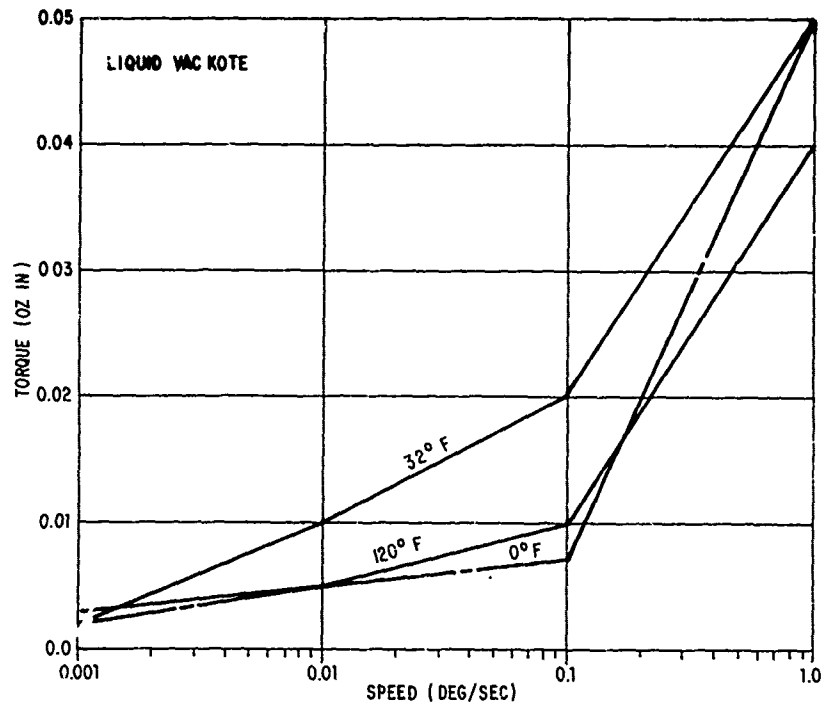


Figure 55 Bearing SR156-A Temp. Tests at 5 Lbs. Preload

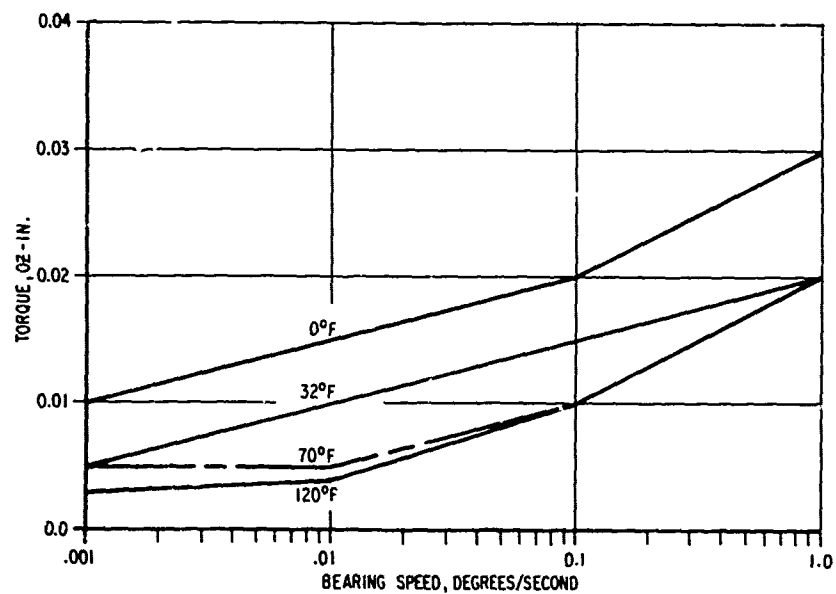


Figure 56 Bearing SR156-B Temperature Tests

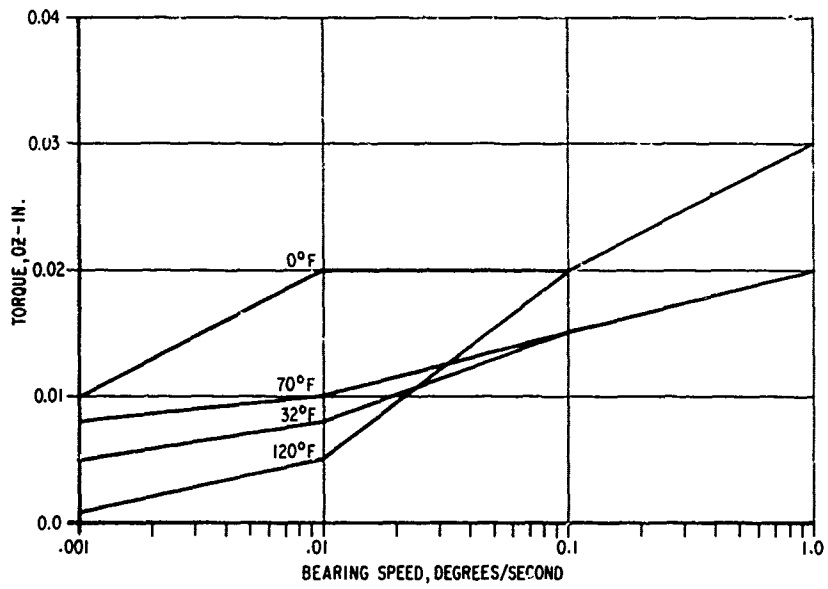


Figure 57 Bearing SR156-C Temperature Tests

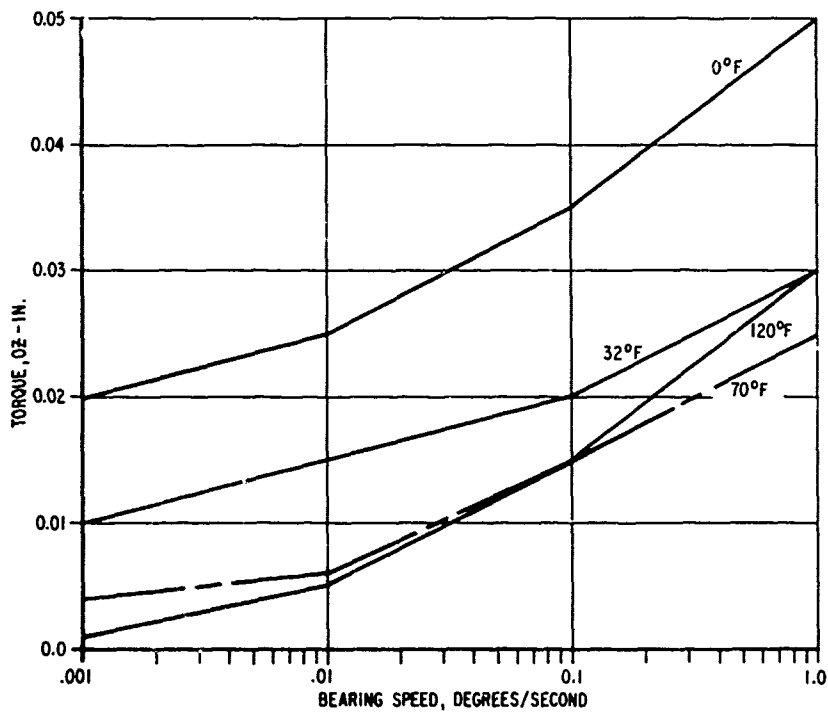


Figure 58 Bearing SR156-D Temperature Tests

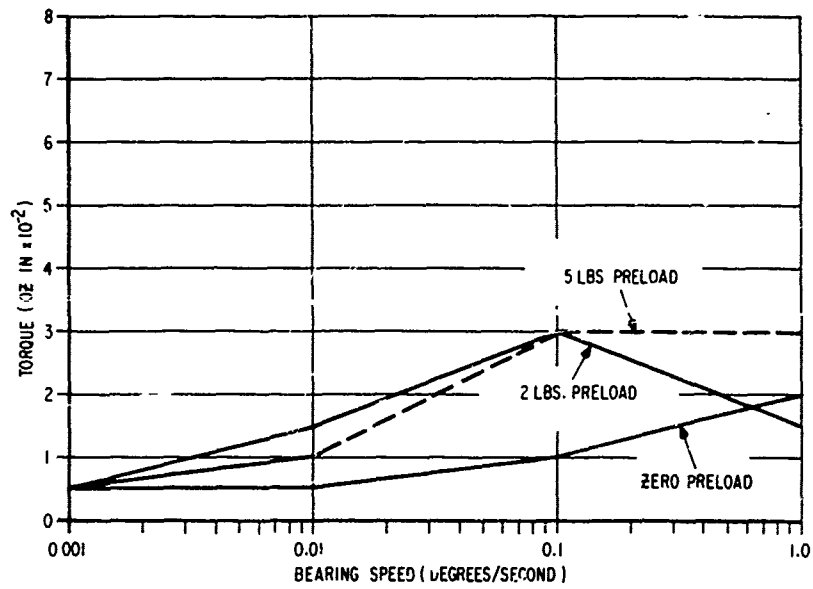


Figure 59 Bearing SR156-E Speed Vs. Torque

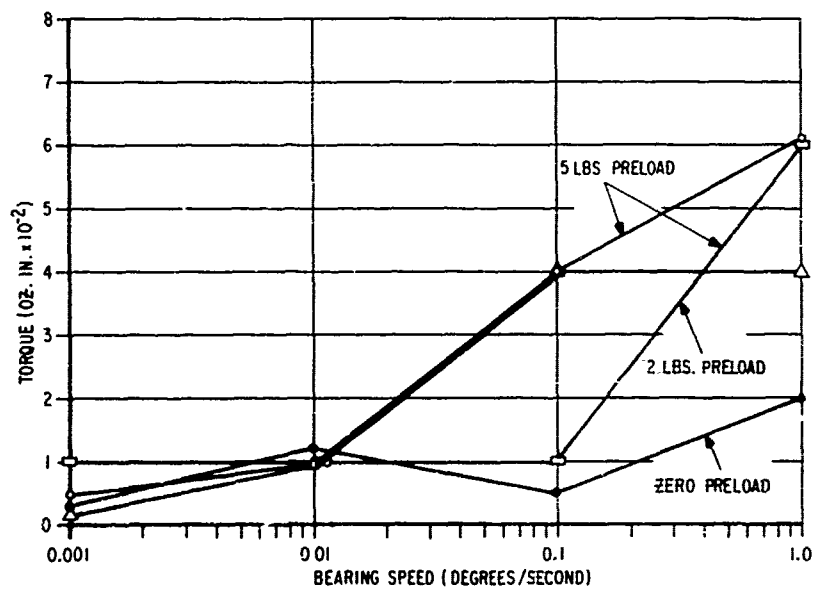


Figure 60 Bearing SR156-F Speed Vs. Torque

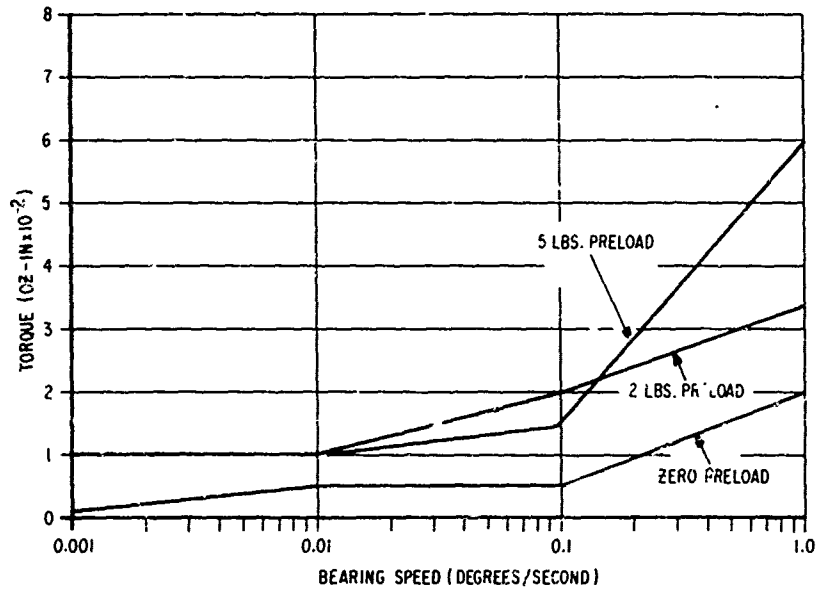


Figure 61 Bearing SR156-G Speed Vs. Torque

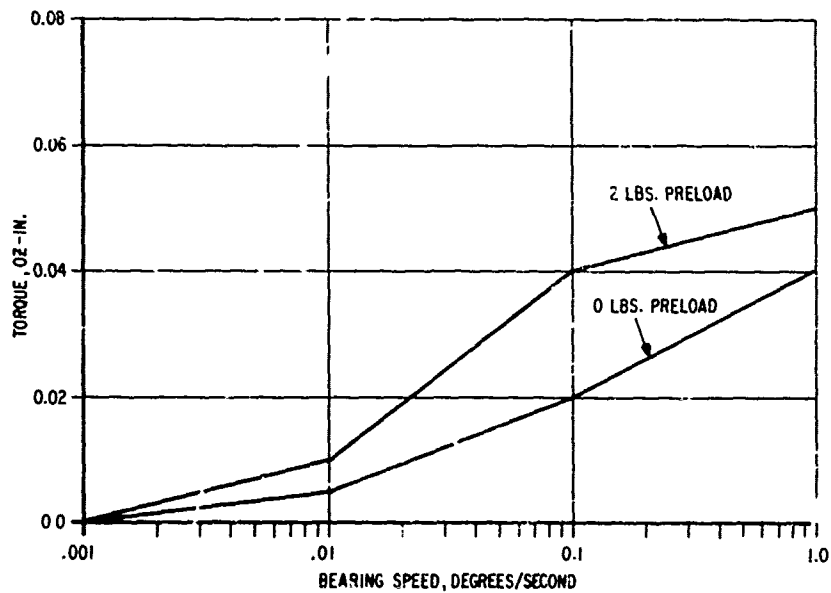


Figure 62 Bearing SR156-H Speed Vs. Torque

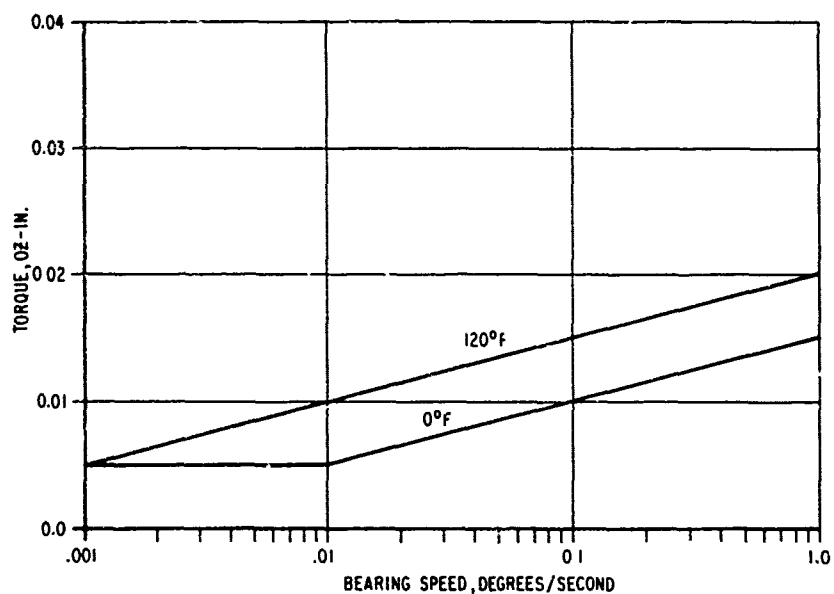


Figure 63 Bearing SR156-F Temp. Tests, Zero Preload

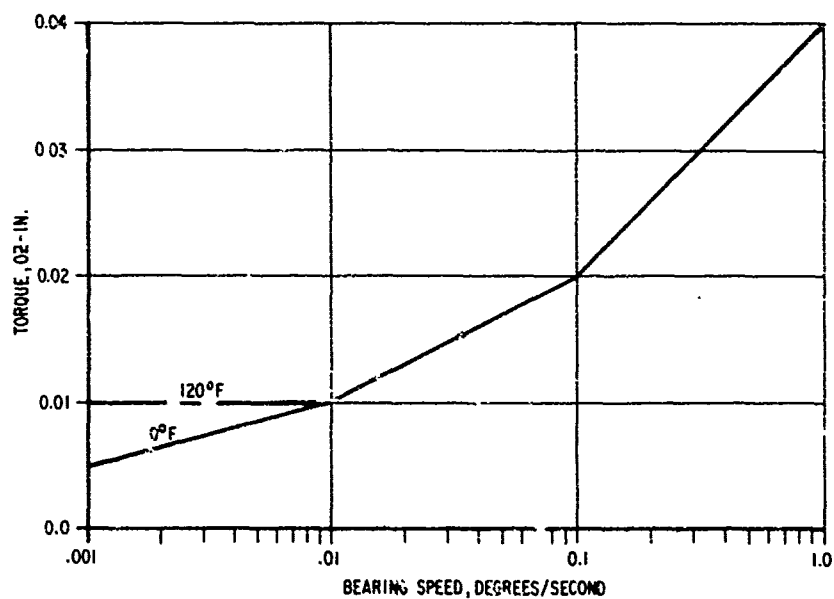


Figure 64 Bearing SR156-F Temp. Test, 2 Lb. Preload

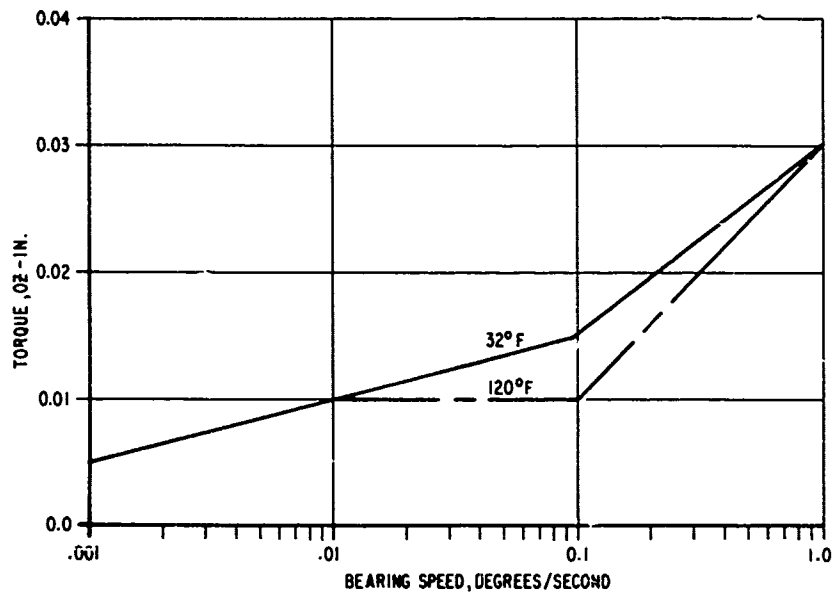


Figure 65 Bearing SR156-F Temp. Test, 4 Lb. Preload

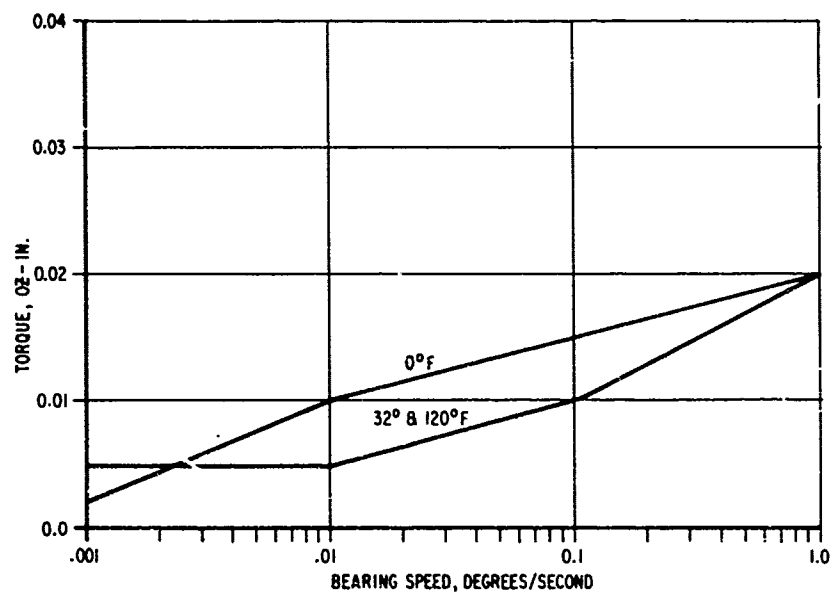


Figure 66 Bearing SR156-E Temp. Test, 2 Lb. Preload

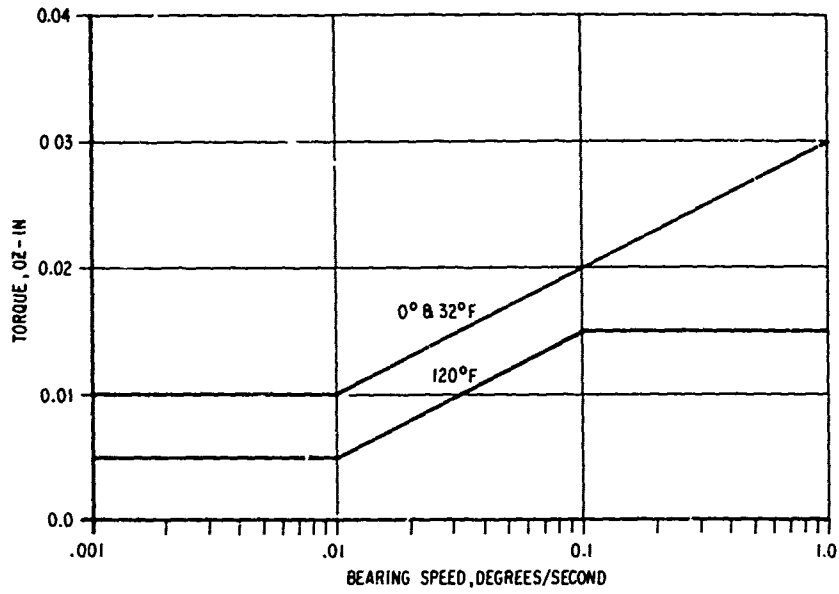


Figure 67 Bearing SR156-G Temp. Test, 2 Lb. Preload

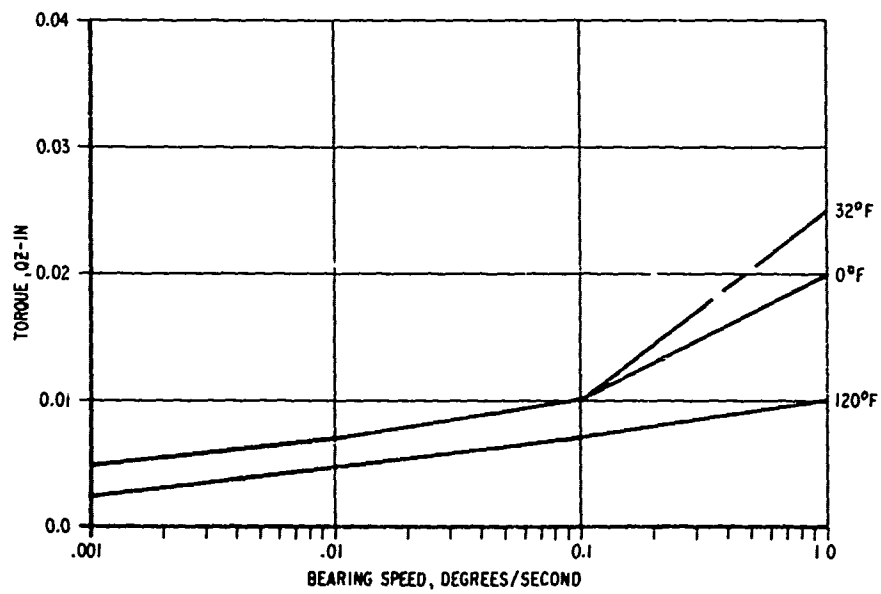


Figure 68 Bearing SR156-H Temp. Test, 2 Lb. Preload

was available on these bearings or other bearings of their size. BBRC has used bearings of this size on a number of aerospace flight applications, but because the friction torque is so small and the project 405B speeds so slow, no accurate correlatable data was ever produced.

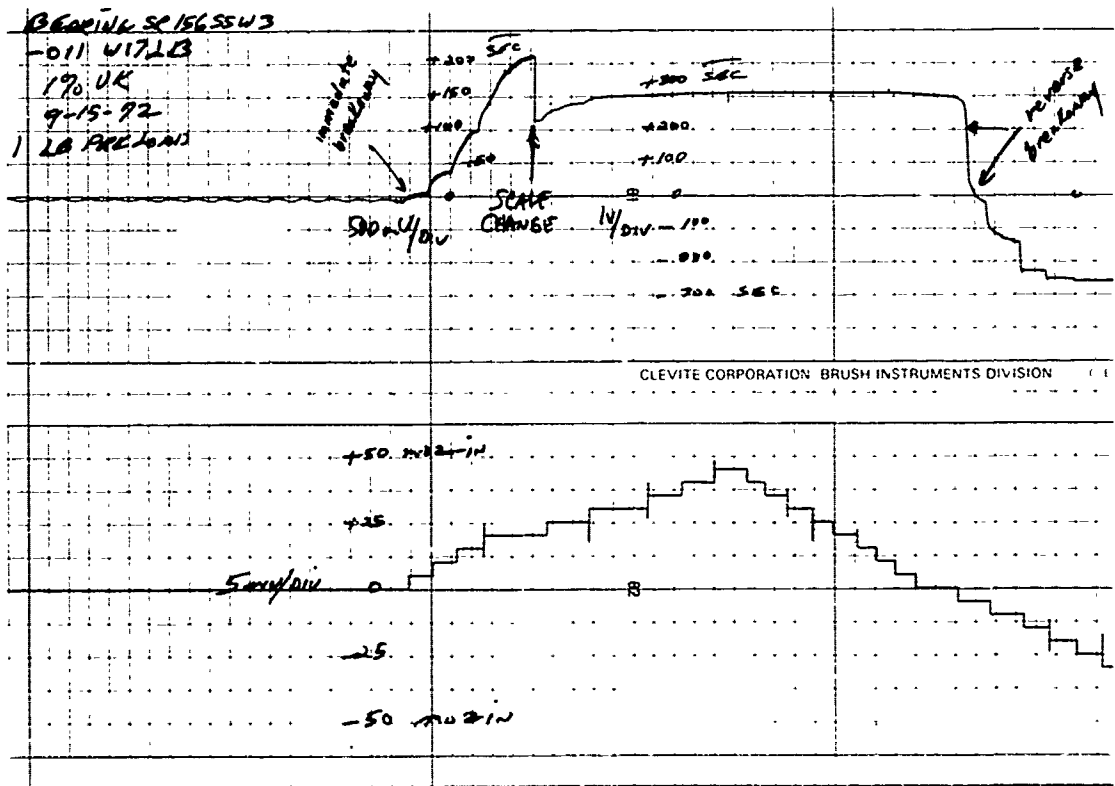
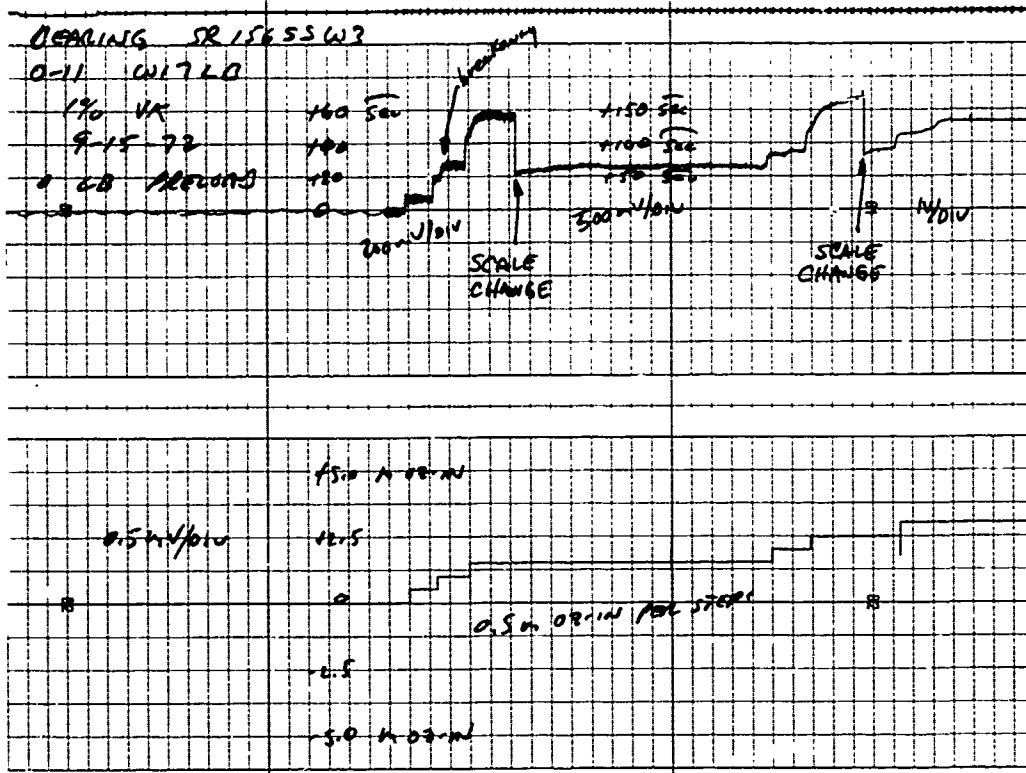
As expected, the torque increased with speed throughout the tests although the increase of torque with preload was not as pronounced. Either of two factors could be responsible for this; the inability to measure torque as accurately as desired or the fact that the entire range of preload was only 10 pounds. The average torque measured (1°/second) at 5 pounds preload was 0.033 oz.in. and at 2 pounds preload was 0.026 oz.in., but the torque variation in individual bearings was greater than this. The peak measured torque was 0.06 oz.in. which occurred on both the dry and liquid lubricated units. The torque magnitude was found essentially the same on both the dry and liquid lubricated bearings, as with the other bearings tested. The liquid Vac Koted bearings at 0°F produced the expected higher torque on three of the four bearings tested.

The starting torque values were also lower than those measured on the two larger bearings. Breakaway generally took place between 0.001 and 0.005 oz.in. and a starting torque higher than running torque was not found. Figures 69 and 70 present raw data taken on the SR156 starting tests. Breakaway is shown in the upper trace of Figure 69 where bearing B rolls continuously at 0.002 - 0.003 oz.in. and in the lower trace where it rolls immediately and rapidly when steps of 0.005 oz.in. were applied. The breakaway of bearings B and D, preloaded to 5 pounds, are shown in Figure 70 to occur between 0.001 and 0.002 oz.in. As with the running friction tests, the sensitivity and noise immunity of the test equipment was challenged by the small torques measured. The traces of Figure 70 show how the mechanical noise of the laboratory, which varied from day to day, is reflected as noise on the data.

No discernible difference was seen between the starting torque values with different preloads, as was found on the 33267 bearing. This is probably due to the limited preload range and the inability of the test equipment to measure more sensitively. Likewise, there was no discernible difference between the results of the liquid and dry lubricated bearings or the temperature tests.

4.4.5 Test Conclusions

The test results reflect very favorably on the use of bearings in high accuracy pointing systems. At these test speeds, running friction was at or below that which would have been predicted and a starting friction peak was virtually non-existent within the capability of the equipment to measure. We conclude, therefore,



CLEVITE CORPORATION BRUSH INSTRUMENTS DIVISION

Figure 69 SR156 Breakaway - 0 & 1 LB. Preload

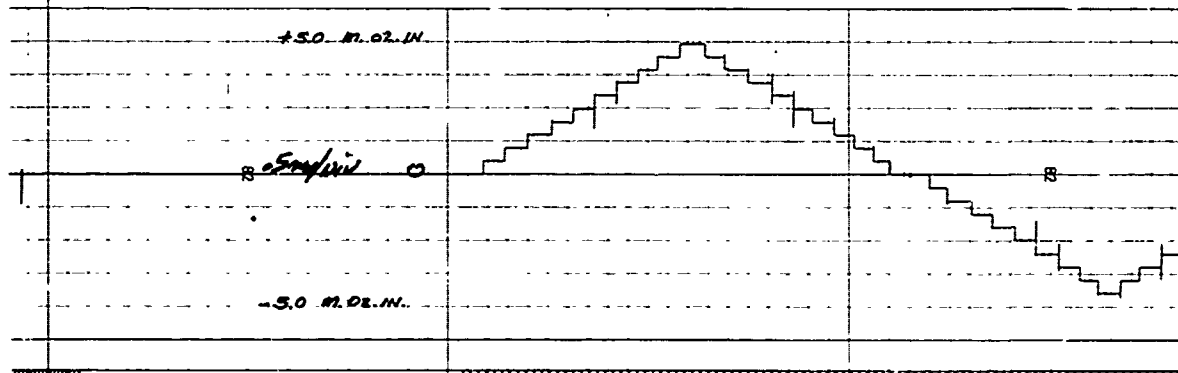
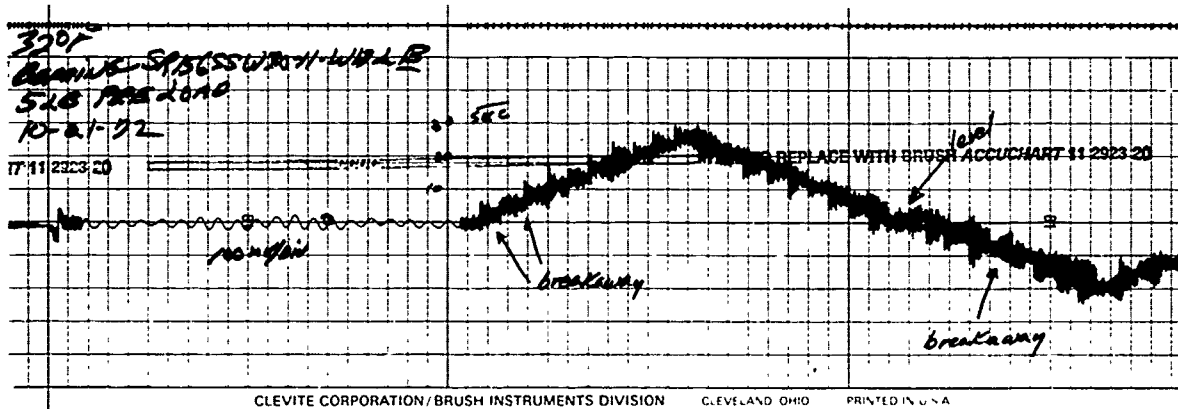
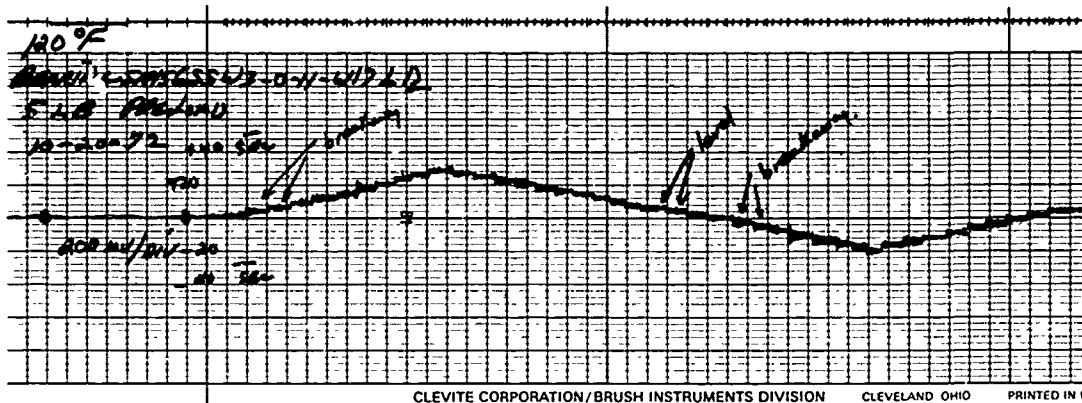


Figure 70 SR156 Breakaway - 5 Lbs. Preload

that the bearings will not present a limiting characteristic to either of the 405B study applications.

Probably the most important test discovery is that the starting friction torque (stiction) is not higher than the low speed running torque. A peak of starting friction 2-3 times higher than the running friction had always been assumed, but was not detectable on any bearing tested. In addition, the starting torque was much lower than expected. These results indicate that if the friction models used in servo analyses could be modified accordingly, that higher pointing accuracies could be achieved. Over extremely small angles (10-50 microrad) the spring effect of the bearings could also be incorporated into the model, giving a combined spring-rolling model. In any case, the stiction torque predicted for most models appears to be higher than necessary, i.e., control systems will not be as severely affected by stiction as previously thought.

In a number of previous examples of drive or pointing systems there appeared to be friction torque, particularly starting torque, in excess of that measured in these tests. It seems likely that a large portion of this torque came from either the torque motors or the power transfer device. The residual torque of a brushless torque motor is taken as approximately 1% of the peak torque. This means that a torque motor could easily have residual torque on the order of one oz.in. which is many times higher than our measured breakaway torque. Most power transfer devices are either slip rings or flex cables. The slip ring has pure sliding friction rather than the rolling friction of a bearing. The starting and running torque magnitudes are on the order of the bearing torque and must be evaluated. The flex cable torque has the form of a spring constant rather than sliding friction and for this reason may be preferable for less than continuous rotation. Measurement of the torque of these devices was not a part of this program, but is the next logical step to be taken in the evaluation of high accuracy pointing systems such as 405B.

The running friction variations do not have the form (at these test speeds) of noise riding on an apparent dc level. The slowness of the torque variations means that bearing torque disturbances which are above the servo bandpass on higher speed applications may be well within the control frequency range of servos operating between 0.001 and 1.0 degree/second. For this reason additional compensation considerations may be necessary for extremely high accuracy applications. The fact that the friction torque is speed dependent at even these slow speeds is not seen as a limiting factor in high accuracy applications because the dependence is small and regular, i.e., not discontinuous.

The performance of the bearings tested was not significantly affected by the use of wet or dry Vac Kote. This allows the lubricant choice to be made on considerations such as applied

loads, optical cleanliness, bearing life, bearing temperatures, etc. Other wet and dry lubricants may have different effects, of course, but a large amount of test data is available on most of them. The tests also showed that for operating temperatures above the pour point of liquid lubricant and for dry lubricant, that the minimum amount of preload corresponds to minimum bearing friction. Bearings used for high accuracy systems should therefore be as lightly preloaded as possible.

SECTION V
POINTING TEST EQUIPMENT DESCRIPTION

5.1 INTRODUCTION

The equipment used to perform the system pointing tests consists of two major assemblies; the test fixture and the electronics assembly. These assemblies were used to evaluate the ability of a standard state-of-the-art control system to point a mass suspended on bearings and to evaluate the effect of friction on this pointing capability. The evaluation of pointing to the accuracy range listed in Section I (10-35 microrad) was a major goal. The test equipment was designed to measure system pointing capability in the presence of bearing motion, with different friction levels and sources, and with simulated disturbance torques.

The fixture shown in Figure 71 combines a pointing gimbal with gimbal support, measurement, and motion input mechanisms. The control electronics use a major portion of the bearing test electronics with only new gain and compensation electronics required by the test gimbal.

5.2 TEST FIXTURE

The test fixture is composed of a heavy structure which supports the pointing gimbal and the gimbal input motion mechanism. The pointed mass is the large aluminum disc which is 21.75 inches in diameter and 1/4 inch thick. It weighs approximately 9.5 pounds and its moment of inertia is 22.8 oz-in-sec². The position sensor is an LVDT which has the winding mounted on the support structure and the core mounted on the pointed disc. The LVDT is a linear device which is used to measure the angular position. Since it is mounted at an 11.5 inch radius and has a linear range on the order of $\pm .050$ inch, the error introduced by using the linear device is negligible. The support structure is massive to eliminate structural resonances which would mask or disturb the friction effects we want to evaluate.

5.2.1 System Test Gimbal and Motion Input Mechanism

The system test gimbal and the motion input mechanism are shown in the layout of Figure 72. The double bearings shown allow both the shaft and the housing of the test gimbal to be rotated with respect to the structure. The shaft is the innermost member. The motion input mechanism drives the gimbal housing which is attached to the inner race of the motion input bearings. These are Kaydon KA40AH bearings purchased as shelf articles. The input mechanism is composed of a dc motor/gearhead combination, two drive belts, and a reduction gear pair. The motor, via the belts and gears, drives the test gimbal housing in either direction

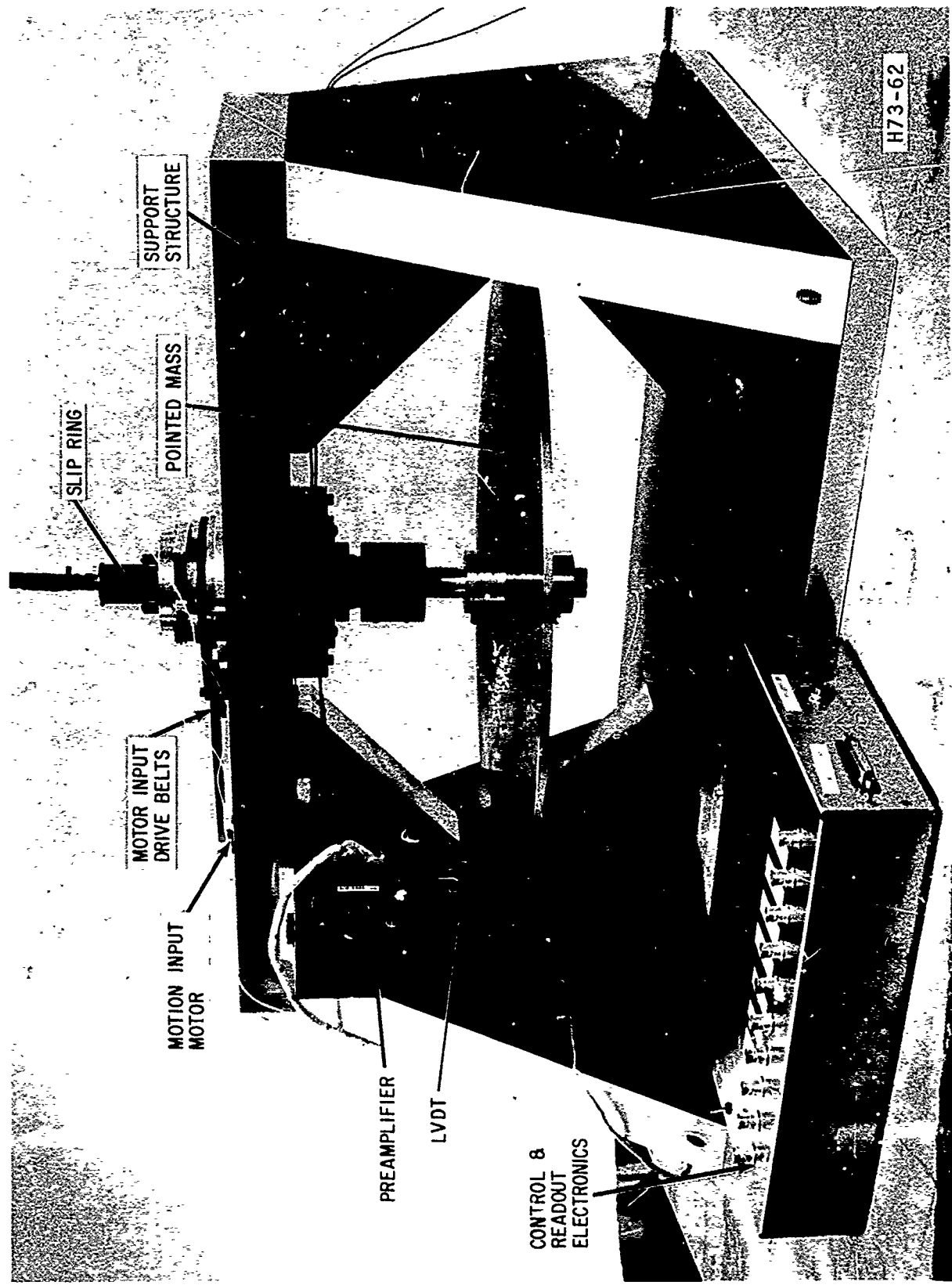


Figure 71 Pointing Test Fixture

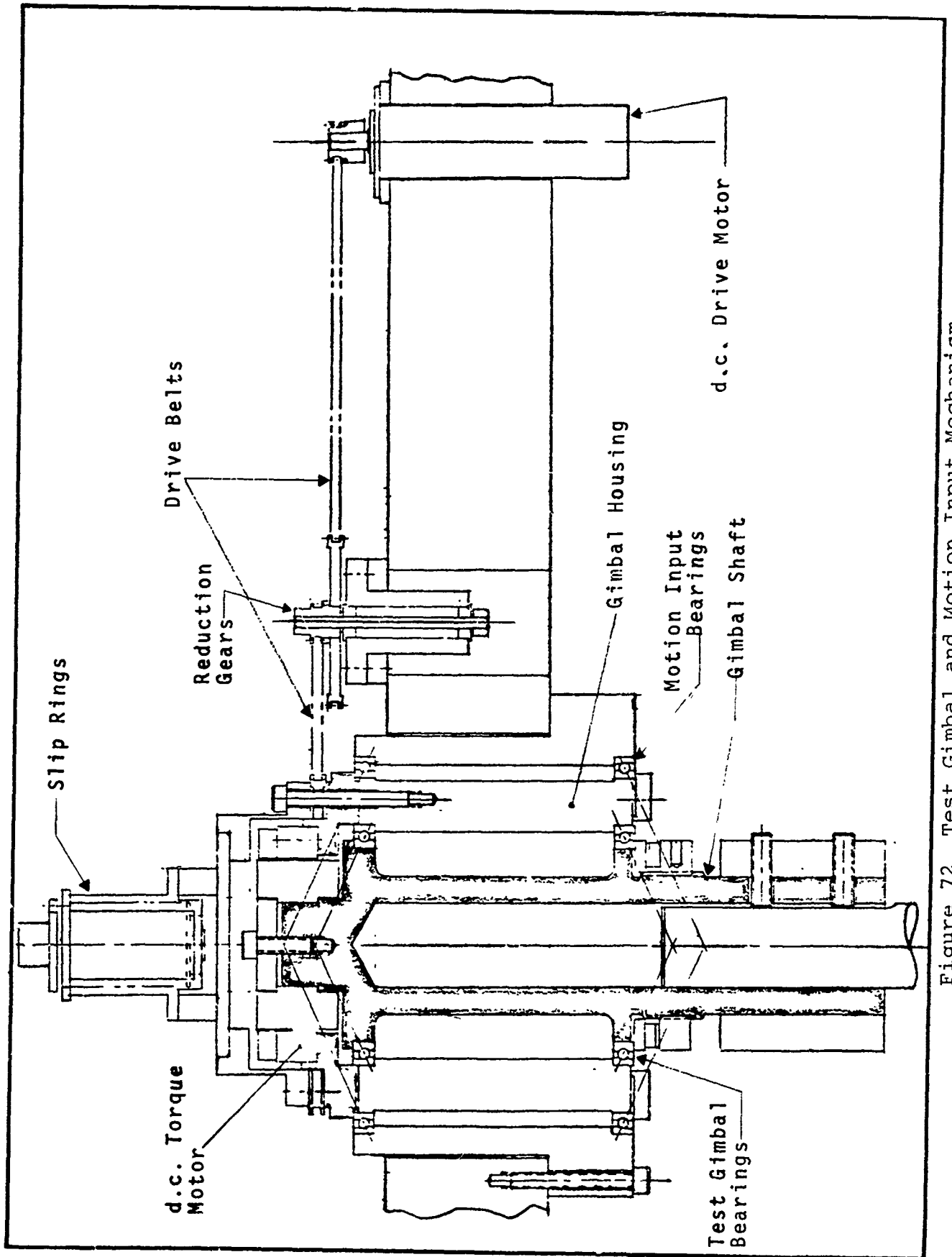


Figure 72 Test Gimbal and Motion Input Mechanism

and at the desired speed in response to the polarity and magnitude of the dc voltage applied to it. The total gear reduction from the motor to the housing is 46,200:1 with 1108:1 in the gear head, 4.57:1 in the first belt pass, and 9.15:1 in the second pass. The dc motor must therefore run at 7700 rpm when the gimbal housing turns at 1 degree/second. This requires approximately 9 volts on the motor which is a good midpoint for motor operation. The belt drive system was used rather than a gear drive system to minimize the high frequency noise transmission through gears. This "soft" system was much more noise free than the "hard" system used in the bearing test fixture.

The test gimbal is composed of a housing and shaft separated by angular contact ball bearings, a dc torque motor, a slip ring, and the pointed disc. The housing and shaft were machined of aluminum. The bearings are the 36563-1 bearings described in Section IV above, and previously tested. Both were cleaned and relubricated with liquid Vac Kote prior to assembly. The motion of the outer (motion input) bearings may introduce small disturbances into the outer race of the test bearings, but these were considered analogous to disturbances which could be input to the gimbal bearings in spacecraft use. The torque motor is an Inland model 2149 brush-type device. The reasons for its choice were the brushes, which gave a type of friction we wanted to evaluate, and the ready availability of this particular model. The slip ring was not used to carry current, but only as a friction source. This allows it to be removed from the system to evaluate different friction levels without disturbing the electrical system. Flexible wires were used to carry motor current across the gimbal instead of using the slip ring. The slip ring was a Breeze Corporation unit, part no. 16093. This design was flown on six OSO satellites and operated in space for up to five years, so it was felt to be a representative aerospace model.

5.3 ELECTRONICS ASSEMBLY

The electronics used are essentially the same as those shown in Figure 3 and described in Section III above. The excitation circuit, demodulator, preamplifier and notch filters are exactly the same because of the use of the LVDT as the position sensor. Only the gain of the motor driver was changed to accommodate the new dc motor. The control gain and compensation were modified to give the system described below.

5.3.1 Control System

The gimbal shaft and pointed mass are held by the closed loop control system to the zero position defined by the LVDT. The servo block diagram is shown in Figure 73. A conventional lead-lag servo compensation is incorporated to give a system bandpass of approximately 20 Hz. A 300 rad/second filter is required on the output of the LVDT demodulator and can be considered part of

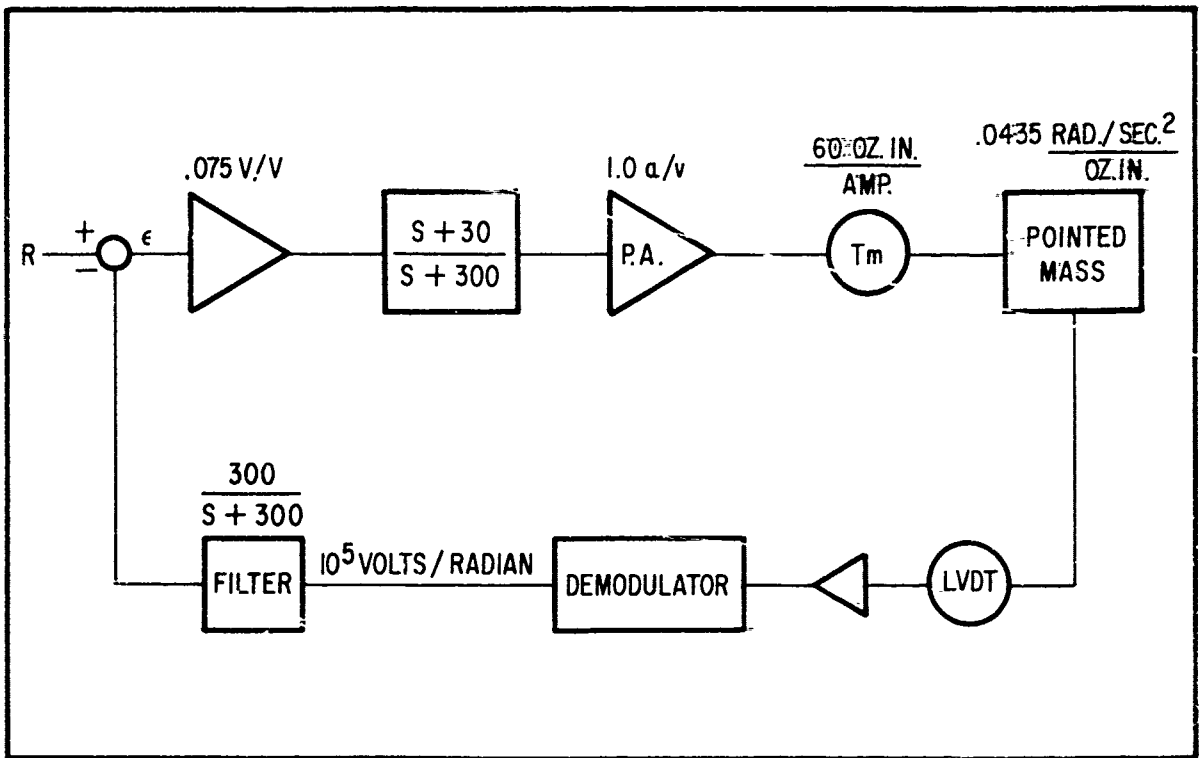


Figure 73 Pointing Gimbal Control System

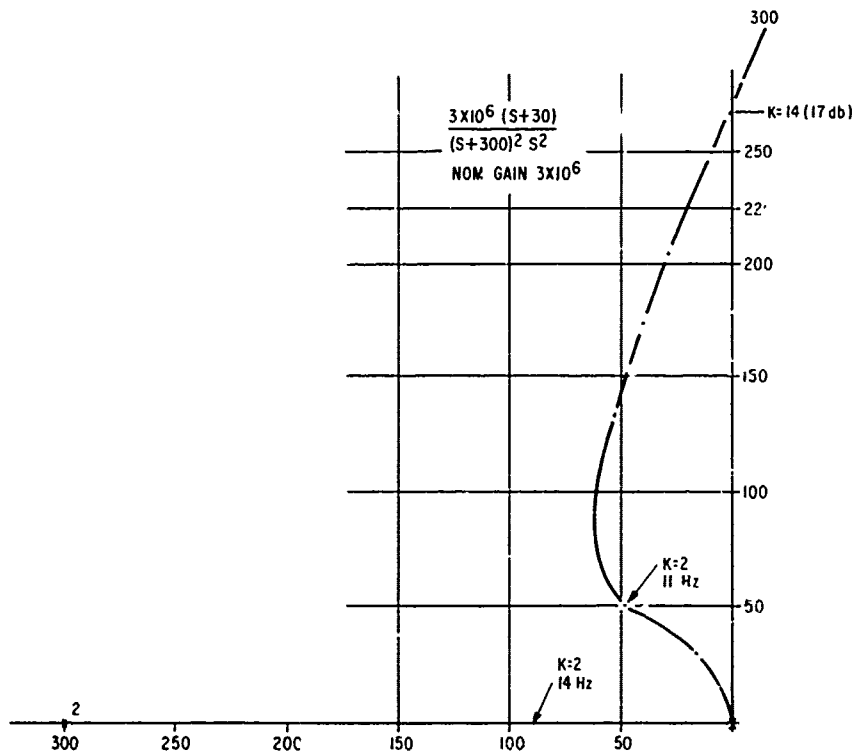


Figure 74 Pointing Gimbal Control Servo Root Locus

the plant. No spring return force or mechanical damping is assumed for the plant so the controlled object is essentially the mass held by the bearings. The effect of friction on this type of system is the object of our evaluation.

The root locus of the system characteristic is shown in Figure 74. The operating point is at the $K=2$ relative gain point. The damping ratio is shown here to be approximately 0.7, i.e., $\cos. 45^\circ$, giving a step response which has a single overshoot. The relative gain at which the locus crosses into the right half plane (system goes unstable) is 14, or 17 db above the operating point.

The closed loop frequency response of this system is shown in Figure 75. It shows a bandpass of approximately 20 Hz to the -3 db point and a rolloff rate of 40 db/decade above 50 Hz.

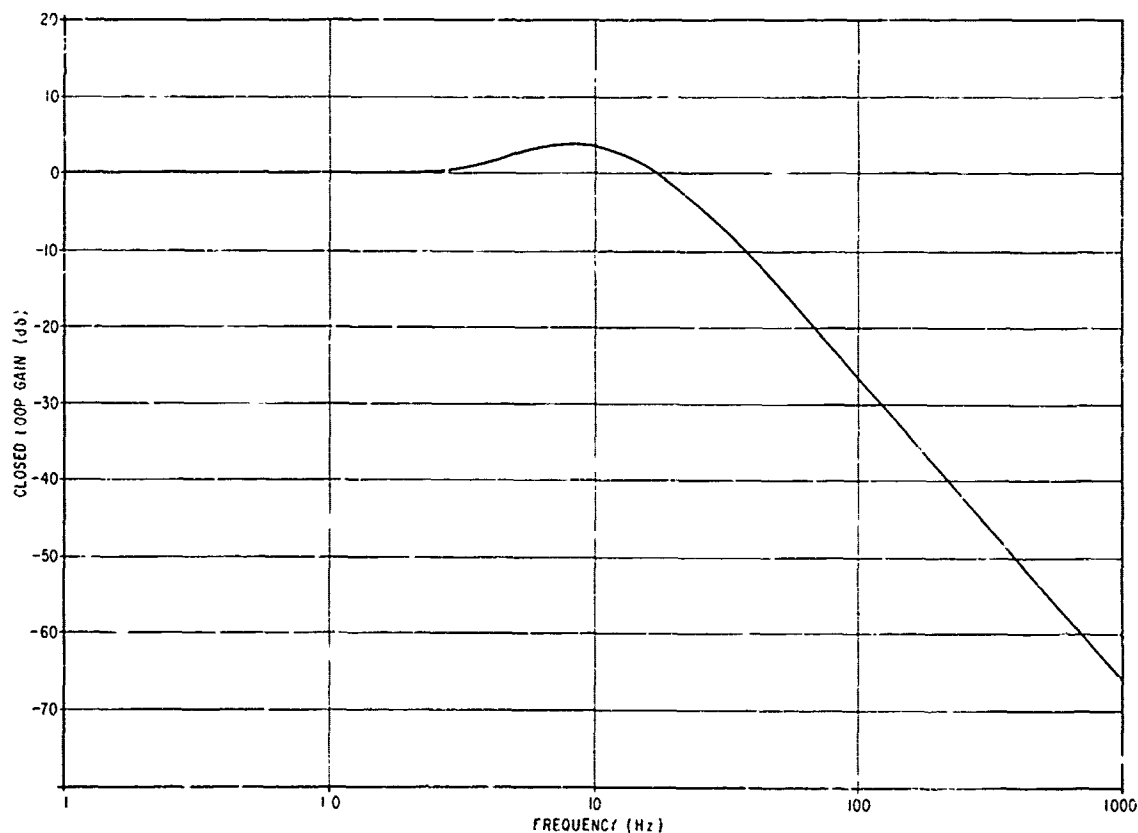


Figure 75 Closed Loop Frequency Response of the Pointing Servo

A root locus analysis of the system was performed to show that its stability would not be affected by the addition of friction, i.e., in Figure 76, the fact that the entire locus lies to the left of the imaginary axis means that the friction will not cause the loop to go unstable.

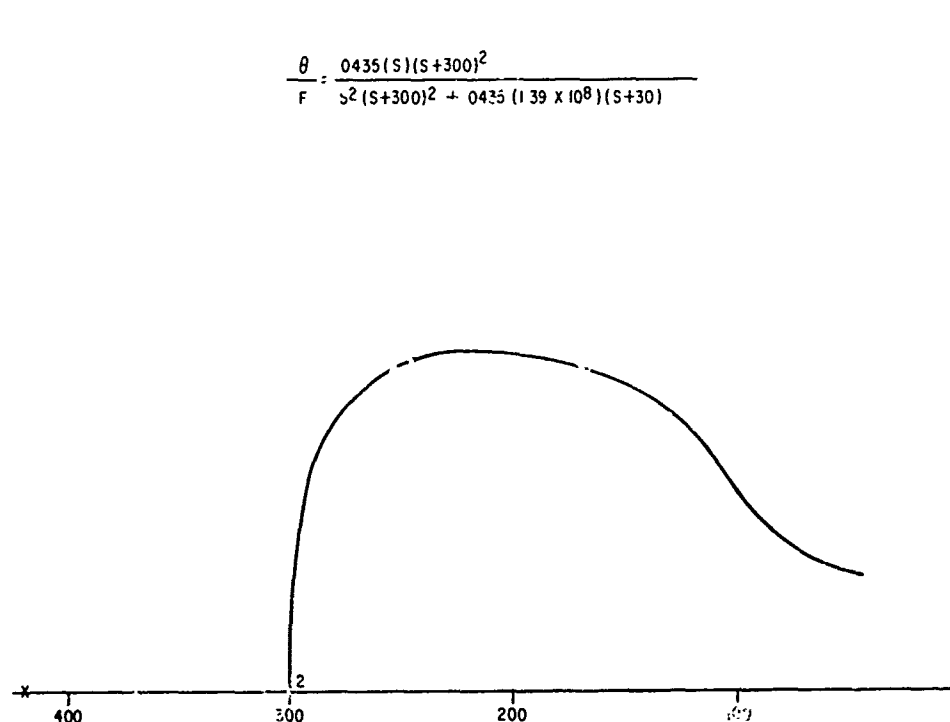


Figure 76 Root Locus for Friction Effects

Since the loop will always drive towards zero, the task is to evaluate the accuracy or closeness that it will drive to in the presence of friction. A theoretical number can be achieved based on the theoretical system friction and the gain of the system. When the offset error away from zero produces motor torque that is less than the total gimbal friction, the gimbal will stop at that error angle. Measuring this angle is an indication of the total friction (and hysteresis, etc.) torque in the gimbal system.

The dc gain of the test servo was set at 0.045 oz.in./microrad. As the pointed mass moves toward its final position it will stop in that orientation where the motor torque is less than or equal to the gimbal friction. The bearing tests showed that the friction is not a constant, but varies irregularly as the bearing turns. This leads to the expectation that the system will not always return to or maintain the same pointing angle while dynamically operation, but that the peak error (in microrads) will be no larger than 22.2 times the peak gimbal friction (in ounce inches).

SECTION VI POINTING TESTS

6.1 INTRODUCTION

Three types of pointing tests were performed. The first measured the repeatability of the servo driving to null, the second measured the tracking capability with an input motion of 1 degree/second, and the third measured the system susceptibility to disturbance torque inputs. A description of each test and its results follows.

6.2 NULL REPEATABILITY TEST

The pointed mass (circular disc) was mechanically offset, with the servo loop closed, and allowed to return to null. The offsets were from 0-1° and were repeated many times in both the positive and negative direction to give a large number of data points. The demodulated output of the LVDT was read and recorded to indicate the final position each time. The servo loop was adjusted to that gain which gave the desired dynamic performance, i.e., a loop damping ratio of approximately 0.7. The servo gain could have been increased by as much as a factor of 7, which would have given higher pointing accuracy, but the system would have been poorly damped. Tradeoff between accuracy and dynamic performance are normally run on servos leading to the most realistic compromise for each particular system. The 0.7 damping factor is felt to be realistic for this one.

The graph of Figure 77 is a smooth curve drawn from a frequency of occurrence histogram for the position at which the mass came to rest. It shows that the majority of times the error angle is between two and five microradians. Whether the final resting point is positive or negative depends upon the direction the mass is traveling when it reaches its final position. This is a function of the angle of offset and any initial rates that were imparted to the mass when it was released. If the system were run only in its linear range and no initial rates were imparted to it, the final position would be on the same side of zero consistently, when started from the same point. However, the variations in friction with position are sufficiently random that starting from different points will give widely varying results.

Comparing Figure 77 to the dc gain of the servo, a total friction number for the gimbal can be calculated. The peak number of hangoff occurrence, +4 microrad, corresponds to +0.18 oz-in. This is a very low friction, but is reasonable when the very low speed and the laboratory environment are considered. Certainly the design number for a launchable system that would operate over a wider temperature range for 5-10 years would be much higher.

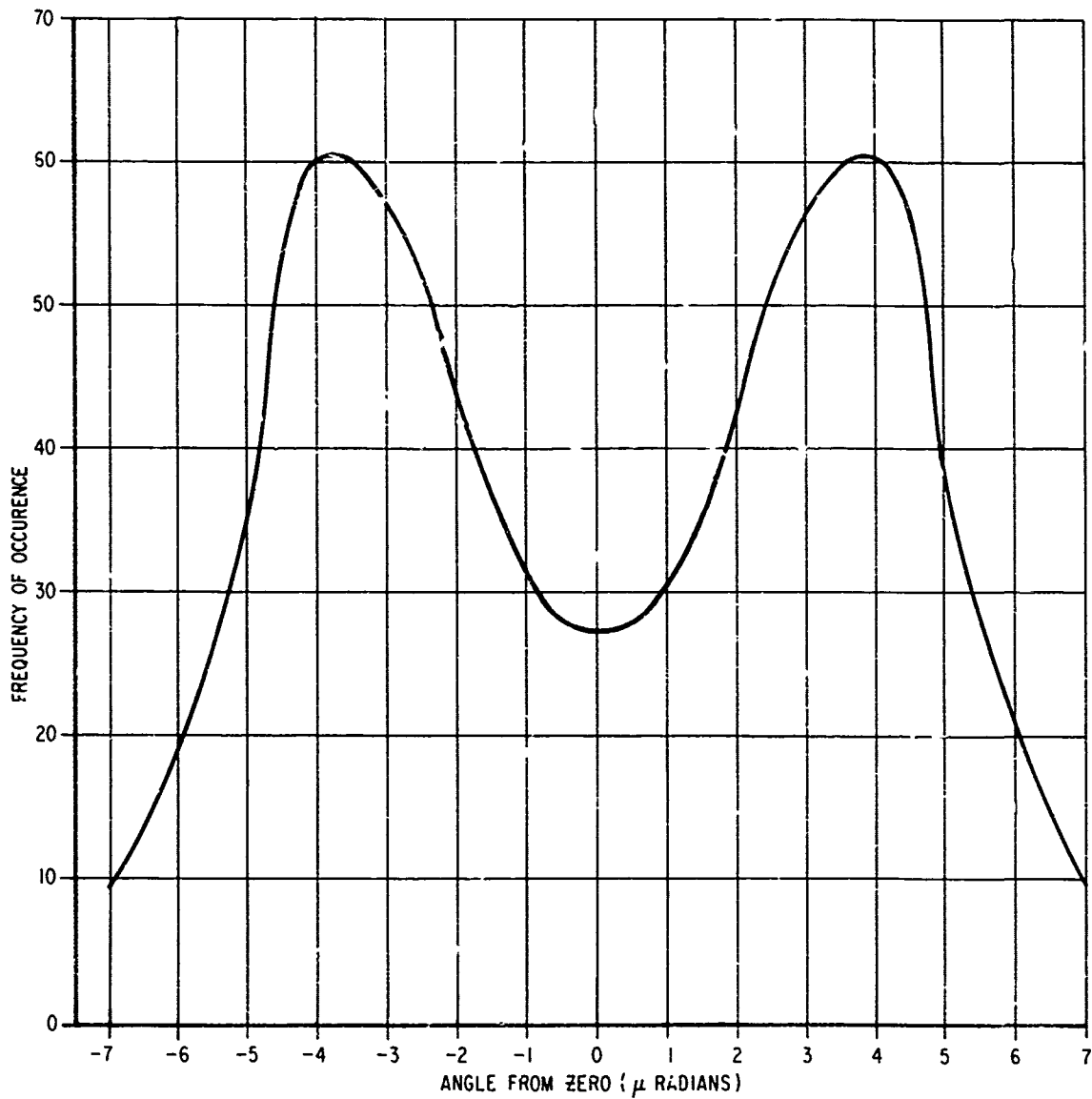


Figure 77 Angular Pointing Frequency Histogram

The system tested incorporated more types of friction than would have to be used in a flight system. A brushless motor, designed for minimum hysteresis torque and flex cables instead of slip rings could be used to improve the pointing misalignment due to friction. Since the pointing accuracy measured in the test is generally better than that required for the pointing tasks of the project 405B demonstrations, it is concluded that this test can only support the use of bearing supported systems to attain the accuracies required by the 405B project.

6.3 MOVING GIMBAL TEST

The gimbal housing was rotated at one degree per second in both the clockwise and counter-clockwise directions. The angular position was measured at the LVDT demodulator output and recorded on a strip chart recorder. As in the previous test the servo gain was set for optimum dynamic response rather than minimum static pointing error.

The position trace recorded for rotation in both directions is given in Figure 78. The dc hangoff in either direction is approximately 50 microradian. Since the dc forward loop gain is 0.045 oz.in./microrad, this corresponds to a running friction of 2.25 oz.in., which is rather low for two bearings, the motor brushes, and the slipring. This steady state pointing error could be eliminated by the addition of a forward loop integrator, but at the expense of added circuit complexity to also accommodate coarse or acquisition maneuvers. This friction level did not significantly decrease when the speed was reduced to 0.5°/second.

At this point, one direct relationship between servo performance and friction can be seen. If the servo does not have a forward loop integrator there will always be a hangoff corresponding to a dc torque level. The hangoff magnitude can be reduced by increasing the loop gain or eliminated by adding the integrator. A penalty of stability or dynamic performance accompanies the integrator. The ideal solution would be to decrease the friction to levels where the hangoff is acceptable.

The ratio between friction and inertia is also important to the servo performance. Since the torque required for control in a friction-free system is proportional to the system inertia, and the system performance depends on the ratio of control torque to friction torque, having more inertia with a constant magnitude of friction will improve system performance. This is the same as saying that the loop gain must be increased to handle a larger inertia, so if the friction does not increase, the gain increase (oz.in./microrad) will give a smaller hangoff due to friction.

The high frequency jitter shown in Figure 78 is caused by gimbal torques and has a peak amplitude of approximately +7 microrad, which is well within the desired 10-35 microrad range. This

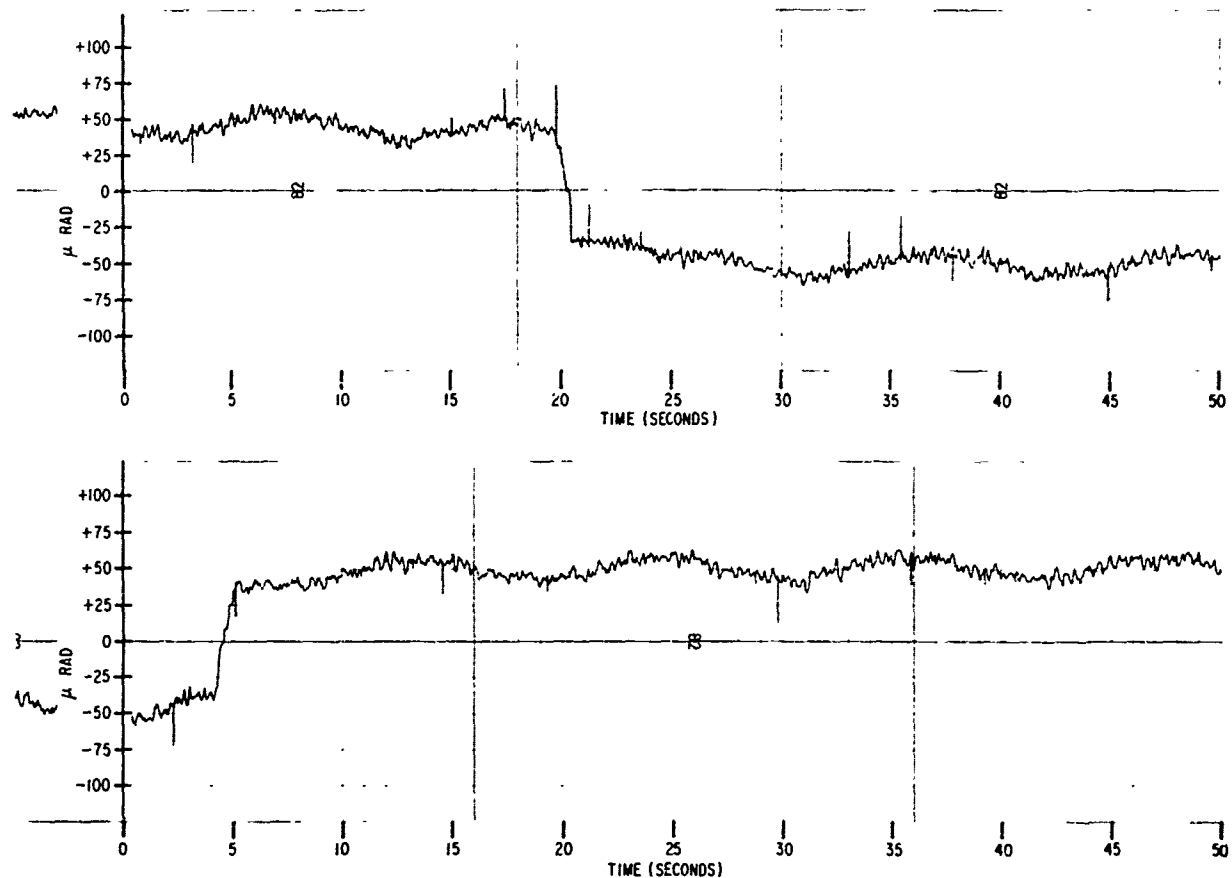


Figure 78 Moving Gimbal Position Traces

corresponds to a friction peak of +0.315 oz.in., which is well above the ripple torque found for the 36561 bearings under light preloads. The level is reasonable when considering the system friction sources in addition to the bearings. An inspection of Figure 78 shows the high frequency ripple to be in the range of 2-4 Hz. This frequency was found to be a function of bearing speed. When the gimbal speed was increased or decreased the ripple frequency varied accordingly.

A slower sinusoidal variation can also be detected on the position trace. Its peak amplitude is approximately ± 10 microrad, which corresponds to +0.45 oz.in. At a gimbal speed of $1^\circ/\text{second}$ this slow frequency is approximately 0.1 Hz, or one cycle in every 10 degrees of gimbal rotation. This frequency is also a direct function of rotation speed, i.e., the torque cycles occur at each 10° of gimbal rotation regardless of speed. There is nothing in the motor or slip ring that is mechanically cyclic at such a rotation angle so this variation is most likely from the bearings. Such variations are relatively common with bearings and with proper analysis can be traced to a cyclic phenomenon such as the

repeated rotation of one particular ball or the movement of one ball after another past a particular spot on one of the races.

The results of this test also tend to confirm that the use of bearing supported systems for pointing accuracies of 10-30 micro-rad is reasonable. That the system pointed as accurately as it did without special precautions or sophisticated servo compensation indicates that a flight system can be designed to do at least as well. The only considerations that would be expected to require a more complex flight servo are problems such as structural resonances, sensor noise, or redundancy requirements of a long life application.

6.4 DISTURBANCE TORQUE TEST

Controlled disturbance torques were input to the pointed mass by driving the torque motor via an external input to the motor drive amplifier. This gives disturbances around the pointed axis only. The effect of disturbances applied to the other two axes and cross coupled into the pointing axis was not analyzed. The applied disturbance torques were sinusoidal because this is the most common form expected in space hardware and because of the ease of analysis of these disturbances.

Figure 79 is a closed loop frequency response curve of the control system susceptibility to disturbance torques applied to the pointed mass. It shows that low frequency disturbances (below 10 Hz) affect the system directly, i.e., the control system does not decouple the disturbance from the controlled mass. The mass follows the disturbance torques as the dc gain of the servo dictates; 22.2 microrad per oz.in. of disturbance torque. Above 10 Hz the effect of the disturbances decrease as the frequency increases. Above 48 Hz (300 rad/second) the response to disturbance decreases at the rate of -40 db/decade.

The tests run confirmed the curve of Figure 79. The laboratory data followed the curve within measurement accuracy over the entire frequency range. The data was taken by applying a voltage of known frequency and amplitude to the motor drive amplifier and measuring the responses at the demodulated output of the LVDT. The dc gain was confirmed by applying a dc voltage and making a static measurement of the servo hangoff.

This servo system was not designed to accommodate any known disturbance torques, but could have been if such torques could have been defined. If the disturbances occur at low frequencies (below 10 Hz) the most common solution is to raise the dc loop gain to the point where the offset caused is acceptably small for the applied torque. At higher frequencies (more common) the natural roll off of the system minimizes the disturbance effects. A type of servo disturbance input that is often encountered is a structural resonance in the pointed hardware that is excited from

outside the system. It can be concluded from Figure 79 that such resonances should be driven well above the 50-100 Hz range if at all possible. When this cannot be done, notch filters can sometimes be incorporated into the control electronics to partially diminish the servo response at this frequency.

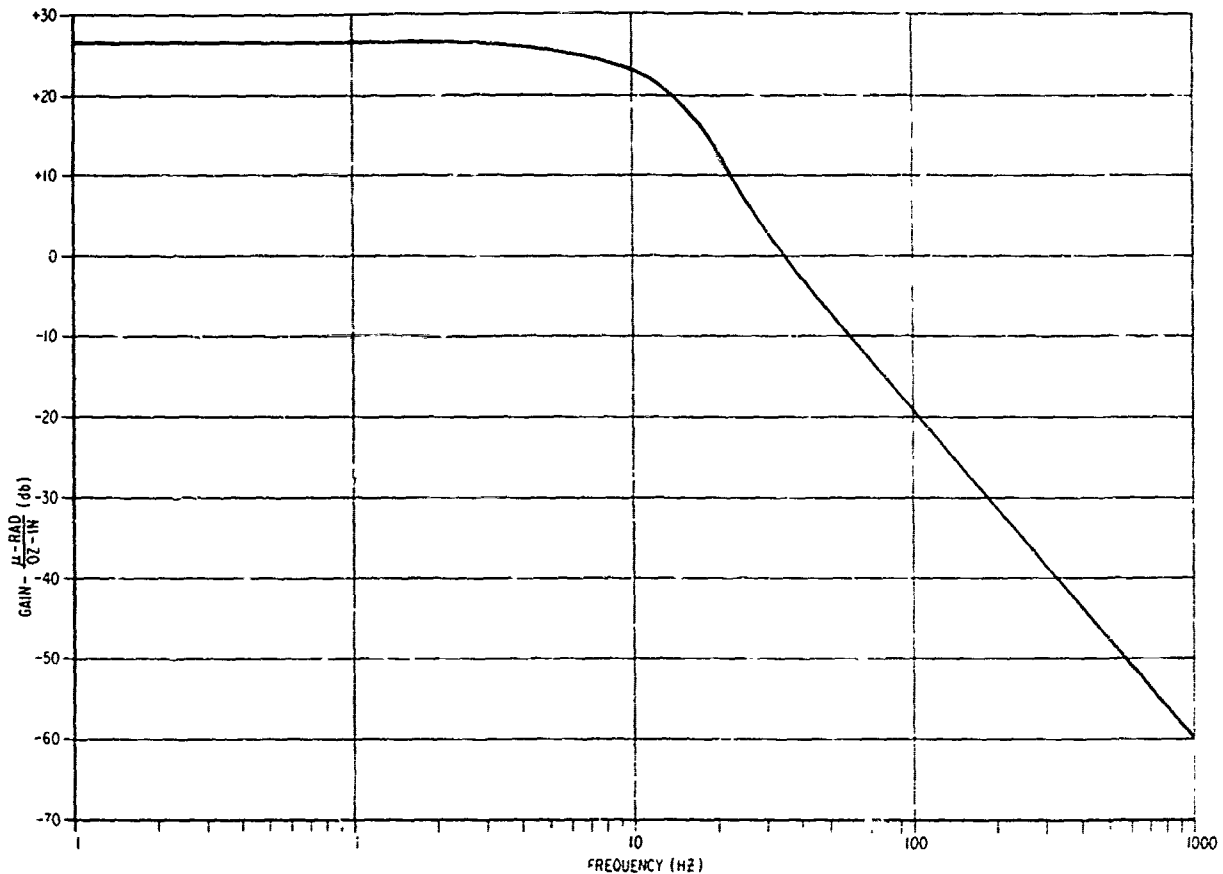


Figure 79 Closed Loop Response to Disturbance Torques

Since the expected disturbance inputs of a flight system are as yet undefined and the mechanical disturbances of the demonstration models expected to be minimal, this test provides more background information to the laser pointing task than immediately applicable data. It does, however, illustrate the potential effect of disturbance torques on flight systems and the necessity of defining these torques as early as possible in the design phase of the flight system.

SECTION VII

ALTERNATE APPROACHES TO BEARING SUPPORTED SYSTEMS

7.1 INTRODUCTION

The tests of bearings and of bearing supported systems described in this report indicate that bearings need not impede system pointing accuracy in the range of 10-35 microrad. However, other considerations are sometimes present which could make other support systems more appealing than those which use conventional ball bearings. The effect of bearing-use on systems which require pointing accuracy in the range of 0.01 - 0.1 microrad could not be sufficiently evaluated by these tests. Pointing in this range would require either a much longer, more complex series of tests or an alternate support system. Spacecraft lifetimes in excess of 10 years have not been demonstrated in space flight or test at this writing, and the use of ball bearings or an alternate is one of the major tradeoffs in such designs. Two alternate concepts have been investigated for a number of applications and are briefly reviewed herein. They are magnetic bearings and flexure pivots. Magnetic bearing technology is still in the development stage, but a number of demonstration models have been successfully operated. Specialized and conventional flex pivots are being used in a number of applications of flight hardware.

7.2 MAGNETIC BEARINGS

Magnetic bearings as a means of suspension must be included in any discussion of high accuracy pointing. These bearings have been developed to the point that they are reasonable in stiffness and size, take virtually no power, and are completely non-contacting. They hold the promise of eliminating friction as a source of pointing inaccuracy; static and viscous friction are both extremely low in well-designed magnetic bearings. Also, angular range is unlimited and there is no wear-out mechanism.

The recent work in this field has been sponsored by NASA and INTELSAT. Developmental work has been performed by Cambion (Cambridge Thermionic Corporation) and General Electric in this country and Teldix in West Germany. The emphasis in these contracts has been on capitalizing on the long-life aspects of these bearings as applied to momentum wheels for spacecraft, but much of the work applies equally well to high accuracy pointing applications.

7.2.1 How a Magnetic Bearing Works

Magnetic bearings have been slow to be developed because entirely passive magnetic suspension in three degrees of freedom is not possible using any normal materials. Many have tried. Some have

even been issued patents for their unworkable schemes. But the use of closed-loop feedback control systems has resulted in practical magnetic bearings that use a combination of active and passive means to achieve true three-dimensional stability.

The rudiments of a typical magnetic bearing are shown in Figure 80. The shaft is supported by being "stretched" between two axially-located permanent magnets. The attraction of these magnets resists any motion of the shaft in a radial direction, hence the shaft is said to be passively supported in the radial direction. In the axial direction, the shaft is unstable. It wants to clamp itself to either the right or the left magnet. The system can be made stable, however, by use of electromagnets that modify the flux in the right and left magnets as a function of the axial position of the shaft. The axial system is thus "active" suspension. The position sensors can be optical, capacitive, or magnetic.

This kind of bearing typically uses air gap separations of several thousandths of an inch. Axial stiffness can be 10,000 to 100,000 pounds per inch and radial 1/2 to 1/10 of axial stiffness.

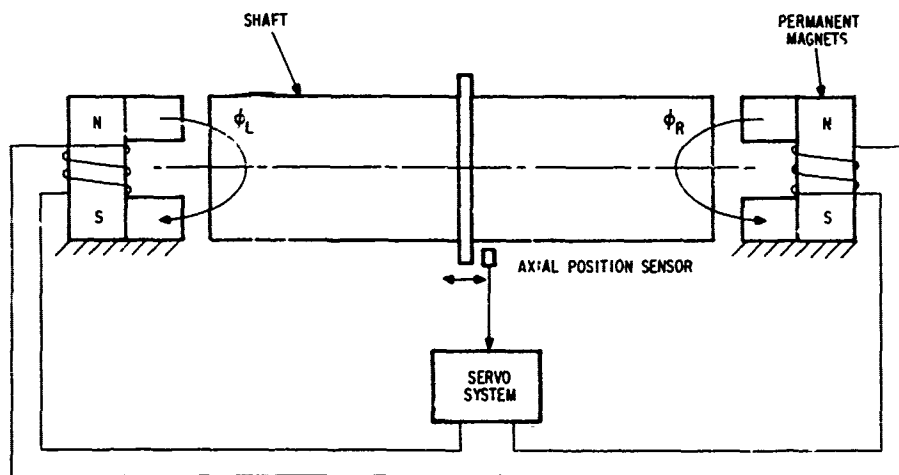


Figure 80 A Simplified Magnetic Bearing

Development of magnetic bearings has gone far beyond the basic system shown in Figure 80. The two most unique developments are (1) the use of the combination of permanent and electromagnets in such a way that no steady-state electrical power is required, and (2) a system using active radial and passive axial control to yield very high radial bearing stiffness.

7.2.2 Application of Magnetic Bearings to the 405B Program

The following factors would affect the use of magnetic bearings in a laser pointing application.

Advantages:

1. Negligible static friction
2. Very low viscous friction
3. Unlimited angular range
4. No lubrication required
5. No wear-out mechanism.

Disadvantages:

1. The "softness" of the bearings would preclude their use during launch. A mechanical locking device would be required.
2. Special torque motors would be required. Conventional torque motors have unacceptably large de-centering forces.
3. Precision angular read-out is difficult because of slight uncertainties in the location of the axis of rotation in a "soft" magnetic bearing.
4. Magnetic bearings are more expensive than ball bearings.
5. Magnetic bearings are less reliable than ball bearings at the present state of their development, and from an inherent "parts-count" reliability concept may continue to be. However, the expected long life is one of their outstanding features.

7.2.3 Magnetic Bearing Conclusions

Magnetic bearings hold great promise for use in high accuracy pointing. However, they are in their infancy and, moreover, the results of the ball bearing tests reported in this document indicate that the friction improvements possible with magnetic bearings are not required for 405B as presently defined. If expected progress in magnetic bearings takes place, they may someday serve to combine the coarse and fine pointing tasks in a single magnetic bearing supported system.

7.3 FLEXURE PIVOT SUPPORTS

The flexural pivot is a device whereon the mass to be pointed is suspended from flexible members which bend as the pointed mass is rotated. Because of the flexures it is inherently a limited angle device. The most common example is the taut wire suspension of a D'Arsonval meter movement. As torque is applied, the flexible wire rotates, generating a restoring torque which is linear with the angle of rotation.

7.3.1 Types of Flexure Pivots

A large number of flexure devices have been used on mechanical and electrical designs. Three flex pivot concepts are shown in the section views of Figure 81. In each case the inner member rotates with respect to the outer member causing the webs to flex.

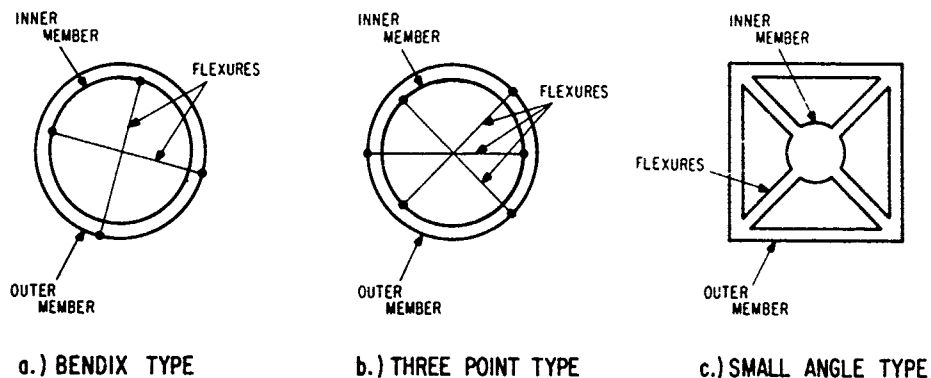


Figure 81 Flexure Pivot Types

a. Bendix Type - This pivot is commercially available and has been used in a large number of industrial and aerospace applications. The only real weakness it has is that the centers of rotation of the inner and outer members do not remain aligned as the members are rotated. From Figure 81a, it can be seen that the centroids of the inner member translates with respect to the outer member as the inner member rotates. When the inner member is attached to a precise optical component this translation may not be acceptable. The typical rotation angle for this type of pivot is ± 5 degrees, but models are available with excursions as large as ± 13 degrees for indefinite life and higher with reduced life spans.

b. Three Point Type - This device has the inner web slotted so that each web passes through the near side of the inner member and is attached to the far side. As the inner web is rotated, a buckling compression rather than tension is applied to each web. If the webs have equal mechanical characteristics the centers of rotation of the inner and outer members will remain aligned. None of this type is known to have flown on an aerospace application.

c. Limited Angle Pivots - The pivot shown in Figure 81 c is limited to extremely small angular excursions. This is because the centers of rotation of the inner and outer members are rigidly

aligned and very high tension is generated in the webs as the inner member is rotated. Two versions of this type of pivot were developed by BBRC for use on experiments for NASA's Apollo Telescope Mount. The inner members of each pivot were attached to an optical component which was required to maintain precise alignment while being rotated. Each pivot was operated at excursions of less than +300 microrad.

7.3.2 Flexure Pivot Tradeoffs

As with ball bearings and magnetic bearings, the use of flex pivots in a specific application is limited by the requirements of that application. The advantages and disadvantages of flex pivots for the known laser pointing applications are given below.

Advantages:

- a. The flexure pivot is a friction-free device; it has no rubbing or sliding contacts.
- b. The transfer function between applied torque and rotated angle can be extremely linear and repeatable.
- c. For angles small enough to operate in the elastic range of the web material there is no detectable hysteresis, no dead zone and no non-linearities.
- d. There is no wear out mechanism other than fatigue. For small angles the theoretical life is close to infinite.

Disadvantages:

- a. The angular freedom is limited. Models have been conceived with angular excursions of up to 90 degrees but they have not been built and tested. There is no way to get continuous motion, in any case.
- b. The flex pivot use requires a tradeoff between the strength of the pivot (structural considerations) and the amount of power required to drive it. If the pivot is very soft, launch locks are required to support it during the launch environment. If the pivot is strong enough to sustain the launch environment, the torque required to drive it will also be high. Since dc motor torque is a function of current but motor power loss a squared function of current, a very strong flex pivot may require an unreasonable amount of power.
- c. Using the flex pivot usually means a mass supported on an undamped spring. This requires either an unconventional control system or the addition of a damping mechanism which can be heavy, unreliable, or cause friction similar to that which the design was meant to avoid originally.
- d. The flex pivot to be used for a specific application must usually be developed for that application. This will generally result in costs considerably in excess of a bearing supported system.

7.3.3 Conclusions

For extremely small pointing angles at very high accuracy, flex pivots are the best known method. Under these circumstances their life, reliability and performance characteristics are all superior. However, the number of cases where these requirements are called for has been small and thus insufficient development has occurred to make them a common, inexpensive device. For this reason they are a relatively small part of the total pointing system picture. They are, however, ideally suited to the fine pointing requirements defined in the project 405B studies.

APPENDIX A
REFERENCE BIBLIOGRAPHY OF BEARING TECHNOLOGY

The following references are not directly applicable to the bearing tasks of the 405B project, but they do contribute a wealth of general and specific background data.

<u>Title</u>	<u>Author</u>	<u>Ref. No.</u>
"Molecular Approach to Dry Film Lubrication in a Vacuum (Space) Environment"	R. M. Van Vliet	AD-245272L
"Behavior of Materials in Space Environments"	Jaffe & Rittenhouse	AD-266548
"Evaporation Effects on Materials in Space"	Jaffe & Rittenhouse	AD-266906
"Materials Evaluation under High Vacuum and Other Satellite Environmental Conditions"	Blackmon, Clauss, Ledger, & Mauri	AD-270279
"Analytical and Experimental Study of Adapting Bearings for Use in an Ultra-High Vacuum Environment"	P. H. Bowen	AD-282625
"Program 461 Reliability Materials Research and Application Evaluation of Bearing Materials and Lubricants for Space Environment"	No Author	AD-405572
"Lubrication of Bearings and Gears in Aerospace Environmental Facilities"	P. H. Bowen	AD-411430
"Behavior of Slip Rings in a Space Environment"	Clauss, O'Hare, & Kassebaum	AD-416945
"New Candidate High Temperature Lubricants for Advanced Aerospace Systems"	R. F. Dolle	AD-449716
"Evaluation of Slip Ring Capsules"	Sperry Gyroscope Co.	AD-449800

<u>Title</u>	<u>Author</u>	<u>Ref. No.</u>
"Performance Test of Power Transmission Slip Rings in Vacuum Environments"	D. L. Adkins	AD-451412
"Vac-Kote Lubrication Technology for Long Space Life Bearing Applications"	B. J. Perrin (BBRC)	TN66-35
"Dry Film Lubricant Evaluation with Various Anodic Coatings"	North American Aviation	AD-457441
"Tests of Dry Composite Lubricated Bearings for Use in an Aerospace Environmental Chamber"	T. L. Ridings	AD-458414
"Tests of Dry Composite Lubricated Gears for Use in an Aerospace Environmental Chamber"	T. L. Ridings	AD-460502
"Lubrication of Bearings and Gears for Aerospace Facilities"	P. H. Bowen	AD-461390
"Fundamental Mechanisms of Lubrication in Space Environment"	Brown & Burton	AD-468097
"Vacuum Test of Slip Ring/Motor Assemblies and Bearings"	R. W. Mayer (BBRC)	TR-63-36
"Friction and Wear Behavior of Solid Films"	Bryant & Gutshall	AD-479698
"Friction and Wear Characteristics of Materials Under Ultrahigh Vacuum and High Temperature Conditions"	A. J. Haltner	AD-480552
"Fundamental Mechanisms of Lubrication in Space Environment"	Brown & Burton	AD-481492

<u>Title</u>	<u>Author</u>	<u>Ref. No.</u>
"Greases Based on Perfluvoro Polymeric Fluids - A New Class of Greases for Aerospace Use"	Christian & Bunting	AD-484607
"Friction and Wear Behavior of MoS ₂ in Air, Vacuum, and Dry N ₂ "	Wm. Wolkowitz	AD-486042
"In-Space Friction Tests"	R. L. Hammel	AD-505552
"Air Force Materials Laboratory Solid Film Lubrication Research"	B. D. McConnell	AD-604654
"Solid Film Lubricated Bearing Research Program"	Brown, Hawkins, Maguire & Pitek	AD-608629
"Research and Development of a Friction-Controlled Face Seal"	R. J. Smith	AD-609174
"Evaporation of Organic Compounds from Metal Surfaces at High Vacuum"	Gisser & Sadjian	AD-612158
"Lubricants for the Space Environment"	F. J. Clauss	AD-627578
"Lubrication Evaluation"	F. J. Clauss	AD-635078
"Space Materials Handbook, 3rd Edition"	Rittenhouse & Singletary	AD-692353
"Liquid Lubricant Handbook for Use in the Space Industry"	Campbell, Thompson, & Hopkins	X67-21565
"Lubricants for Use in the Space Environment"		AD-702550
"Friction of Tungsten Disulfide Sliding in an Ultrahigh Vacuum"	A. J. Haltner	AD-823171
"Lubricants for the Space Environment"	Flom & Haltner	AD-829345

<u>Title</u>	<u>Author</u>	<u>Ref. NO.</u>
"Friction and Wear of Solid Materials Sliding in Ultrahigh Vacuum and Controlled Gaseous Environments"	A. J. Haltner	AD-832431
"Aerospace Greases - Lubrication Demands and the State-of-the-Art"	J. B. Christian	AD-844498
"Friction and Wear of Solid Materials Sliding in Ultrahigh Vacuum and Controlled, Gaseous Environments"	Haltner & Feingold	AD-853047
"The Lubricating Behavior of MoS ₂ and PTFE Double Layers in High Vacuum"	Spengler & Hellwig	AD-856289
"Lubricants for Use in the Space Environment"	Benzing & McConnell	AD-867903
"Lubrication Techniques for Use in Vacuum"	R. Courtel	A68-27386
"Friction in Vacuum"	Briscoe and Dauphin	A68-34571
"A Short Survey of European Work on Lubrication in Vacuum"	C. L. Harris	A69-18564
"Vacuum Evaluation of Lubricants and Techniques for Space Exposed Components"	H. T. Azzam	A70-17340
"Testing Solid Lubricants"	J. S. Kummins	A70-23914
"Improved Silicones"	Bowen, Boes, Grossett & Bober	N66-27232
"Lubricant Study in Ultrahigh Vacuum and in Various Gas Environments"		

<u>Title</u>	<u>Author</u>	<u>Ref. No.</u>
"Lubricants and Self-Lubricating Materials for Spacecraft Mechanisms"	F. J. Clauss	LMSD 894812
"Lubrication of Sliding and Rolling Element Electrical Contacts in Vacuum"	J. Przybyszewski	168-16665
"Lubrication and Bearing Problems in the Vacuum of Space"	E. E. Bisson	168-19608
"Development of a Bearing for the Despun Antenna of a Spin Stabilized Satellite, Part I: Basic Investigation"	Granzow, Hauser, & Rieger	168-21201
"Lubrication and Bearing Problems in the Vacuum of Space"	E. E. Bisson	N68-27414
"Materials for Lubrication Applications"	H. I. Silversher	N70-26346
"Comparative Friction and Wear Behavior of New Materials Usable in Ultrahigh Vacuum"	(BBRC)	TN61-38 & 47
"Results of Vacuum Environmental Tests: On Slip Rings (TN61-47A), On Bearings (TN61-38A), On DC Motor (TN61-48A), All Treated with VacKote"	(BBRC)	LOCK-001
"LMSC Study on D-C Brushes for Hard Vacuum Applications"	Campbell, Thompson, & Hopkins	TN62-22
"Solid Lubricant Handbook for Use in the Space Industry"	(BBRC)	
"Qualification Report: Lubrication, S-17 Orbiting Solar Observatory"		

<u>Title</u>	<u>Author</u>	<u>Ref. No.</u>
"Accelerated Vacuum Testing of Long Life Ball Bearings and Slip Rings"	R. I. Christy & A. C. Cunningham	(Hughes) 007
"Lubrication in Space Environments"	Adamczack, Benzing, & Schwenker	ASD TDR 62-541
"Status of Lubricants for Manned Spacecraft"	de Laat, Shelton, & Kimzey	66AM7A2
"Space Mechanism Lubrication"	Perrin & Mayer (BBRC)	M68-08
"Evaluation of Slip Rings for Communications Satellite Applications"	(BBRC)	F69-07
"Lubricator: Evaluation"	Silversher & Drake	Lockheed MRI 503.01
"Final Report, Lubricant Evaluation"	Silversher & Drake	Lockheed MRI 503.02
"Sintered Skeleton Sweats Lead to Control Friction"	Tom Balmer	
"Design Study Report : Lubrication System for Comsat Intelsat III Antenna Despin Assembly"	R. W. Mayer (BBRC)	TR-68-37
"Lubrication of Ball Bearings for Space Applications"	Young, Clauss, & Drake	
"Solid Film Lubricants in a Vacuum Environment"	J. A. Wolterbeek	LMSC 67-22
"Investigation of a Dry Lubricant Surface Treatment for Bearings"	A. L. Kay (BBRC)	TR-64-8

A P P E N D I X B

Figures 82 and 83 are the schematics of the test equipment electronics which were used on both the bearing test and on the gimbal test fixture. Figure 82 shows the preamplifier and board no. 1 of the control electronics. Figure 83 is board no. 2 of the control electronics.

The only differences in the electronics when used for the pointing tests are changes in some of the component value of the compensation amplifier (on board 2) to make the compensation be

$$\frac{S + 30}{S + 300} \text{ rather than } \frac{S + 628}{S + 6280} .$$

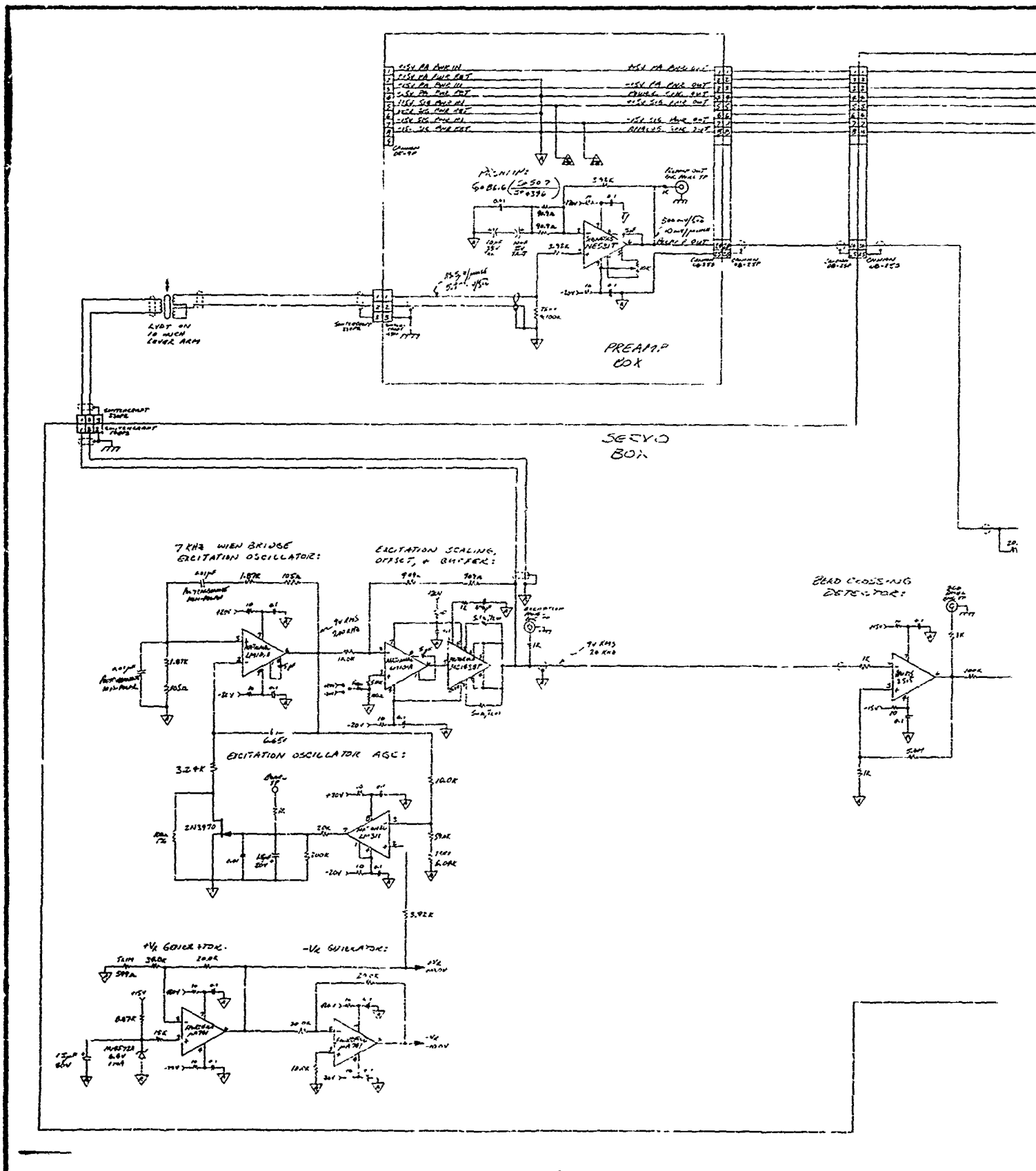
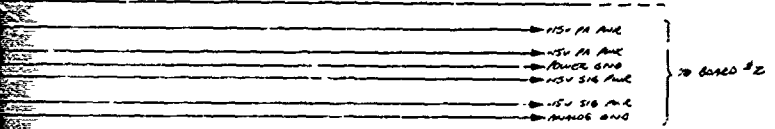
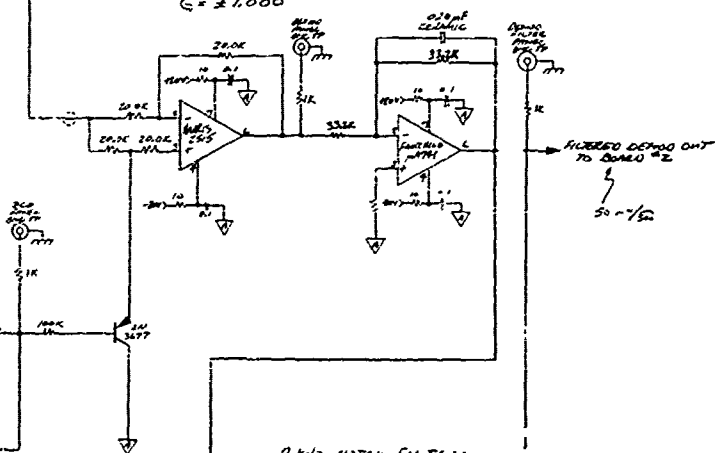


Figure 82 Preamplifier and Board No. 1

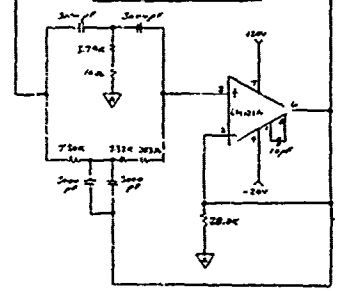


DENOMINATOR:
 $G = \pm 1,000$

DC100 FILTER:
 $G = \frac{-300}{s+300}$



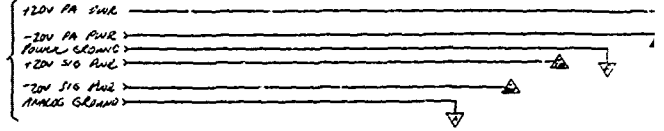
7 kHz NOTCH FILTER:



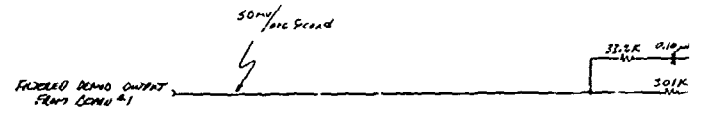
BOARD #1 — BOARD #2

REVISION C - 6-12-73 PLG
 REVISION A - 9-12-72 PLG

FRONT BOARD #1



6



43

BOARD #1 ——— BOARD #2

Unclas.

Security Classification

DOCUMENT CONTROL DATA - R & D

(Security classification of title, body of abstract and indexing annotation must be entered when the overall report is classified)

1. ORIGINATING ACTIVITY (Corporate author)		2a. REPORT SECURITY CLASSIFICATION	
BALL BROTHERS RESEARCH CORPORATION		Unclas.	
2b. GROUP			
3. REPORT TITLE			
EVALUATION OF CONCEPTS FOR A LASER ACQUISITION AND TRACKING SUBSYSTEM			
4. DESCRIPTIVE NOTES (Type of report and inclusive dates)			
FINAL REPORT, JUNE 1972 - APRIL 1973			
5. AUTHOR(S) (First name, middle initial, last name)			
ROBERT C. CULVER			
6. REPORT DATE		7a. TOTAL NO. OF PAGES	7b. NO. OF REFS
JUNE 1973		97	
8a. CONTRACT OR GRANT NO.		9a. ORIGINATOR'S REPORT NUMBER(S)	
F33615-72-C-2053		AFAL-TR-73-180	
b. PROJECT NO.		9b. OTHER REPORT NO(S) (Any other numbers that may be assigned this report)	
405B			
c.			
d.			
10. DISTRIBUTION STATEMENT Distribution is limited to U.S. Government agencies only, by reason of inclusion of test and evaluation data; applied March 1972, other requests for this document must be referred to AFAL/TEL/405B Wright Patterson AFB, Ohio, 45433			
11. SUPPLEMENTARY NOTES		12. SPONSORING MILITARY ACTIVITY	
		AFAL/TEL/405B ADP Wright Patterson AFB Ohio 45433	
13. ABSTRACT			
<p>The program objective was to evaluate the starting and running friction characteristics of bearings rotating at 0.001 - 1.0 degree/second and to determine the pointing accuracy that can be achieved on a bearing supported gimbal system. The bearing tests measured the friction of bearings with pitch diameters of 0.25, 1.4 and 2.6 inches, using liquid and dry film lubricants, at high and low temperatures, and with various axial preloads. The running friction results were generally lower than predicted, varying from less than detectable to 0.9 ounce inches. The starting friction tests showed that the bearings have a spring-like characteristic when small torque levels are applied, that the starting friction levels were much lower than expected (0.03 ounce inch), and that a starting friction peak larger than the low speed running friction level does not exist. The pointing accuracy tests were performed on a single axis gimbal which was controlled by a conventional servo system. Tests were run on the repeatability of the system in attaining null, the ability to point while the gimbal housing was rotating at 1°/second, and the effects of disturbances on the system. The tests showed that pointing accuracies in the range of 10 - 35 microradian can be achieved on bearing supported systems and that the bearings are not the limiting cause of errors.</p>			

14. KEY WORDS	LINK A		LINK B		LINK C	
	ROLE	WT	ROLE	WT	ROLE	WT
Bearings						
Bearing Friction						
Starting Friction						
Pointing Accuracy						
Gimbal						
Laser Pointing						
Laser Tracking						